

Physical Sciences

- Geology, Geochemistry and Geotectonic Setting of the Pan-African Granites and Charnockites Around Ado-Ekiti, Southwestern Nigeria
Akindele O. Oyinloye and Romanus Obasi 299
- Effect of Excess Metal Concentration on the Extraction Potential of Di-(2-Ethylhexyl) Phosphoric Acid
A. S. Ahmed, M. B. Bhatti, M. T. Saeed and S. K. Afridi 309
- Evaluation of Locally Available Fuller's Earth for the Bleaching of Soybean Oil
M. Sharif Nizami and M. Iqbal Chaudhry 314
- Studies on the Laboratory Scale Synthesis of 4, 4'-Diaminodiphenylurea and Preparation of Direct Dyes from the Compound
S. Rehman Khan, A. M. Gilani, Asma Inayat and Shaheena Waheed 319
- Synthesis and Fungicidal Activity of Some Sulphide Derivatives of O-Ethyl-N-Substituted Phenylcarbamates
F. Adelowo-Imeokparia and I. A. O. Ojo 324
- Isolation and Characterization of *Kappa*-Carrageenan from *Hypnea musciformis* (Red Alga) Collected from Karachi Coast, Pakistan
Fatima Bi, Muhammad Arman, Mahmood-ul-Hassan and Seema Iqbal 330
- Comparative Studies on the Adsorption Properties of Powdered Activated Carbon and Propenoic Acid Modified Sawdust in the Treatment of Secondary Palm Oil Mill Effluent
M. O. Osuide, C. M. A. Ademoroti, V. U. Okojie and F. E. Igbinavbiere 335

Short Communication

- Some Studies on the Changes in the Composition of Coal Ash and Bottom/Fly Ash Produced in Atmospheric Fluidized Bed Combustor
Ismat Ali and M. Mohsin Ali 341

Biological Sciences

- High Frequency *In vitro* Propagation of *Polianthes tuberosa*
Muhammad Saeed Ahmad, Tauqeer Ahmad, Nasreen Zaidi and Idress Ahmad Nasir 344
- Morphological Changes in Cotton Roots in Relation to Soil Mechanical Impedance and Matric Potential
Ghulam Nabi and C. E. Mullins 349

Multiple Parameters for Ascertaining Yield Stability of Upland Cotton Varieties Tested Over Number of Environments Muhammed Jurial Baloch and Nasreen Fatima Veesar	355
---	------------

Technology

Isolation and Stabilization of Dark Red Food Dye from <i>Beta vulgaris</i> Alim-un-Nisa, Shamma Firdous and Nusrat Ijaz	360
---	------------

The Effect of Substitution on the Dyeing and Spectroscopic Properties of Some Monoazo Disperse Dyes Ausaf Aleem, Mohammad Naeem, M. Aleem Ahmed, Kamran Ahmed and Mansoor Iqbal	364
---	------------

Physicochemical Characteristics of Rayon Grade Dissolving Pulp and the Effects of Metallic-Ions on the Viscose Rayon Process Atif Latif, Asad Ullah Jan, Farid Ullah Khan and Amin Ur Rahman	368
--	------------

Short Communication

The Study of Electrolytes on the Dye Uptake of Bifunctional Reactive Red Dyes on a Cellulosic Substrate (Cotton K-68) Javaid Mughal, Ausaf Aleem, Qasim Siddiqui and Mansoor Iqbal	371
--	------------

Geology, Geochemistry and Geotectonic Setting of the Pan-African Granites and Charnockites Around Ado-Ekiti, Southwestern Nigeria

Akindele O. Oyinloye^{a*} and Romanus Obasi^b

^aDepartment of Geology, University of Ado-Ekiti, PMB-5363, Ado-Ekiti, Nigeria

^bDepartment of Mineral Resources Engineering, Federal Polytechnic, Ado-Ekiti, Nigeria

(received April 8, 2006; revised August 21, 2006; accepted September 19, 2006)

Abstract. The geology, petrology and geochemistry of the coarse-grained and fine-medium-grained gneissic charnockites and the porphyritic biotite-hornblende and medium-grained older granites in the Ado-Ekiti area were studied. Xenoliths of schistose quartzite occur within these charnockitic and granitic rocks. The porphyritic older granite and the coarse-grained charnockite occur in very close association in the field. All these rocks contain monazite, in their mineralogical composition, which indicate crustal input into their original magma. Aluminium-total iron-magnesium (AFM) plot for these rocks indicated that they were calc-alkaline in nature and were formed in a subduction related tectonic setting. Percentage normative corundum versus mol. $Al_2O_3/(Na_2+K_2O+CaO)$ plots for the older granites and the charnockites from the Ado-Ekiti area revealed that their original magma was derived from a mixed source (igneous and crustal). Y+Nb versus Rb plots for the older rare earth granites and the charnockites indicated that they originated from a volcanic arc and within-plate environments. The normalised rare earth elements (REE) patterns showed that these rocks were genetically related, and the feldspar fractionation took place during their formation as revealed by Eu depletion patterns in the REE diagrams. The negative Eu/Eu^* (ratio of absolute europium to normalized europium) anomaly and $(La/Yb)_N$ ratios higher than 5 obtained in these rocks indicated that they were emplaced through magmatic fractionation. The mixed magma from which these rocks were derived was formed in a back arc tectonic setting where an ocean slab was subducted into the mantle leading to the generation of magma, which intruded into the earlier formed rocks in a back arc basin. The charnockites and the older granites were the end products of the differentiation of such magma.

Keywords: monazite, xenolith, calc-alkaline, subduction, southwestern Nigeria, geotectonic setting, Pan-African granites, charnockites

Introduction

Nigeria lies within the Pan-African mobile belt in between the West African and Congo cratons (Akande, 1991; Woakes *et al.*, 1987; Odeyemi, 1981). The geology of Nigeria is dominated by the precambrian basement (crystalline and schistose meta-sediments) and recent-cretaceous sedimentary rocks, almost in equal proportions (Rahaman *et al.*, 1988). There is a high level intrusion of jurassic younger granites into the basement complex in Jos area of central-northern Nigeria. The precambrian basement in Nigeria consists of migmatite-gneissic complex within the muscovite-quartzite schists. In the Ado-Ekiti area, the basement complex, apart from the migmatite-gneissic-quartzite complex, includes granitoid plutons which are mostly older granites and charnockites with other minor granite associations (Fig. 1). These rocks have intruded into both migmatite-gneissic complex and the schists. Older granites and charnockites occur prominently in southwestern Nigeria at Iwo, Akure, Idanre, Ikare, Ikere and Ado-Ekiti (Olawaju, 1987). According to Dada *et al.* (1989), charnockites also occur at Bena, Makichi, Toro and Zurami in northern Nigeria. The Toro charnockite complex in the north-

central Nigeria is Pan-African in age based on a U-Pb-zircon dating, which places the Toro complex in the context of Pan-African granitoid (Dada *et al.*, 1989), making Toro charnockite to be similar in occurrence to those described in the southwestern Nigeria. Recently, Ekwueme (2003) also reported the occurrence of similar Pan-African charnockites in the Oban massives and Obudu plateau in the southeastern Nigeria. On the basis of geochronological and structural evidence, Tubosun *et al.* (1984) and Annor (1995) believe that the emplacement of granitic and charnockitic complex in southwestern Nigeria took place during the Pan-African tectonic episodes. Olawaju (1988) suggested on the basis of chemical studies that the Pan-African granites and charnockites in the Ado-Ekiti area are 'magmatic' in origin.

The present study focuses attention on the geology and geochemistry of the older granites and the charnockites in the Ado-Ekiti area with a view to explaining their possible geotectonic origin by comparing the concentration of some index elements in the rocks with those of a pure mantle. Discrimination diagrams, based on the chemical contents of the rocks, have been also used to infer the possible tectonic environment(s) in which their magma originated.

*Author for correspondence; E-mail: akinoyinloye@yahoo.com

Materials and Methods

Twelve (12) representative samples each of the older granites and charnockites (making a total of twenty four rock samples) were selected from the fieldwork collections in the Ado-Ekiti area. Petrographic studies were carried out during the fieldwork, as well as in the laboratory, using conventional thin sections of each rock type. Analysis of major elements was carried out on rock glass beads and trace elements on compressed rock powder pellets using X-ray fluorescence (XRF) equipment, which had computer and printer facilities, at the Cardiff University, Wales, UK, by the first author. The detection limits of the XRF used for the analysis of these elements varied from 0.0009% (CaO) to 0.03% (MgO) for the major elements and from 2 ppm (Ni) to 27 ppm (Ba) for the trace elements.

The initial rock sample preparation for the analyses of rare earth elements (REE) was carried out by the first author. This involved selection and pulverising the samples to produce rock powder and transporting them in polythene sample bags. The REE analyses were carried out at the Department of Geology, Royal Holloway and Bedford, New College, University of London, Surrey, UK, using the inductively coupled plasma spectrometry (ICPSS) as outlined by Walsh *et al.* (1982). The ICPSS used was a Phillips model OV8210 1.5 5-m, which was capable of evaluating spectral lines and measuring the REE concentration in each sample. Precision level attained was better than 1%.

Results and Discussion

Fieldwork carried out in the Ado-Ekiti area by the authors provided opportunity for studying the rocks in place and collecting fresh samples for the laboratory analyses. Apart from the migmatite gneissic-quartzite basement complex in the Ado-Ekiti area, the older granites and charnockites constituted prominent rock groups in this area. The Pan-African granites are called older granites in order to distinguish them from the non-orogenic, high-level jurassic granite intrusion confined in occurrence to the central-northern Nigeria around the Jos plateau (Falconer, 1911).

Field description and petrography. (a) *Migmatite-gneissic complex.* In the Ado-Ekiti area, the migmatite-gneissic complex forms the country rock into which the granitoids intruded. This group of rocks is usually low-lying and distinctively made up of three parts. The first part is a pale-coloured quartzo-feldspathic portion composed of quartz, plagioclase and K-feldspar. This portion of the migmatite is texturally medium grained but with relatively coarse crystals of plagioclase. This portion forms the leucosome of the migmatite in Ado-Ekiti area. The melanosome portion of the migmatite in

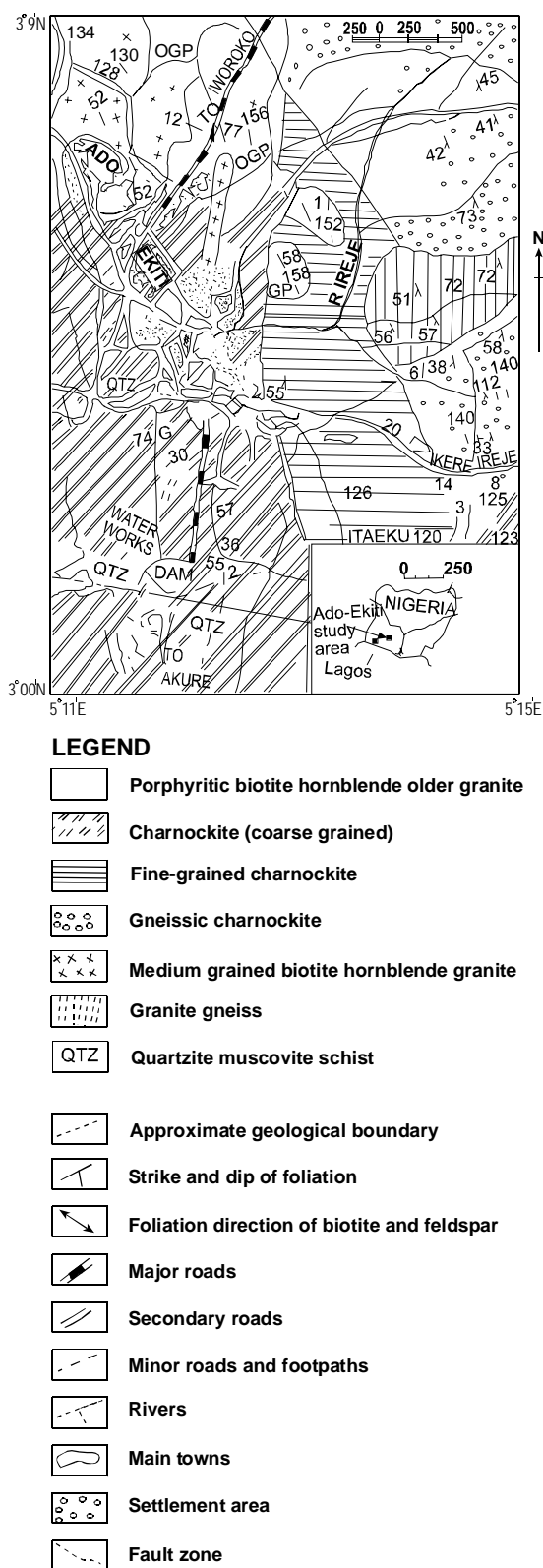


Fig. 1. Geological map of Ado-Ekiti, southwestern Nigeria (after Olarewaju, 1987); G = granite, GP = porphyritic granite, OGP = older granite porphyrite, R = river, QTZ = quartz.

this area is dark coloured and very rich in biotite. Other minerals in the melanosome include hornblende and garnet. Texturally, the melanosome of the migmatite here is medium-coarse grained. The palaeosome portion of the Ado-Ekiti migmatite, which is the third component, has the appearance of an ordinary metamorphic rock (gneiss), which is intermediate in colour between the leucosome and the melanosome. This portion is composed of quartz, plagioclase, biotite, muscovite and hornblende with a medium-coarse grained texture. Strong axial planer foliations, which have been refolded in places, are observed on the migmatite-gneiss complex here. The migmatite-gneiss in the Ado-Ekiti area is a layered type, which can be classified as a stromatolite type. A common feature of the migmatite-gneiss here is the layering with quartzofeldspathic veins, which are deformed into pygmatic folds. In such folds, synformal and antiformal axes are often very prominent.

The granite gneisses in the Ado-Ekiti area are biotite granite gneisses. These rocks are medium to coarse-grained in texture consisting of quartz, K-feldspar, biotite, muscovite, plagioclase, hornblende, and at times garnet. In places, the biotite granite gneiss may form fresh hilly outcrops, which are quarried for construction purposes. This is a mafic rock which shows a strong mineralogical banding. The biotite-gneiss has also been refolded in places indicating a polycyclic history like the migmatite-gneiss complex, which they are closely associated with.

(b) Metasediments. Metasediments in the Ado-Ekiti area are represented by quartzites, which occur as ridges and as xenoliths in the granitic and charnockitic rocks. The quartzite ridges vary in length and height. They often contain massive quartz at the crest and quartz veins in places. Elsewhere, pegmatitic bodies may be found in the quartzite ridges. These quartzites are composed mainly of quartz, minor muscovite and zircon. The xenolithic variety of quartzite in Ado-Ekiti is darkish in outlook and highly schistose. They occur as remnants within the older granites and the charnockites. These xenolithic quartzites are fine-grained in texture and are composed of quartz, relatively abundant biotite, muscovite and garnet.

(c) Older granites. There are broadly two major textural varieties of older granites, which are: (i) medium to coarse-grained biotite and biotite-hornblende granite; and (ii) the coarsely porphyritic biotite-hornblende granite. Microgranite (aplite) occurs as a minor rock intruding the older granites. The biotite hornblende granite occurs as inselbergs all over the Ado-Ekiti area. These inselbergs can be as high as 600 m above the sea-level. It appears as if the older granites exploit the north-

south trending regional foliation direction in this area. In places, some of the outcrops of this variety of older granites are covered with sub-angular to rounded boulders and can be very fresh. Elsewhere, they are covered with very thick vegetation, and outcrops may not be visible. Whitish feldspar-dominated pegmatitic bodies are often found associated with the older granites. In thin section, the older granites are composed of quartz, biotite, K-feldspar, monazite, muscovite and hornblende. The porphyritic older granite is the major type of granite in the Ado-Ekiti area. This type of granite occurs as low lying outcrops, which may be flat, forming a table land in places and may form hills in close association with the coarse charnockite elsewhere. This rock type is characterised by large phenocrysts of K-feldspar in a ground mass of fine-grained quartz, biotite and hornblende. In places, the K-feldspar phenocrysts are aligned. Microgranite (aplite) of fine texture, which may be upto 2 m in width, often intrude into the porphyritic older granite outcrop. The microgranite in the older granite may be faulted in places.

The porphyritic older granite is composed of quartz, K-feldspar, biotite, hornblende, plagioclase, monazite, zircon, apatite and opaques.

(d) Charnockites. Although about three textural varieties of charnockites have been reported in literature in the Ado-Ekiti area (Olawaju, 1987), only two of the three major textural varieties were sampled and have been described here. These are: (i) the coarse-grained charnockite; and (ii) the fine-medium-grained gneissic charnockite. In places, both the charnockite types exist as low lying outcrops, which are exposed. Elsewhere, the coarse-grained charnockite type occurs as hills. The coarse-greenish type often occurs in close association with the porphyritic older granite in the field. The darkish gneissic charnockite outcrops contain angular boulders of rock (charnockite) littering the surrounding. Both the charnockite types were observed as intrusive rocks in the Ado-Ekiti area. Like the older granites, xenoliths of dark schistose quartzite were found within the outcrops of charnockites in many localities in the Ado-Ekiti area. In the boundary areas, where older granites, charnockites and microgranites occur, it was usual to observe on a single outcrop, a section of porphyritic granite intruded by microgranite separating porphyritic older granite from the coarse-grained charnockite. The boundary between the microgranite and the older granite is gradational, but very sharp between the microgranite and the charnockite. The occurrence of the charnockite and the porphyritic older granite together on an outcrop tend to confirm the earlier suggestion by Tubosun *et al.* (1988) and Olawaju (1988; 1987) that the older granites and the charnockites in the Ado-Ekiti area were formed contemporaneously. In thin section, the

charnockites were observed to be composed of quartz, plagioclase and alkaline feldspars, hornblende, biotite, monazite, apatite, zircon, pyroxene and opaques. The occurrence of monazite in all the rocks in the Ado-Ekiti area raises very serious question as to whether these rocks were derived from a magma originating from the primitive mantle. For all intents and purposes, the presence of monazite (Ce, La, Y, Th)PO₄ (as identified and confirmed using a Cambridge 250 scanning electron microscope sport chemical analysis at the Department of Earth Sciences, University of Cardiff, Wales, UK) in an igneous rock indicated crustal or sedimentary input into its original magma.

Geochemistry. (a) The older granites. The chemical data of major elements for six samples of the porphyritic older granite (ADG1-ADG6) and six samples of the medium-grained biotite older granite (ADG7-ADG12) are shown in Table 1. The major and trace elements data for these granites were similar, with little differences in their respective concentration values. The SiO₂ component of the porphyritic older granite ranged from 74.25%-76.5%, while it ranged in the medium-grained biotite older granite from 73.52-75.63%. The content of Al₂O₃ in the porphyritic older granite varied from 13.04-13.69%, while the variation in the biotite older granite was between 13.81% and 14.51%. The oxides, Fe₂O_{3(T)}, MgO,

MnO, CaO and P₂O₅, occurred as minor components of both the older granites. In both granites, K₂O concentrations were consistently higher than the Na₂O component, giving K₂O/Na₂O ratio greater than 1 in both the rocks (Table 1).

(b) The charnockites. Major elements for the six coarse-grained charnockite (CHK1-CHK6) and six fine-grained gneissic charnockite (CHK7-CHK12) are shown in Table 2. Like the older granites, the chemical data of the charnockites were remarkably similar with only slight differences in the concentration values. The SiO₂ content of the coarse-grained charnockite (CHK1-CHK6) varied from 58.60-62.77%, while it varied from 58.8%-62.07% in the gneissic charnockite (CHK7-CHK12). The oxides, Al₂O₃, Fe₂O_{3(T)}, CaO, Na₂O and K₂O occurred prominently in both the charnockites. Unlike in the older granites, however, K₂O was consistently lower than Na₂O giving the K₂O/Na₂O ratio lower than 1 in both the charnockites. This might be due to more abundant sodic rock forming minerals like (plagioclase) in the charnockites than was observed in the older granites.

On the plot of aluminium-total iron-magnesium (AFM) diagram, the older granites and the charnockites plotted in the calc-alkaline trend, but in the case of charnockite, samples reached the crest of the curve separating the tholeiitic and

Table 1. Chemical data of major elements (wt, %) for representative samples of the older granites from the Ado-Ekiti area, southwestern Nigeria

Chemical constituent	ADG1	ADG2	ADG3	ADG4	ADG5	ADG6	ADG7	ADG8	ADG9	ADG10	ADG11	ADG12
SiO ₂	76.52	75.50	74.25	74.31	74.50	76.52	75.43	75.63	73.52	74.18	75.06	75.24
TiO ₂	0.09	0.063	0.13	0.13	0.13	0.10	0.10	0.10	0.13	0.13	0.13	0.01
Al ₂ O ₃	13.69	13.04	14.30	14.45	14.32	13.92	3.67	13.81	14.14	14.51	14.48	13.87
Fe ₂ O _{3(T)*}	1.59	1.38	1.30	1.26	1.33	1.61	1.63	1.64	1.27	1.32	1.31	0.18
MnO	0.07	0.01	0.02	0.01	0.01	0.05	1.03	0.07	0.01	0.01	0.01	0.02
MgO	0.05	0.03	0.06	0.06	0.05	0.03	0.06	0.03	0.05	0.70	0.06	0.05
CaO	0.68	0.49	0.51	0.51	0.72	0.72	0.63	0.62	0.47	0.54	0.53	0.48
Na ₂ O	2.66	2.38	2.26	2.29	2.24	2.64	2.49	2.48	2.21	2.53	2.31	2.32
K ₂ O	5.14	6.04	6.95	6.53	7.03	4.96	5.43	5.41	6.83	6.37	6.36	6.28
P ₂ O ₅	0.01	0.02	0.01	0.02	0.02	0.01	0.01	0.01	0.02	0.02	0.02	0.02
LOI	0.39	0.52	0.46	0.97	0.54	0.38	0.30	0.42	1.93	0.20	0.33	0.36
Total	100.89	100.04	100.54	100.54	100.57	100.94	99.78	100.22	100.58	100.51	100.60	100.02
Na ₂ O + K ₂ O	7.80	8.42	9.21	8.82	9.27	7.60	7.92	2.18	3.09	2.52	2.75	2.71
MgO/MgO + Fe ₂ O _{3(T)}	16	10	16	13	10	17	18	7.89	9.04	8.90	8.67	8.60
K ₂ O/Na ₂ O	27	29	26	46	28	42	44	28	31	46	38	38
Y + Nb	0.08	0.02	0.04	0.05	0.04	0.02	0.04	0.01	0.04	0.35	0.04	0.04
Na + K + 2Ca/Al	0.67	0.72	0.72	0.68	0.72	0.7	0.67	0.66	0.69	0.69	0.67	0.69

* = total iron as Fe₂O_{3(T)}; LOI = loss on ignition; ADG1-ADG6 = porphyritic biotite hornblende older granite; ADG7-ADG12 = medium-grained biotite older granite

Table 2. Chemical data of major elements (wt, %) for representative samples of charnockites from the Ado-Ekiti area, southwestern Nigeria

Chemical constituent	CHK1	CHK2	CHK3	CHK4	CHK5	CHK6	CHK7	CHK8	CHK9	CHK10	CHK 11	CHK12
SiO ₂	59.20	60.73	62.77	58.60	64.33	61.70	62.07	61.63	59.70	58.80	60.80	60.10
TiO ₂	0.16	0.22	0.46	0.19	0.53	0.14	0.42	0.43	0.26	0.37	0.39	0.40
Al ₂ O ₃	13.75	14.59	16.45	13.05	14.60	14.35	16.16	15.80	14.10	14.62	16.60	16.89
Fe ₂ O ₃ (T)*	4.04	3.93	5.89	6.93	5.99	4.72	5.26	5.71	4.60	4.10	5.60	5.39
MnO	0.15	0.20	0.10	0.22	0.10	0.17	0.79	0.08	0.13	0.20	0.07	0.14
MgO	1.86	3.16	1.80	3.29	1.79	2.10	1.14	1.70	2.50	4.50	1.30	2.59
CaO	8.29	8.04	5.26	8.95	5.40	6.57	6.73	6.14	8.33	9.10	5.18	6.01
Na ₂ O	5.07	5.60	3.70	4.57	4.74	3.99	4.96	4.78	4.89	2.81	5.15	4.30
K ₂ O	3.27	2.60	3.41	2.80	2.01	3.41	2.69	3.27	3.60	2.10	3.13	3.10
P ₂ O ₅	2.34	0.55	0.01	2.31	0.09	3.13	0.17	0.07	1.84	2.55	1.01	0.09
LOI	2.40	0.31	0.60	0.11	0.04	0.20	0.60	0.07	0.40	0.60	0.70	0.05
Total	100.50	100.46	100.45	100.60	99.80	100.48	99.99	100.51	100.35	99.76	99.93	99.49
K ₂ O/Na ₂ O	0.65	0.46	0.92	0.61	0.42	0.86	0.57	0.68	0.53	0.75	0.60	0.72
Na ₂ O + K ₂ O	8.34	9.20	7.11	7.37	6.85	7.40	7.65	8.05	8.49	4.91	8.28	7.40
MgO/MgO + Fe ₂ O _{3(T)}	0.32	0.50	0.23	0.32	0.23	0.31	0.18	0.23	0.35	0.52	0.19	0.33
Y + Nb	78	74	74	76	68	74	55	58	77	77	60	70
Na + K + 2Ca/Al	1.81	1.66	1.07	1.94	1.13	1.43	1.24	1.29	1.78	1.58	1.12	1.5
NCOR	0.11	0.15	1.25	0.21	1.21	0.24	1.09	1.70	1.68	1.34	1.87	1.33

* = total iron as Fe₂O₃ (T); LOI = loss on ignition; NCOR = normative corundum; CHK1-CHK6 = coarse-grained charnockite; CH7-CHK12 = fine-medium-grained charnockite

calc-alkaline fields (Fig. 2). According to Wilson (1991), this indicates that the magma from which these rocks were formed was calc-alkaline in nature and was totally restricted in occurrence to the subduction-related environment. This, by implication, means that the older granites and the charnockites in the Ado-Ekiti area were derived from a subduction-tectonic environment. Normative values of quartz-albite-orthoclase (Q-Ab-Or) plotted for the porphyritic older granite and the fine-grained older granite showed the rock samples plotting close to the granite minimum point on the liquidus surface and above it (Fig. 3). According to Wilson (1991), igneous rocks whose data plot as discussed above were formed at low H₂O pressure of 1 kb and a temperature of 720 °C. In both the varieties of charnockites, the Na₂O + K₂O/Al₂O₃ ratios were greater than 1 (Table 2), which implies that these rocks were paralkaline in nature (Wilson, 1991). In the older granites (both types), the Na₂O/Al₂O₃ ratios were less than 1, which means that these rocks were not paralkaline granites according to Wilson (1991). Both the varieties of charnockites studied during the present study showed that all the rocks contained Na₂O + K₂O + 2CaO/Al₂O₃ ratios higher than 1, implying that these rocks were not peraluminous in nature, whereas the older granites had Na₂O + K₂O + 2CaO/Al₂O₃

ratios that were less than 1, making the older granites in the Ado-Ekiti area peraluminous granites. According to Wilson (1991), peraluminous granites contain crustal or sedimentary materials in their original magma. The MgO/MgO + Fe₂O_{3(T)} ratios in these rocks (0.30 in the charnockites and 0.06 in the granites) were lower than the mean upper mantle values of 0.70 (Wilson, 1991; Tables 1 and 2). This implies that the original magma of these rocks was not from a purely primitive mantle.

A plot of mol. Al₂O₃ / (Na₂O + K₂O + CaO) versus percent normative corundum for the classification of igneous rocks is shown in Fig. 4. Majority of the charnockites and older granite samples plotted in the S-type field. This type of plot implies that the original magma from which these rocks were formed contained substantial amount of sedimentary or crustal materials with little mantle component as few samples of both rocks plotted in the I-type field. Histogram of mol. (%) Al₂O₃ / (Na₂O + K₂O + CaO) for the charnockites and older granites of the area is drawn in Fig. 5. It was observed that the rock samples plotted in the I-type and S-type fields. However, majority of the charnockite samples plotted in the I-type field, while most of the older granite samples plotted in the S-type field. Nevertheless, few samples of the charnockite plotted in

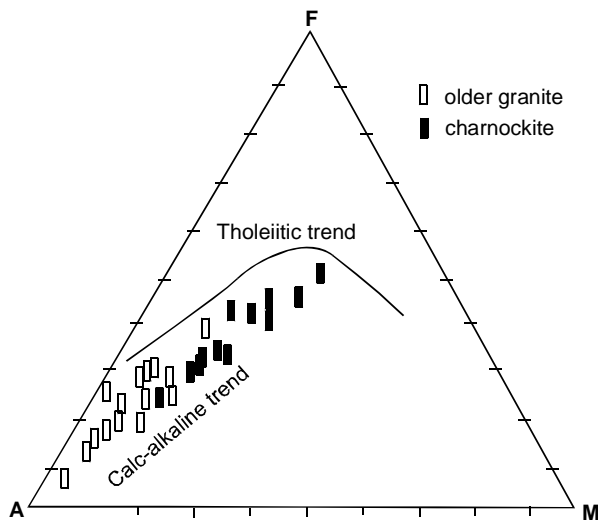


Fig. 2. Aluminium-total iron-magnesium (AFM) diagram showing the tholeiitic and calc-alkaline differentiation trend for the charnockite (CHK) and the older granite (ADG) from the Ado-Ekiti area, Nigeria.

the S-type field and few of the older granite samples plotted in the I-type field (Fig. 5). This implies that while it may be said that the charnockites originated from a mantle source with some crustal or sedimentary contamination in its original magma, the older granites were largely derived from a magma which was highly contaminated by a crustal or a sedimentary source, as is noted in the case of a back arc tectonic setting.

Trace elements. The elements Ba, Rb, Sr were highly concentrated in the charnockites. These elements recorded lower concentrations in the older granites (Tables 3 and 4). This might be due to the presence of more plagioclase in the charnockite, which harbours Ba. Barium also substitutes for K in the biotite in the charnockites and in the older granites. Strontium and rubidium are anomalous in the charnockites due to substitution of these elements for Ca in plagioclase and hornblende, which are abundant in the charnockites but either absent or low in the older granites. The concentrations of Ni, Cr, Co and V though higher in the charnockites than in the older granites, are by far lower than those for rocks that originated from the primitive mantle sources, which are in hundreds of ppm. This suggests again, that the magma of these rocks cannot be from a pure primitive mantle source (cf. Wilson, 1991).

The plot of Y + Nb versus Rb for these rocks shows that the older granites plotted in the volcanic arc granite (VAG)-field (Fig. 6), while the charnockite samples plotted in the 'within plate granite (WPG)-field'. This implies that these rocks were

formed in a volcanic arc tectonic environment, and the movement of plates was important in the generation of their magma.

Rare earth elements (REE). Table 5 shows the REE data for the charnockites and the older granites from the Ado-Ekiti area. The charnockites contained higher absolute REE concentrations than the older granites, which might be due to the presence of high values of light rare earth elements (LREE). This implicates REE concentrating minerals (especially, monazite,

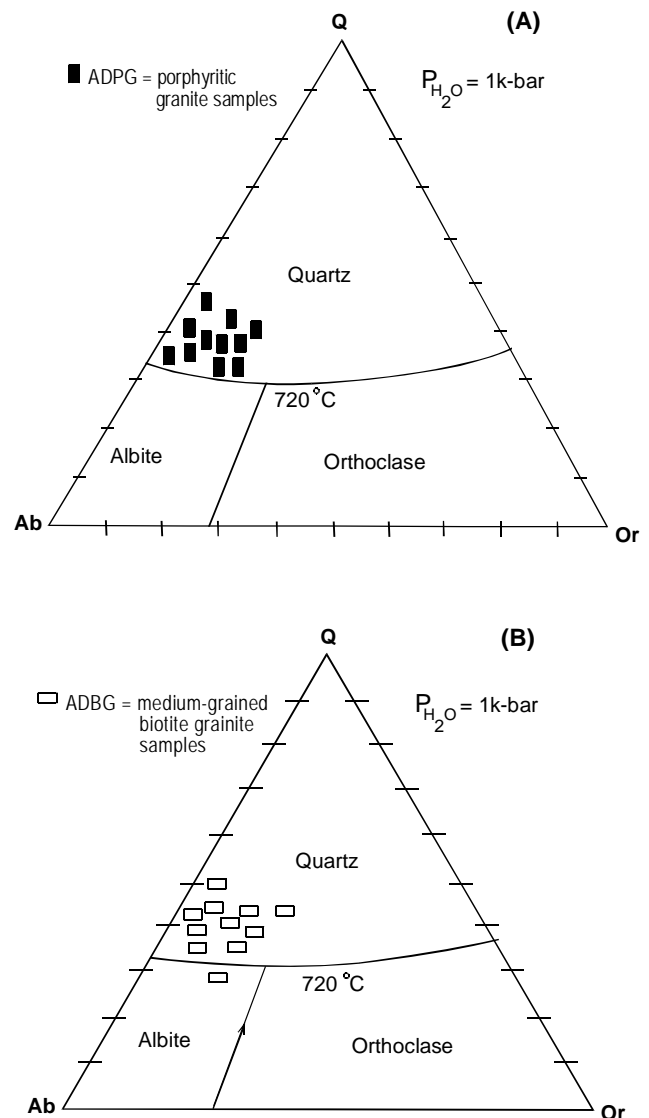


Fig. 3. Normative albite (Ab)-orthoclase-(Or)-quartz (Q)-H₂O system for the: (A) porphyritic granite (ADPG), and (B) biotite granite (ADBG) from the Ado-Ekiti area, southwestern Nigeria (P_{H₂O} = 1k-bar = pressure equivalent of water = 1 kilobar).

which contains LREE in the rocks), indicating that their original magma had crustal input. When the REE values for normalized chondrite were plotted for these rocks (Fig. 7), all showed similar stepped relationship. However, the charnockites showed slightly stepped patterns with very little Eu depletion in the coarse-grained charnockite and relatively marked Eu depletion in the gneissic charnockite variety (Fig. 7). The charnockites contained higher LREE than heavy rare earth elements (HREE) as in the older granites. The older granites showed slightly more marked stepped patterns than the charnockites and more pronounced Eu depletion (Fig. 7), implying higher feldspar fractionation in this rock group than in the charnockites.

The charnokites and the older granites showed negative normalized Eu/Eu^* (ratio of absolute Eu to normalized Eu) anomaly as well as high $(\text{La}/\text{Yb})_N$ ratios. According to Feng

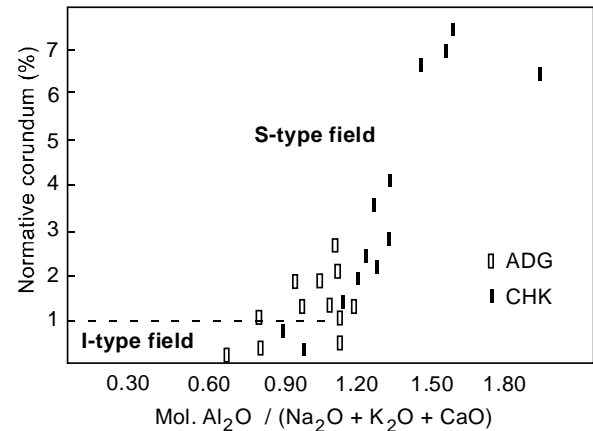


Fig. 4. Normative corundum versus mol. $\text{Al}_2\text{O}_3 / (\text{Na}_2\text{O} + \text{K}_2\text{O} + \text{CaO})$; ADG = porphyritic biotite hornblende Ado-Ekiti older granite; CHK = fine-medium grade charnockite.

Table 3. Chemical data of trace elements (ppm) for representative samples of older granites (ADG1-ADG12) from the Ado-Ekiti area, southwestern Nigeria

	ADG1	ADG2	ADG3	ADG4	ADG5	ADG6	ADG7	ADG8	ADG9	ADG10	ADG11	ADG12
Ba	211	239	251	147	166	236	173	265	272	154	199	153
Ni	10	13	11	9	11	11	10	9	1.0	11	11	11
Cr	8	6	7	8	9	10	11	10	9	8	7	10
V	8	6	5	5	4	10	8	11	9	4	3	10
Co	68	73	70	58	59	72	57	73	71	60	53	50
Rb	182	162	182	190	180	195	185	186	181	174	160	199
Sr	148	183	170	158	159	172	157	172	171	160	167	158
Y	19	19	18	27	23	25	28	22	24	30	30	23
Zr	121	135	113	128	137	148	169	132	131	148	134	161
Nb	8	10	8	19	15	17	16	6	7	16	8	15
Th	42	58	52	29	30	31	32	22	45	34	41	29
Ta	1.93	2.54	3.08	2.85	3.14	1.88	2.18	16	16	12	14	13

Table 4. Chemical data of trace elements (ppm) for representative samples of the charnockite (CHK1-CHK12) from the Ado-Ekiti area, southwestern Nigeria

	CHK1	CHK2	CHK3	CHK4	CHK5	CHK6	CHK7	CHK8	CHK9	CHK10	CHK11	CHK12
Ba	1450	1399	1490	1290	1480	1440	1550	1100	1250	1050	1440	1241
Ni	18	20	24	24	16	24	30	24	29	20	30	34
Cr	11	14	20	16	20	11	26	11	20	29	24	32
V	20	24	26	24	14	24	22	20	40	46	41	24
Co	13	29	30	38	12	18	24	29	34	49	39	42
Rb	165	154	175	153	100	162	180	183	180	147	186	178
Sr	172	187	148	208	239	230	232	193	245	249	298	355
Y	40	42	48	50	24	39	29	26	49	41	31	44
Zr	34	40	56	47	52	46	24	50	54	32	85	75
Nb	38	32	26	26	34	35	26	32	28	36	29	26
Th	17	18	20	15	30	24	23	17	18	17	11	21
Ta	8	9	10	4	5	6	7	9	17	10	4	6

and Kerrich (1990), negative Eu/Eu* anomaly and (La/Yb)_N ratios higher than 5 in an igneous rock are indications of magmatic differentiation. The implication of this for the magma of the charnockites and the older granites here is that even though the magma might have originated from a mixed source (mantle and crust), differentiation was important in the formation of these rocks.

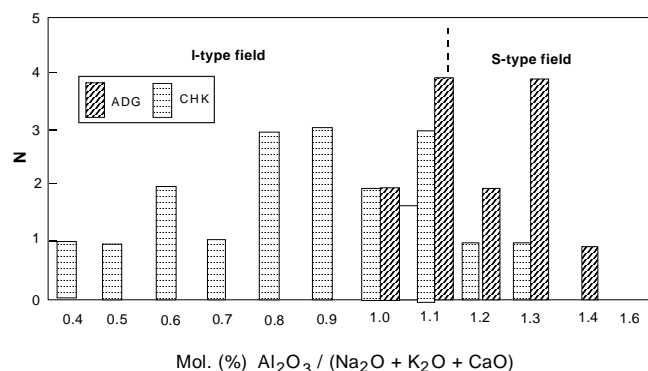


Fig. 5. Histogram of mol. (%) Al₂O₃/(Na₂O + K₂O + CaO); CHK = charnockite samples; ADG = Ado-Ekiti older granite; methods of classification of igneous rocks after Vivallo and Rickard (1990); N = frequency; bar value is 2 on N column.

Conclusion. The geological, petrological and geochemical results described here revealed that the charno-ckites and the older granites were genetically related and were formed in the same environment. Presence of monazite in the mineralogy of the charnockites and the older granites from the Ado-Ekiti area indicated crustal or sedimentary input into the original magma of these rocks. The AFM plot (Fig. 2) for both the rocks

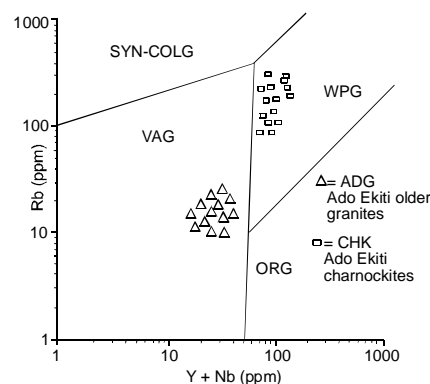


Fig. 6. The Y + Nb versus Rb discrimination diagram for the Ado-Ekiti charnockite (CHK) and older granites (ADG); SYN-COLG = syn-collision granite; ORG = ocean ridge granite; WPG = within plate granite; VAG = volcanic arc granite (after Pearce *et al.*, 1984).

Table 5. Data (in ppm) of absolute rare earth elements (REE) for the charnockites and the older granite from the Ado-Ekiti area, southwestern Nigeria

Elements	CHK(1)	CHK(2)	CHK 2	ADK (1)	ADK(2)	ADK (2)
La	520	750	580	400	280	320
Ce	840	1240	980	280	220	230
Br	87	130	110	200	180	170
Nd	300	455	365	160	110	120
Sm	36	60	40	60	40	50
Eu	12	9	9	20	15	15
Gd	37	26	22	25	20	20
Dy	12	22	14	10	10	10
Ho	2	4	3	6	8	6
Er	6	10	6	8	5	6
Yb	3	6	3	2	2	2
Lu	0.40	0.80	0.50	0.20	0.20	0.20
Total	1855.40	2712.80	2132.50	181.20	930.21	949.21
LREE	1795	2644	2084	1150	885	905
HREE	60.40	68.80	48.50	51.20	45.21	44.21
LREE/HREE	29.72	38.43	43.96	22.07	19.58	20.47
Eu/Eu*	0.36	0.34	0.35	0.24	0.22	0.20
(La/Yb) _N	91	132	122	129	115	117

HREE = heavy rare earth elements; LREE = light rare earth elements; Eu/Eu* = normalised Eu/Eu* anomaly (ratio of absolute Eu to normalized Eu); (La/Yb)_N = normalised La/Yb; CHK(1) = coarse charnockite; CHK(2) = gneissic charnockite; ADK(1) = porphyritic hornblende-biotite granite; ADK(2) = medium-grained biotite granite

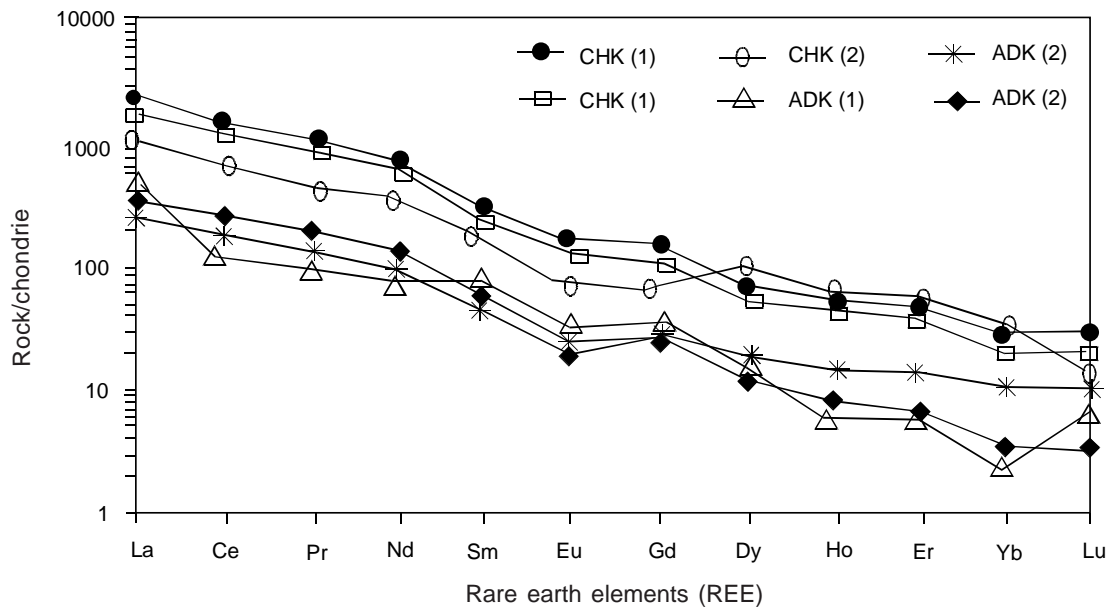


Fig. 7. Chondrite normalised rare earth elements (REE) patterns for the charnockite and older granites from the Ado-Ekiti area, southwestern Nigeria; CHK (1) = coarse-grained charnockite; CHK (2) = fine medium-grained gneissic charnockite; ADK (1) = porphyritic biotite hornblende older granite; ADK (2) = medium grained biotite older granite.

revealed that these rocks were calc-alkaline, typical of a subduction tectonic environment. The percentage corundum versus mol. $\text{Al}_2\text{O}_3/(\text{Na}_2\text{O} + \text{K}_2\text{O} + \text{CaO})$ and the histogram of molecular (%) $\text{Al}_2\text{O}_3/(\text{Na}_2\text{O} + \text{K}_2\text{O} + \text{CaO})$ indicated that the charnockites and the older granites were derived from a mixed source of crustal and mantle materials. The Y + Nb versus Rb discrimination plot for both the rocks showed that these rocks were derived from a volcanic arc and 'within plate tectonic environments'. The charnockites and the older granites from the Ado-Ekiti area contained high REE, indicating REE concentrating minerals, especially the LREE, whose hosts are known to be crustal in origin. The similarity in patterns of the normalised $(\text{La}/\text{Yb})_N$ and Eu/Eu^* data for both rocks (charnockites and older granites), indicated that feldspar fractionation and magmatic differentiation were responsible for the formation of these rocks. Generally, the geochemistry of these rocks did not implicate either a purely mantle or crustal source, exclusively. Rather, the geology, petrology and geochemistry implicated a mixed magmatic source of subduction-type geotectonic environment. This type of environment is most likely to be the one in which an ocean slab (with crustal materials) had been subducted into the mantle as in a back arc environment.

Acknowledgement

The authors wish to acknowledge the technical assistance extended by Dr. J. N. Walsh of the Department of Geology,

Royal Holloway and Bedford New College, University of London, Surrey, UK for analysing rock samples for rare earth elements. Thanks are due to Dr. G. M. Steed, Department of Earth Sciences, University of Cardiff, Wales, UK, who read the initial draft of this manuscript and offered useful suggestions.

References

- Akande, S.O. 1991. Geological setting and evolution of vein gold deposits in the Nigerian schist belts (poster presentation) Brazil Gold '82, E. A. Ladeira (ed.), pp. 257-260, Balkema, Rotterdam.
- Annor, A.E. 1995, U-Pb zircon age for Kabba-Okenne granodiorite gneiss; implication for Nigeria's basement chronology. *African Geoscience Review* **2**: 101-105.
- Dada, S.S., Lancelot, J.R., Briquia, I. 1989. Age and origin of the annular charnockite complex at Toro, northern Nigeria; U-Pb and Rb-Sr evidence. *J. Afric. Earth Sci.* **2**: 227-234.
- Ekwueme, B.N. 2003. *The Precambrian Geology and Evolution of the Southeastern Nigerian Basement Complex*, University of Calabar Press, Calabar, Cross River State, Nigeria.
- Falconer, J.D. 1911. *The Geology and Geography of Northern Nigeria*, Macmillan, London, UK.
- Feng, R., Kerrich, R. 1990. Geochemistry of fine grained clastic in Archean Abitibi Green-Stone belt, Canada; impli-

- cation for provenance and tectonic setting. *Geochimica et Cosmochimica Acta* **54**: 1061-1081.
- Odeyemi, I.B. 1981. A review of the orogenic events in the precambrian basement of Nigeria. *West Africa Geology Rundsch* **70**: 897-909.
- Olarewaju, V.O. 1988. Petrology and geochemistry of the charnockite and associated granitic rocks of Ado-Ekiti Akure, S.W. Nigeria-I. *Precambrian Geology of Nigeria*, P.O. Oluyide (co-ordinator), pp. 129-143, Geology Survey of Nigeria Publications, Lagos, Nigeria.
- Olarewaju, V.O. 1987. Charnockite-granite association in SW Nigeria, Rrapakivi granite type and charnockite plutonism in Nigeria. *J. Africa Earth Sci.* **6**: 67-77.
- Pearce, J.A., Harris, N.W., Tindle, A.G. 1984. Trace element discrimination diagrams for tectonic interpretation of granite rocks. *J. Petrology* **25**: 956-983.
- Rahaman, M.A., Ajayi, T.R., Oshin, I.O., Asubiojo, F.O.I. 1988. Trace element geochemistry and geotectonic setting of Ile-Ife schist belt. In: *Precambrian Geology of Nigeria*, P.O. Oluyide (co-ordinator), pp. 241-256, Geology Survey of Nigeria Publications, Lagos, Nigeria.
- Tubosun, J.R., Lancelot, J.R., Rahaman, M.A., Ocan, O. 1984. U-Pb Pan-African ages of two charnockite-granite association from southwestern Nigeria: contribution. *Mineral Petrol.* **88**: 188-195.
- Vivallo, W., Rickard, D. 1990. Genesis of an early proterozoic zinc deposit in high grade metamorphic terrain, Saxberget, central Sweden. *Econ. Geol.* **85**: 714-736.
- Walsh, J.N., Buckley, F., Baker, J. 1982. Simultaneous determination of the rare earth elements in rocks using inductively coupled plasma source spectrometry (ICPSS). *Chemical Geology* **33**: 141-153.
- Wilson, M. 1991. *Igneous Petrogenesis, A Global Tectonic Approach*, pp. 227-241, second impression, Harper Collins Academy, New York, USA.
- Woakes, M., Ajibade, C.A., Rahaman, M.A. 1987. Some metallogenic features of the Nigeria basement. *J. Afric. Earth Sci.* **5**: 655-664.

Effect of Excess Metal Concentration on the Extraction Potential of Di-(2-Ethylhexyl) Phosphoric Acid

A. S. Ahmed*, M. B. Bhatti, M. T. Saeed and S. K. Afridi

Glass and Ceramics Research Centre, PCSIR Laboratories Complex, Ferozepur Road, Lahore-54600, Pakistan

(received April 19, 2005; revised August 30, 2006; accepted September 2, 2006)

Abstract. The extraction potential of di-(2-ethylhexyl) phosphoric acid (DEHPA) in kerosene increases manyfold on loading calcium into the organic phase before equilibration with aqueous copper feed. The control of pH was unnecessary in the range from pH 5.0 to pH 3.0. It was found that copper can easily replace nickel, sodium and calcium in the organic phase because of the difference in the dissociation constants of copper and other metals studied. The hydrolysis of calcium maintains the pH of the aqueous phase in favour of higher extraction of copper by DEHPA.

Keywords: dissociation constant, di-(2-ethylhexyl) phosphoric acid, copper extraction

Nomenclature

A⁻ = anions in the aqueous phase

CaR₂ = calcium-DEHPA complex

H⁺ = free hydrogen ions

HR = concentration of organic acidic extractant

OH⁻ = hydroxyl ions

M²⁺, X²⁺ = free metal ions (M²⁺ refers to free metal ions of low dissociate constants, while X²⁺ refers to free metal ions of high dissociate constants)

MR₂, XR₂ = concentration of metals in the organic phase

R⁻ = dissociated ions of extractant

XA = concentration of metal salt in the aqueous phase

Introduction

Hydrometallurgical operations using di-(2-ethylhexyl) phosphoric acid (DEHPA) for the extraction of copper have been reported to give lower loadings, as compared with the more expensive second generation extractants (Borowiak-Resterna and Lenarcik, 2004; Cox, 1992; Yoshizuka *et al.*, 1990), such as LIX 864, 865, 984, 622, P5100, 5300, PT5050, SME529, ABF2, and OMG. A number of authors have tried to improve extraction with DEHPA by studying various factors, such as concentration of solvent and solute, effect of pH, influence of sulphate and chloride ions, and the nature of diluents (Cerpa and Alguacil, 2004; Saeed and Jamil, 1998; Ahmed *et al.*, 1994). The principal objective in the application of solvent extraction process is to minimize the control of influencing factors on the separation of competing metals and hence to attain maximum loading of the desired metal in the organic phase.

In order to improve the extraction potential of DEHPA, some researchers (Ajawin *et al.*, 1983; Joe *et al.*, 1966) have used

*Author for correspondence; E-mail: drrashid_azri@yahoo.com

sodium or ammonium salts of DEHPA. The presence of sodium or ammonium ions suppresses the ionization of the metal hydroxide and increases the metal loadings of the organic phase. However, in most cases, a third phase is formed (Ajawin *et al.*, 1983), which reduces the concentration of the metal in the extract phase.

In the present study, a series of experiments were conducted to find out the most suitable metal to form a metal salt of DEHPA that can be employed to achieve maximum extraction. Apropos to this, a number of metal hydroxides, such as sodium hydroxide, calcium hydroxide and nickel sulphate, were initially contacted with DEHPA to make a metal-DEHPA complex before equilibrating it with the aqueous phase. The presence of metal iron in the form of metal-DEHPA complex in the organic phase increased the total metal ions concentration in the equilibrated phases, as compared to the anion concentration in the system. At equilibrium, the exchange of competing metal ions in the aqueous phase was elucidated in the light of much less considered dissociation constants of these metals involved in the process. Other factors, such as concentrations of the solvent and solute and pH of the aqueous phase, were also considered to describe the present process.

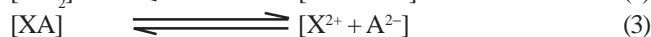
Theoretical background. The extraction of metal ions from the aqueous phase by DEHPA in the organic solute has been shown to conform to the following general equation (Ahmed *et al.*, 1994; Rydberg and Serine, 1992):



This is an ion exchange reaction and the final equilibrium depends on dissociation and distribution constants of the various species in the system. The release of hydrogen ions decreases pH of the aqueous solution causing the formation

of non-extractable metal species (Saeed and Jamil, 1998; Yoshizuka *et al.*, 1990), while protonation of the extractant in the aqueous phase results in a very low distribution constant of the metal species (Ahmed *et al.*, 1998; Ritcey and Ashbrook, 1984).

Now, consider a metal M^{2+} forming a metal-DEHPA complex (MR_2) in the organic phase, which is equilibrated with an acidic aqueous solution containing a divalent metal X^{2+} and anions A^{2-} . The reaction mechanism in the aqueous phase may be described by the following equations:



The amount of metal ions ($X + M$) in the system exceeds the stoichiometric proportion of anions A^{2-} . The condition of electrical neutrality in the aqueous phase at pH 4.29 requires that the metal ions can only be equal to the anions in the aqueous phase. Therefore, the excess metal (X or M) transfers into the organic phase and remains there in undissociated form. The condition of electrical neutrality in the aqueous phase requires that:

$$2[X^{2+}] + 2[M^{2+}] + [H^+] = 2[A^{2-}] + [OH^-] \quad (6)$$

The pH of the aqueous phase is 4.29, thus the total concentration of hydrogen and hydroxyl ions can be neglected as compared to total cations and anions. Therefore, equation (6) may be simplified as:

$$2[X^{2+}] + 2[M^{2+}] = [A^{2-}] \quad (7)$$

The amount of metal, in excess, is equal to the total metal in the system minus anions. Therefore, this excess metal will remain in undissociated form in the organic phase so as to maintain electrical neutrality in the aqueous phase. The distribution constant of the undissociated complex has been reported to be very high (Marcus and Kertes, 1969). In the present study, the M^{2+} ions (calcium, sodium, or nickel) chosen had a higher dissociation constant than that of X^{2+} ions (copper). Therefore, M^{2+} ions will be more in the dissociated form and remain in the aqueous phase allowing X^{2+} ions to be extracted into the organic phase.

It is clear from these facts that the exchange of two metals between the organic and aqueous phases depends on their dissociation and distribution constants of their undissociated species formed with DEHPA. Moreover, this process enhances the extraction potential of DEHPA manyfolds because of the presence of a large amount of metal species as compared to anions in the system.

Materials and Methods

To determine the extractability of DEHPA, a series of tests were carried out which can be divided into two groups. The first set of experiments was conducted with DEHPA diluted in kerosene as a solute. In each case, 50 ml of the organic phase was equilibrated with 50 ml of aqueous copper solution of varying pH in 200 ml bottles. The bottles were shaken continually for 30 min at room temperature to ensure complete equilibrium. Equilibrated phases were allowed to be disengaged and the aqueous phase was withdrawn for analysis. The concentration of metal ions was analysed using Spectronic-20 spectrophotometer. The pH of the aqueous phase was measured with Toptronic pH meter. The concentration of metal ions in the organic phase was obtained by difference. To ensure the accuracy of the analysis, the organic phase was stripped with 1 N sulphuric acid and analysed for copper concentration.

The second set of experiments was performed with nickel-DEHPA, sodium-DEHPA and calcium-DEHPA complexes. The experimental procedures were the same as adopted in the first set of experiments. The analysis technique used for copper, nickel, calcium and sodium was described earlier (Ahmed *et al.*, 1989). The concentration of metals in the aqueous phase was analyzed spectrophotometrically.

All the chemicals used in the present investigation were of reagent grade (E. Merck), except kerosene. Commercial kerosene was washed with distilled water to remove colour or any other impurities and centrifuged prior to its use.

Results and Discussion

The influence of pH on the extraction of copper ions solely with DEHPA and with various metal complexes of DEHPA in the organic diluent kerosene are shown in Fig. 1 and Fig. 2. The **curve-1** (Fig. 1) depicts that copper and sulphate ions are in stoichiometric proportion, giving a very low distribution constant of copper for the system. It is evident from equation (1) that for every mole of copper extracted into the organic phase, 2 moles of H^+ ions are released into the aqueous phase to maintain electrical potential of the system. So, in this system, one of the parameters that controlled the reaction was the acid contents (H^+ ions) of the aqueous phase. At pH 4.29 of the aqueous solution, copper extracted was 0.165 g/l from the total feed concentration of 3.0 g/l copper with 0.1 M DEHPA. The **curve-2** shows an improvement in the extraction of copper from 3.0 g/l copper solution of pH 4.29 with 0.1 M nickel-DEHPA complex. The total metal ions present in the system were in excess of the stoichiometric amount of sulphate ions. The dissociation constant of the nickel-complex is

higher than the copper complex, therefore, some of the nickel-DEHPA complex dissociates in the aqueous phase and nickel is replaced by copper to form copper-DEHPA complex in the aqueous phase. The copper-DEHPA complex was extracted into the organic phase because of the low dissociation constant of copper. The release of H^+ ions in this system was much less than that of the results given in **curve-1** (Fig. 1), hence, resulting in a favourable pH of the aqueous phase to give higher extraction of copper as illustrated in **curve-2** (Fig. 1). The loading of copper in the organic phase was 0.182 g/l for this system, which was better than the results illustrated in **curve-1** (Fig. 1).

These results confirm the presented theory that as the amount of excess metal in the system increased, the amount of copper extracted in the organic phase also increased. This exchange of two metals between the organic and aqueous phases is the result of dissociation constants and distribution constants of their undissociated species formed with DEHPA.

Considering the above findings, metal hydroxides of calcium and sodium were chosen because they have much higher dissociation constants as compared to copper. The extraction of copper from the aqueous phase with calcium or sodium complexes of DEHPA is illustrated in Fig. 2. The curves in Fig. 2 illustrate significantly higher extraction potential of DEHPA as compared to the results presented in Fig. 1.

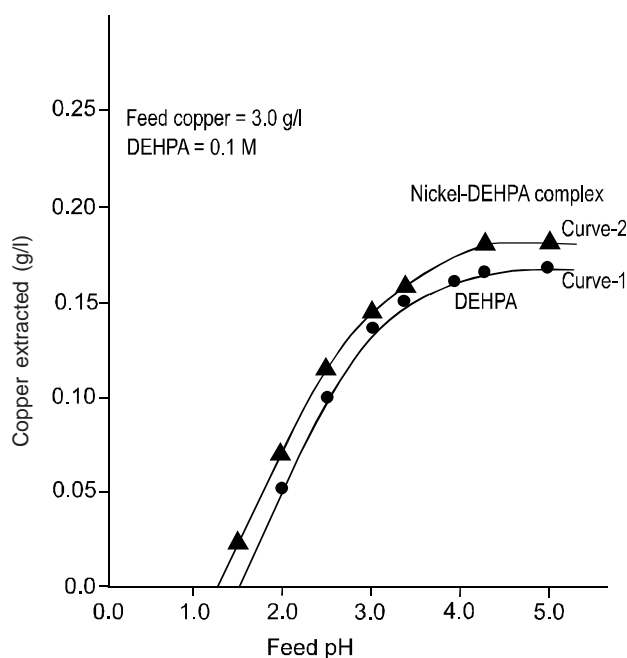


Fig. 1. Extraction of copper with di-(2-ethylhexyl) phosphoric acid (DEHPA) and nickel-DEHPA complex.

It was found that sodium concentrations in 0.1 M DEHPA can be increased upto 20 g/l. However, theoretically, 0.1 M DEHPA can only load metal ions equivalent to its molar concentrations, whereas sodium ions present in the organic phase were almost nine times higher. The higher concentration is attributed to the ability of kerosene to dissolve sodium hydroxide solution, as such, which consequently results in an increase in the volume of the organic phase. Moreover, the sodium-DEHPA complex formed, presumably had very low concentration. The higher concentrations of excess metal in the system improved the extraction of copper as compared to the results given in **curve-1** and **curve-2** (Fig. 1). Copper extracted was 1.080 g/l from the total metal concentration of 23 g/l (3 g/l copper + 20 g/l sodium) in the system with the DEHPA concentration of 0.1 M. Moreover, the third phase was not observed under the present conditions of the system.

The influence of calcium ions, as an excess metal in the system, is also shown in Fig. 2. The results indicate that calcium had a greater effect on the extraction of copper than any other metal studied. Copper extracted was 2.12 g/l from the total metal concentration of 4.64 g/l (3.0 g/l copper + 1.64 g/l calcium) with the DEHPA concentration of 0.1 M. This is an increase of 1.955 g/l, 1.938 g/l and 1.04 g/l over the results reported in **curve-1** and **curve-2** (Fig. 1) for solely DEHPA and nickel-DEHPA complex and the sodium-DEHPA curve in Fig. 2, respectively, under similar conditions.

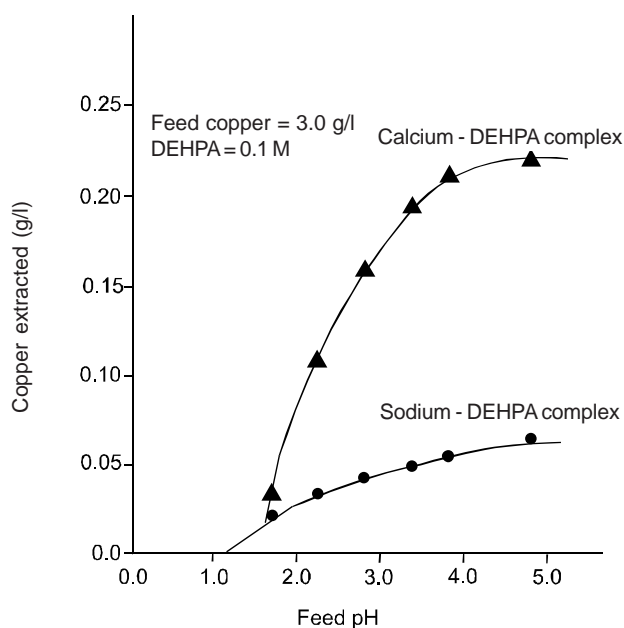


Fig. 2. The effect of excess metal on the equilibrium distribution of copper, using calcium and sodium-di-(2-ethylhexyl) phosphoric acid (DEHPA) complexes.

These results prove that the introduction of calcium ions as an excess metal in the organic phase improves the extraction potential of DEHPA as compared to the other metals examined. Therefore, a series of distribution data was obtained to investigate the influence of other salient parameters on the extractability of DEHPA. These salient parameters were pH, concentrations of DEHPA and copper, solvent losses, and solubility of DEHPA in the aqueous phase.

The extraction of copper from 1 g/l to 5 g/l copper in the aqueous feed solution at pH 4.29, with calcium-DEHPA complex, is shown in Table 1. The results show that the extraction of copper did not increase proportional to its increase in concentration in the aqueous feed solution. It is attributed to the release of large sulphate ions into the aqueous phase which are associated with copper salt, since 1 g of copper is associated with 1.511 g of sulphate ions as given in Table 1. In 1 g/l copper in the aqueous feed solution having total metal ions concentration of 3.36 g/l (2.36 g/l calcium), the concentration of sulphate ions was less than half, i.e., 1.511 g/l. It resulted in giving a distribution coefficient of 1.179. As the concentration of aqueous copper feed solution increased to 5 g/l, the concentration of associated sulphate ions also increased to 7.554 g/l in the system. The sulphate ions were thus more than the total concentration of metal ions (5 g/l copper + 2.36 g/l calcium) resulting in a very low distribution coefficient of 0.414. This trend is evident from Table 1 for the other concentrations of copper, i.e., 2 g/l, 3 g/l and 4 g/l.

Moreover, the results given in Table 1 show that 0.5 M DEHPA carries only 1.818 g/l to 2.155 g/l total metal (0.053 M copper + 0.037 M calcium). If the extracted complex is represented by XR_2 , according to equation (1), then it would appear that only a small proportion of DEHPA molecules is directly involved in the formation of metal complex. This shows that the process demanded further contacts of the loaded extract phase with fresh copper feed to involve all molecules of DEHPA for maximum extraction of metal ions from the aqueous feed.

The results given in Table 2 give feed pH, equilibrium pH, sulphate ions added, and distribution of copper and calcium in the conjugate phases at equilibrium. The influence of sulphate ions becomes more evident on the extraction capacity of DEHPA as shown in Table 2. The concentration of sulphate ions was increased by the addition of sulphuric acid, whereas concentration of total metal (copper + calcium) ions was kept constant. The distribution of both metals decreased as the concentration of sulphate ions increased. It is due to excess sulphate ions in the aqueous phase. These excess sulphate ions function as coordinating ligands (Marcus and Kertes, 1969; Joe *et al.*, 1966) and compete with DEHPA for

the metal ions resulting in reduced extraction of metal by DEHPA.

The results in Table 2 show that change in the feed pH from 4.29 to 3.40 gives almost the same distribution of copper for 5 g/l copper feed solution extracted with 0.5 M Ca-DEHPA complex. Similarly, an increase in pH to 5.0 by the addition of sodium hydroxide gives the same distribution of copper. The pH of the aqueous feed solution reduces the extraction of copper as shown in Fig. 1, Fig. 2 and Table 2. The extraction of copper at pH 4.29 was 0.995 g/l, and at pH 1.50 it reduced to only 0.165 g/l. This shows that the effect of pH on the extractability of DEHPA was more profound at the pH values lower than 2.0.

Another interesting fact emerging from Table 2 is that the pH of the aqueous phase, after achieving equilibrium, was higher than that of the aqueous feed pH. This increase of pH of the equilibrated aqueous phase may be explained by considering the following reactions occurring in the aqueous phase:

Table 1. Distribution of copper and calcium in the equilibrated phases*

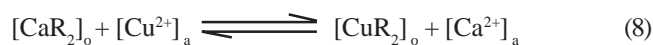
Total copper (g/l)	Associated SO_4^{2-} ions (g/l)	Organic phase		Aqueous phase		Distribution coefficient
		copper (g/l)	calcium (g/l)	copper (g/l)	calcium (g/l)	
1	1.511	0.338	1.480	0.662	0.88	1.179
2	3.022	0.500	1.385	1.500	0.975	0.762
3	4.533	0.650	1.325	2.350	1.035	0.583
4	6.043	0.800	1.263	3.200	1.097	0.480
5	7.554	0.995	1.160	4.005	1.200	0.414

* = calcium = 2.36 g/l; di-(2-ethylhexyl) phosphoric acid (DEHPA) = 0.5 M; feed pH = 4.29

Table 2. Effect of sulphate ions on the extraction of copper*

Feed pH	Equilibrium pH	Added SO_4^{2-} ions (g/l)	Organic phase		Aqueous phase	
			copper (g/l)	calcium (g/l)	copper (g/l)	calcium (g/l)
4.29	4.16	-	0.995	1.160	4.005	1.200
3.40	4.10	0.017	0.960	1.092	4.040	1.268
2.50	3.79	0.149	0.750	1.088	4.250	1.272
2.00	3.50	0.478	0.472	1.015	4.528	1.345
1.50	2.89	0.518	0.165	0.900	4.835	1.460
5.00	4.15	-	0.995	1.150	4.005	1.210

* = di-(2-ethylhexyl) phosphoric acid (DEHPA) = 0.5 M; feed copper = 5 g/l; calcium = 2.36 g/l



These equations show that a large number of calcium ions are transferred to the aqueous phase as is also evident from Table 1. These calcium ions hydrolyse and consequently increase or maintain pH of the aqueous phase (Sato *et al.*, 1977). It is also apparent from these equations that calcium ions have higher dissociation constant and are suitable to replace copper by an ion exchange mechanism.

It has been reported (Cox, 1992; Yoshizuka *et al.*, 1990; Korodosky *et al.*, 1987) that Salicylaldoxime (strong copper extractant) as in higher series, and Ketoxime (moderate copper extractant) LIX65N, SME 529, OMG and ABF 2 are widely used extractants for extraction purposes. Ketoxime can load upto 5.0 g/l copper at about 20% concentration in kerosene, however, this resulted in viscous, hard to handle, organic phase. The salicylaldoxime shows very high distribution constant but is sparingly soluble in the aqueous phase showing excessive losses. However, the results presented for the extraction of copper with DEHPA show high extraction without becoming viscous, and the losses by evaporation or absorption in the aqueous phase are minimal which agree with earlier findings (Cox, 1992; Joe *et al.* 1966).

It is evident from the results given in Tables 1 and 2 that the extraction potential of DEHPA was greatly influenced by the presence of excess metal. The added metal ions remained in the organic phase and can be replaced by repeated contact of the organic phase with fresh feed. It will obviously give higher loadings of only copper ions in the extract phase. In other words, the real benefit of the cheap DEHPA may be achieved by the addition of excess metal in the system and by using multistage extraction process.

Conclusion

The overall distribution of metal ions depends on the amount of total metal concentration and total anions present in the system. The pH of the aqueous phase may be unnecessary to control when using this process. The number of extraction stages in a mixer-settler would be reduced due to quick exchange of metal ions by this process.

References

- Ahmed, A.S., Shaheen, M.Y., Hussain, L., Chaudhry, A.B. 1989. Dissociation aspects in solvent extraction of metals. *Pak. J. Sci. Ind. Res.* **32**: 507-509.
- Ahmed, A.S., Ahmad, S., Akram, A., Jamil, M. 1994. Experimental and theoretical studies of solvent extracton of copper(II) with di-(2-ethylhexyl) phosphoric acid. *Pak. J. Sci. Ind. Res.* **37**: 71-76.
- Ahmed, A.S., Ahmad, S., Jamil, M., Shaheen, M.Y. 1998. Effect of sulphate ions on the extraction of zinc ions. *J. Pak. Inst. Chem. Engrs.* **27**: 29-32.
- Ajawin, L.A., Perez de Ortiz, E.S., Sawistowski, H. 1983. Extraction of zinc by di-(2-ethylhexyl) phosphoric acid. *Chem. Engg. Res. Design* **61**: 62-65.
- Borowiak-Resterna, A., Lenarcik, B. 2004. Effect of the alkyl chain length in N,N-dialkylpyridine-3-carboxamides upon their extraction of copper(II) from aqueous chloride solutions. *Solvent Extraction and Ion Exchange* **22**: 913-931.
- Cerpa, A., Alguacil, F.J. 2004. Separation of cobalt and nickel from acidic sulfate solutions using mixtures of di-(2-ethylhexyl) phosphoric acid (DP-8R) and hydroxyoxime (ACORGA M5640). *Chem. Technol. Biotechnol.* **79**: 455-460.
- Cox, M. 1992. Solvent extraction in hydrometallurgy. In: *Principles and Practices of Solvent Extraction*, J. Rydberg, C. Musikes, G.R. Choppin (eds.), pp. 357-412, Marcel Dekker, Inc., New York, USA.
- Joe, E.J., Ritcey, G.M., Ashbrook, A.W. 1966. Uranium and copper extraction by liquid ion exchange. *J. Metals* **18**: 18-21.
- Korodosky, G.A., Olafson, S.M., Lewis, R.G., Deffner, V.L. 1987. State-of-the-art discussion on the solvent extraction reagents used for the recovery of copper from dilute sulphuric acid leach solutions. *Separation Sci. Technol.* **22**: 215-232.
- Marcus, Y., Kertes, A.S. 1969. *Ion Exchange and Solvent Extraction of Metal Complexes*, pp.169-175, Wiley-Interscience, London, UK.
- Ritcey, G.M., Ashbrook, A.W. 1984. *Solvent Extraction*, pp. 82-89, Elsevier Scientific Publishing Co., New York, USA.
- Rydberg, J., Sekine, T. 1992. Solvent extraction equilibria. In: *Principles and Practices of Solvent Extraction*, J. Rydberg, C. Musikas, G.R. Choppin (eds.), pp. 101-156, Marcel Dekkar, Inc., New York, USA.
- Saeed, M.T., Jamil, M. 1998. Modelling of zinc stripping from its loaded di-(2-ethylhexyl) phosphate complex with acidic solution. *Bangladesh J. Sci. Ind. Res.* **33**: 397-399.
- Sato, T., Ikoma, S., Nakamura, T. 1977. The extraction of vanadium(IV) from hydrochloric acid solution by long-chain alkyl amine and alkyl amononium compound. *J. Inorg. Nucl. Chem.* **39**: 395-399.
- Yoshizuka, K., Arito, H., Baba, Y., Inoue, K. 1990. Equilibria of solvent extraction of copper(II) with 5-dodecyls-allylaldoxime. *Hydrometallurgy* **23**: 247-261.

Evaluation of Locally Available Fuller's Earth for the Bleaching of Soybean Oil

M. Sharif Nizami* and M. Iqbal Chaudhry

PCSIR Laboratories Complex, Ferozepur Road, Lahore-54600, Pakistan

(received February 4, 2005; revised June 24, 2006; accepted June 27, 2006)

Abstract. Locally available Fuller's earth was investigated for bleaching soybean oil. Investigations showed that raw earth samples possessed desirable physical properties and consisted of the clay minerals suitable for bleaching edible oils. The Fuller's earth sample was also activated by refluxing with 4 N hydrochloric acid for 3 h at 100 °C. Fresh volumes of soybean oil were bleached with 3% of the activated earth and its bleachability was determined by Lovibond tintometer. The efficiency of bleachability was compared with that of Tarana Optimum, the standard bleaching earth of German origin for comparison. It was found that bleachability of the activated earth samples and that of Tarana Optimum was quite comparable.

Keywords: oil bleachability, Fuller's earth, soybean oil, Fuller's earth activation

Introduction

Impurities resulting from the raw material breakdown, or oxidation, impart undesirable colouration to edible oils, which is therefore required to be bleached during the refining process, (Hamilton and Bhatti, 1980). Activated charcoal and earths of specific nature are commonly utilized for this purpose. However, the latter being low cost materials are economically very attractive and popular (Brady *et al.*, 1997; Mahatta, 1985). Fuller's earth, the most important among these, is widely used on account of its low cost. In addition to the cost factor, it has large surface area and possesses the desirable adsorptive properties (Worral, 1986). Several researchers, due to this reason, have studied and attempted to activate such type of earths/clays for their optimum utilization as edible oil bleaching agents.

Theng and Wells (1995) investigated naturally occurring acid clays of hydrothermal geological formation from New Zealand and found that these were rich in Allophase, Halloysite, Kaolinite and Montmorillonite. They reported, as a result of their studies, that decolourizing capacity decreased in the order Halloysite > Kaolinite > Montmorillonite > Allophase. They also found that the naturally acid leached clays were more effective and required only minor treatment with HCl for optimizing their performance regarding decolourizing properties. Two activated clays, one imported and the other of Brazilian origin, were studied by Cardello *et al.* (1995), who reported that these were equally effective for bleaching the vegetable oil of *Gossypium hirsutum* (cotton). Similarly, a patent was registered in Germany (Haehn and Eisgruber, 1995) showing the importance of Fuller's earth in view of bleachability of

edible oils. It involved the regeneration of the used oil-containing bleaching clays through different steps, such as, decolourization by extraction with a suitable solvent, thermal treatment at 500-650 °C upto 5 h in oxidizing atmosphere, without disturbing the Montmorillonite contents, and treatment with an aqueous acid solution (15-50%) at acid : clay ratio of 0.2-2 : 100.

As Pakistan imports large quantities of bleaching earths for the vegetable oil refining industry, efforts have been made to explore, investigate and activate the locally available earths that have oil bleachability potential. A preliminary attempt was made to achieve the objective by Bogue under the Soil Survey of Pakistan (GSP-GSU, 1962). He investigated a small deposit at Thano Bulla Khan in the Sindh province of Pakistan and determined its chemical composition. Later on, a huge deposit of Fuller's earth was explored in Dera Ghazi Khan district of the Punjab province of Pakistan. Yousaf *et al.* (1989) investigated the deposit physicochemically upto some extent, and reported it to be promising if studied further and activated properly. This source has been, therefore, further investigated for its utilization for bleaching edible oils, which is reported here.

Materials and Methods

Fuller's earth samples. Sixteen samples, belonging to the Dera Ghazi Khan deposit, obtained from four different sites (four replicate samples from each) were selected for the present investigations.

Cation exchange capacity. Since the cation exchange capacity (CEC) of minerals may vary with several factors, it can be exactly comparable only if the values are obtained by the same

*Author for correspondence; E-mail: pcsir@brain.net.pk

standard procedure. Therefore, CEC for all the investigated earth samples was determined. The CEC value of these samples was determined by adding 100 ml of 1 N ammonium acetate to 10 g of the earth sample contained in 500 ml beaker, stirred well and allowed to stand overnight at room temperature. The suspension was filtered through Whatman # 44 filter paper, collecting the filtrate in one litre volumetric flask. The procedure was repeated five times. 200 ml aliquot from this extract was evaporated on waterbath, dried on hotplate, and ignited in a muffle furnace at 1000 °C. To the residue was added 50 ml of 0.05 N HCl when cold, warmed gently, and left to stand for 1 h. The excess acid was titrated with 0.05 N sodium hydroxide and the CEC value was calculated in terms of milliequivalents/100 g by applying the specific formula as reported earlier (Yousaf *et al.*, 1989).

Swelling index. Samples were dried at 100 °C for one h, pulverized to 100 mesh (USS), and then added to 100 ml Nessler's tubes. Their volumes were noted separately and sufficient volume of distilled water was added upto the fixed mark, contents were shaken well, and allowed to stand at room temperature for 24 h. The expanded volumes (EV) were determined to the nearest millimeter and the swelling index (SI) values were calculated as the ratio between the expanded volumes and initial volumes (IV).

Differential thermal analysis. Four representative samples (one from each site) of the unactivated raw earth were finely ground to pass 100 mesh sieve (USS) for differential thermal analysis (DTA). The DTA tests were carried out at the constant heating rate of 10 °C/min within the temperature range 20-1000 °C, on a derivatograph (MOM, Budapest). Calcined Al₂O₃ was used as the reference material throughout all the investigations.

Surface area. Particle size distribution was determined by using Andreasen and Lundberg apparatus. 5% suspension of the earth samples was made up in a 100 ml cylindrical vessel, shook well, and allowed to settle. Samples of the liquid, at the height of 20 cm from the surface, were withdrawn by 10 ml pipette at intervals. These were dried in collecting dishes, on a waterbath, separately, and the obtained powdery residues were weighed accurately. Particle size of the withdrawn fractions of the suspension, was calculated by applying Stokes Law and the surface area was determined by utilizing the accumulated particle size distribution data (Searle and Grimshaw, 1959).

Activation and bleaching. 100 g of each earth sample was ground to pass 60 mesh sieve (USS) and refluxed with 400 ml of 4 N hydrochloric acid at 100 °C, for three h. These were then filtered and washed thoroughly with distilled water, 3% activated earth was added alongwith 0.3% carbon to the soybean

oil samples for bleaching purposes. The resulting mixture was stirred on a waterbath for 45 min and the bleached oil was separated by filtration. The same process was repeated on all the fresh oil samples by using Tarana Optimum, the standard bleaching earth of German origin.

Bleachability determination. The bleachability was determined by applying the Lovibond tintometer method. The bleached soybean oil samples were filtered for removing any impurities and it was made sure that these were absolutely clear and free of turbidity. The Lovibond tintometer glass cell was dried after cleaning with carbon tetrachloride, filled with the sample and placed in the tintometer. Combinations of red and yellow Lovibond glass slides were then placed along the side of the instrument for matching the colour shade. The shade of oil was keenly observed through the combination of slides and the colour count was calculated in terms of Lovibond units by applying the standard formula (Bhatnagar and Dilgit, 1985). The colour count of the unbleached oil samples was taken as 100 during these calculations. All of the oil samples, bleached by Tarana Optimum, were also tested in the same manner for comparison.

Statistical analysis. The data obtained on CEC, SI and bleachability with respect to red pigment (BR) and yellow pigment (BY) were tabulated. These were then subjected to analysis of variance (ANOVA), using completely randomized design (CRD) and comparison of the means was done at 5% level of significance (Steel and Torrie, 1960).

Results and Discussion

Under the modern concepts of mineralogy, clay minerals are classified under three major groups, namely, Kaolinite group, Montmorillonite group and Illite group. These groups are not only distinguishable by their different chemical compositions, but more particularly by their physical differences as influenced by their respective crystal structures. The Kaolinite group, in this perspective, represents a crystal structure wherein gibbsite sheet is condensed with one silica sheet, whereas the remaining two groups consist of crystal lattice in which gibbsite sheet is enclosed between two silica sheets. Secondly, the important factors influencing CEC indicate that its single value cannot be the characteristic of clay minerals, rather, a range of values characterizes each group of such minerals. The obtained results of CEC determinations are presented in Table 1, which show that five samples: RFE-2, RFE-4 (site A) RFE-5 (site B), RFE-11 (site C), RFE-14 (site D) had CEC values between 30 and 40. The data also indicated that ten samples had CEC values between 20-30. Only one sample (RFE-7; site B) was below 20 in this regard. In brief, all samples, except RFE-7 (site B) with CEC 14.0 fell within the

range 20-40, and were thus non-expanding layered structure clay minerals termed as Illite and Montmorillonite (Worrall, 1986).

The adsorption of water by clays leads to expansion or swelling, the magnitude of which varies widely with the kind of clay minerals present therein. It actually depends upon the extent to which the clay mineral adsorbs water between the individual silicate layers. The SI results are given in Table 1, which indicate that four samples: RFE-2 (site A), RFE-5 (site B), RFE-10 (site C) and RFE-15 (site D) had the values between 2.0-2.5. Eight samples: RFE-1, RFE-3, RFE-4 (site A); RFE-6, RFE-8 (site B); RFE-9 (site C), RFE-13, RFE-16 (site D) were in the range 2.5-3.0 in this regard. Table 1 further shows that four samples: RFE-7 (site B); RFE-11, RFE-12 (site C); RFE-14 (site D), had their respective SI values more than 3, but less than 3.5. Evidently, all of the samples were within the range 2.0-3.5, thereby showing low swelling nature of the investigated earth samples. As earths with higher SI values are undesirable for decolourizing edible oils, these samples were found suitable for bleaching soybean oil.

The activity of a powder is well known to be directly proportional to its surface area, which in turn has linear relationship with the particle size. Therefore, finer the particle size of a powdered material, larger will be its surface area. The surface

area of the raw earth samples studied was found between 31570-42850 sq cm/g. Hence, their bleachability was expected to be good due to their high surface area. It was so anticipated, as the adsorptive effect of the bleaching earths depended upon surface tension, which is directly proportional to their surface area. It is also notable here that though the unwanted colour of the edible oil is bleachable using chemical methods, foreign materials, nevertheless, continue to remain present in the form of colourless compounds. The adsorption procedure, on the other hand, makes the bleached oil absolutely free from all the foreign/colouring materials (Mahatta, 1985). This aspect is also favourable for the use of Fuller's earth instead of other materials.

The DTA method is a widely used technique, based on graphic recording of the changes occurring in the tested samples as a function of time, which are manifested by heat-related effects. The information obtained through this technique can be utilized for the identification of clay minerals. The data accumulated with DTA have been shown as curves given in Fig. 1-3. It is evident from these curves that the first endothermic peak in all the samples occurred around 140 °C, indicating the possibility of both Montmorillonite and Illite. However, peaks of the same nature appeared around 600 °C in the case of sample RFE-15 from site D (Fig. 3). Their comparison, with the standard DTA cards, showed that this sample

Table 1. Cation exchange capacity (CEC) and swelling index

Site	Sample*	CEC	Swelling index (milliequiv/g)
A	RFE-1	29.00	2.56
	RFE-2	31.00	2.38
	RFE-3	29.00	2.57
	RFE-4	32.60	2.92
B	RFE-5	30.00	2.50
	RFE-6	24.00	2.78
	RFE-7	14.00	3.12
	RFE-8	22.80	2.99
C	RFE-9	27.60	2.80
	RFE-10	23.80	2.26
	RFE-11	33.20	3.08
	RFE-12	20.00	3.21
D	RFE-13	29.66	3.00
	RFE-14	30.30	3.50
	RFE-15	24.00	2.40
	RFE-16	26.30	2.62

* = raw samples of Fuller's earth investigated before their acid activation

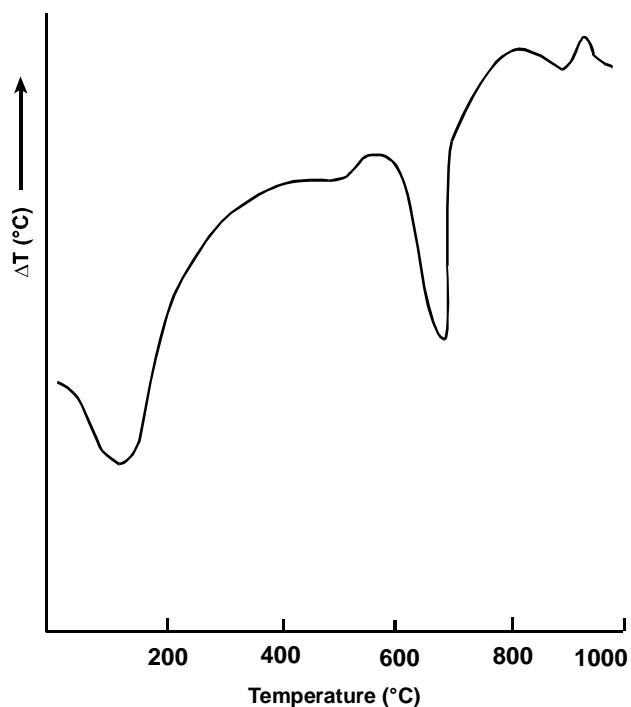


Fig. 1. Differential thermal analysis (DTA) curve of sample RFE-3, site A.

Table 2. Bleachability (%) of soybean oil by different activated Fuller's earth samples

Site	Sample*	Yellow	Red
A	AFE-1	94.2	96.6
	AFE-2	93.8	96.5
	AFE-3	95.5	96.4
	AFE-4	93.8	96.3
B	AFE-5	93.5	96.6
	AFE-6	92.1	93.3
	AFE-7	93.5	96.5
	AFE-8	93.8	96.4
C	AFE-9	95.2	96.5
	AFE-10	93.5	96.5
	AFE-11	91.4	93.3
	AFE-12	94.2	96.4
D	AFE-13	95.5	96.5
	AFE-14	95.2	96.4
	AFE-15	94.5	96.5
	AFE-16	94.8	96.4

* = activated Fuller's earth samples obtained after investigations on the raw earth sample; bleachability of Tarana Optimum (standard/control) was 94.2% for yellow and 94.9% for red pigment

consisted of Illite. While in the case of the curves for samples RFE-3 from site A (Fig. 1) and RFE-11 from site C (Fig. 2), the second endothermic peak occurred at 700 °C, instead of 600 °C. This indicated the presence of Montmorillonite. However, the last endothermic peak, which appeared in all the curves near 920 °C shows the possibility of both the Illite and Montmorillonite. These observations collectively indicate that the investigated samples consisted mainly of Illite and Montmorillonite.

Tarana Optimum bleached 94.2% yellow and 94.9% red pigment of soybean oil. The results obtained for the bleachability potential of the activated Fuller's earth samples are shown in Table 2. It is obvious from the given data that bleachability of most of the samples regarding yellow colouration was comparable with Tarana Optimum. However, the sample AFE-6 and AFE-11 were slightly on the lower side. Table 2 further reveals that sample AFE-3, AFE-9, AFE-13 and AFE-14 even excelled the standard earth sample. Fourteen samples, in view of bleaching red colouration, also excelled the Tarana Optimum, while the remaining two samples, AFE-6 and AFE-11, were fairly comparable.

So far as the bleaching phenomenon is concerned, it seemed to be due to physical adsorption of the colouring material on the activated earth powder. In fact, acid treatment of the raw

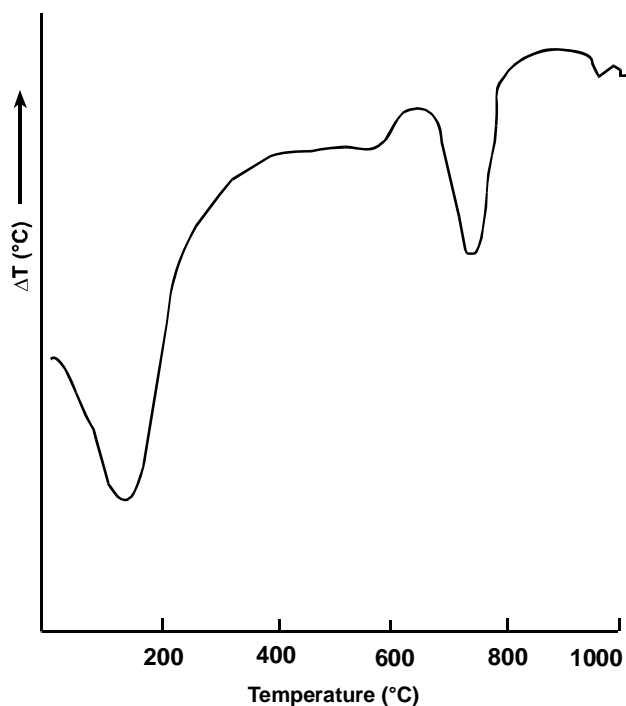
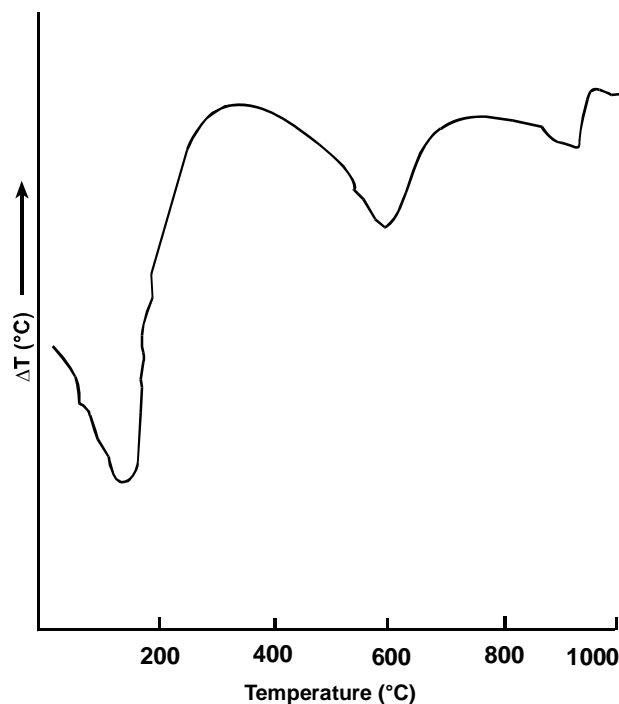
**Fig. 2.** Differential thermal analysis (DTA) curve of sample RFE-11, site C.**Fig. 3.** Differential thermal analysis (DTA) curve of sample RFE-15, site D.

Table 3. Means (\bar{x}) and standard deviations (SD) regarding CEC, SI, BR and BY*

Site	CEC (mean \pm SD)	SI (mean \pm SD)	BR (mean \pm SD)	BY (mean \pm SD)
A	29.06 \pm 1.06 ^a	27.1 \pm 0.23 ^a	96.55 \pm 0.057 ^a	94.6 \pm 0.92 ^a
B	27.27 \pm 3.90 ^a	2.73 \pm 0.55 ^a	95.67 \pm 1.58 ^a	93.65 \pm 1.27 ^{ab}
C	25.05 \pm 8.27 ^a	2.79 \pm 0.36 ^a	95.67 \pm 1.58 ^a	93.72 \pm 1.75 ^{ab}
D	25.42 \pm 5.43 ^a	2.93 \pm 0.24 ^a	96.37 \pm 0.05 ^a	94.15 \pm 0.47 ^b

* = the values with same superscript are non-significant at 5% level of significance; CEC = cation exchange capacity; SI = swelling index; BR = red pigment; BY = yellow pigment

earth removed the foreign matter contained in its capillary tubes and thus made it extremely porous. This, in turn, enhanced the surface area of the so treated earth, the factor which played a vital role to bleach the colouring matter of soybean oil.

The results of statistical analysis have been shown in Table 3. All of the RFE (raw Fuller's earth) samples belonging to sites A, B, C and D indicated non-significant difference for the CEC and SI values. So far as AFE (activated Fuller's earth) samples are concerned, these also showed similar results with respect to bleachability, except those belonging to site A and site D, which indicated significant difference regarding yellow pigment only.

Acknowledgement

The authors are highly appreciated to acknowledge the technical services of Mr. Salam Saeed, Scientific Officer, PCSIR Laboratories Complex, Lahore, Pakistan, for carried out the statistical analysis of different data generated during the experimental work.

References

- Bhatnagar, A.P., Dilgit, S. 1985. *Edible Oil Technology*, pp. 192-198, Small Business Publications, New Delhi, India.
- Brady, G.S., Clauser, H.R., Vaccari, J.A. 1997. *Materials Handbook*, pp. 387-391, 14th edition, McGraw-Hill Book Co., New York, USA.
- Cardello, H.M.A.B., Borghi, A.B.M.P., Vila, M.M.D.C., Goncalves, L.A.G. 1995. Conventional bleaching procedure for cotton seed oil (*Gossypium hirsutum*). *Aliment. Nutr.* **6**: 77-87.
- GSP-GSU. 1962. *Fuller's Earth Deposit Near Thano Bulla Khan*, Technical Report, pp. 1-10, Geological Survey of Pakistan, Quetta, Pakistan.
- Haehn, R., Eisgruber, M. 1995. Regeneration of Used Oil-Containing Bleaching Clays by Extraction and Thermal Treatment, German Patent No. D.E. 4, 330, 274.
- Hamilton, R.J., Bhatti, A. 1980. *Fats and Oils, Chemistry and Technology*, pp. 144-146, Applied Science Publishers, London, UK.
- Mahatta, T.I. 1985. *Technology and Refining of Oils and Fats*, pp. 208-209, Small Business Publications, New Delhi, India.
- Searle, A.B., Grimshaw, R.W. 1959. *The Chemistry and Physics of Clays and Other Ceramic Raw Materials*, pp. 382-385, 3rd edition, Earnest Benn Ltd., London, UK.
- Steel, R.G.D., Torrie, J.H. 1960. *Principles and Procedures of Statistics*, pp. 7-30, McGraw-Hill, London, UK.
- Theng, B.K.G., Wells, N. 1995. Assessing the capacity of some New Zealand clays for decolourizing vegetable oils. *Appl. Clays Sci.* **9**: 321-326.
- Worral, W.E. 1986. *Clays and Ceramics Raw Materials*, 2nd edition, Elsevier Applied Science Publishers, New York, USA.
- Yousaf, M., Mian, M., Iqbal, M., Rafiq, M., Ayoub, M. 1989. Characterization of Fuller's earth from D.G. Khan. *Pak. J. Sci. Ind. Res.* **32**: 798-804.

Studies on the Laboratory Scale Synthesis of 4,4'-Diaminodiphenylurea and Preparation of Direct Dyes from the Compound

S. Rehman Khan*, A. M. Gilani, Asma Inayat and Shaheena Waheed

Leather Research Section, Applied Chemistry Research Centre, PCSIR Laboratories Complex, Ferozepur Road, Lahore-54600, Pakistan

(received October 20, 2005; revised October 3, 2006; accepted October 3, 2006)

Abstract. 4,4'-Diaminodiphenylurea has been synthesized as a potential replacement for benzidine by reaction between *p*-phenylenediamine and urea under different catalytic and reaction conditions. Reaction conditions have been optimized to obtain maximum yield of intermediates. Direct dyes have been prepared from the title compound. The synthesized dyes were used to dye cotton and leather and the colour fastness properties of the dyed cotton and leather were assessed. Results showed that the synthesized dyes have fair to good fastness properties for cotton.

Keywords: 4,4'-diaminodiphenylurea, benzidine substitute, direct dyes

Introduction

The second amendment to German regulations on consumer goods states that the azo dyestuffs, which can release one or more of the listed 23 carcinogenic amines should no longer be used in dyeing of consumer goods (IARC, 1975). Several acid and direct dyes liberate harmful amines, such as benzidine, *o*-tolidine and dianisidine (benzidine derivatives) after reduction. Benzidine is both a genotoxic and harmful carcinogen (IARC, 1975; Case *et al.*, 1954; Scott, 1952). Human exposure to benzidine leading to bladder cancer has been related to the handling of the intermediate itself during the course of tetrazotization (Calogero *et al.*, 1987). Similarly, genotoxic metabolites have been isolated from the urine of animals, which had been fed with some azo dyes containing benzidine as the intermediate (Jocclion *et al.*, 1985). Due to the above stated risks, efforts were made to replace the carcinogenic benzidine and its derivatives by non-benzidine (benzidine-free) based direct dyes. Amide derivatives of the iso- and terephthalic acid (Wajciechowski and Gumulak, 2003), and iso- and terephthalic acid as such, have been used in the synthesis of direct dyes (Wajciechowski *et al.*, 2003). Also, benzidine substituted intermediates, and dyes based on them, have been synthesized in order to overcome the mutagenicity of benzidine (Gong *et al.*, 2002).

In this regard, 4,4'-diaminodiphenylurea (DADPU) has been proposed as a replacement for benzidine (Zhang, 1995), and it has been used to prepare direct dyes. DADPU contains ureylene group (-NHCONH-). 4,4'-Diaminodiphenylurea is normally synthesized using phosgene. Triphosgene has also been used as a substitute for phosgene to prepare urea con-

taining intermediates having ureylene group (Shi *et al.*, 1998; Peng *et al.*, 1996). Keeping in view the toxicity of phosgene and triphosgene, DADPU has been prepared in the present work using *p*-phenylenediamine and urea. The method is economical and reliable, but requires very long reaction time. Also, in the present work, the optimization of the process has been carried out under variable reaction conditions, such as reflux time, and by using different catalysts, which have resulted in better yield of the final DADPU product. DADPU has been further used to prepare direct dyes. Structure of DADPU is shown in Fig. 1(a).

Materials and Methods

p-Phenylenediamine (5.4 g), urea (3.6 g) and water (50.0 ml) were transferred to a flat bottom flask, and stirred on a hot plate. NaHSO₃ (39%; 3.0 ml) was added to the flask and stirring continued. Glacial acetic acid (2.5 ml) was then added, and the contents of the flask were refluxed with continuous stirring at a constant temperature of 102 °C. After refluxing for 24 h, the product was filtered with the help of vacuum filtration apparatus, using Whatman 40 filter paper. The filtered cake was washed thoroughly, first with normal and then with hot distilled water to remove residual urea. The reaction was carried out under the same reaction conditions, but changing the reflux time to 30, 36 and then 40 h. The yields of the DADPU obtained under different refluxing periods are shown in Table 1. The reaction was similarly carried out using ZnCl₂ + CH₃COOH, and Zn + CH₃COOH as catalysts, keeping the reaction time of 30 h constant. Physical appearance and the yield of the final products varied under different catalytic conditions as shown in Table 2.

*Author for correspondence; E-mail: drsrkhan 2004@yahoo.com

Table 1. Yield of 4,4'-diaminodiphenylurea (DADPU) under different periods of reaction time

Reaction time (h)	Yield (%)
24	59.24
30	70.14
36	72.06
40	73.09

Table 2. Yield and appearance of 4,4'-diaminodiphenylurea (DADPU) obtained after the constant reflux time of 30 h, using different catalysts

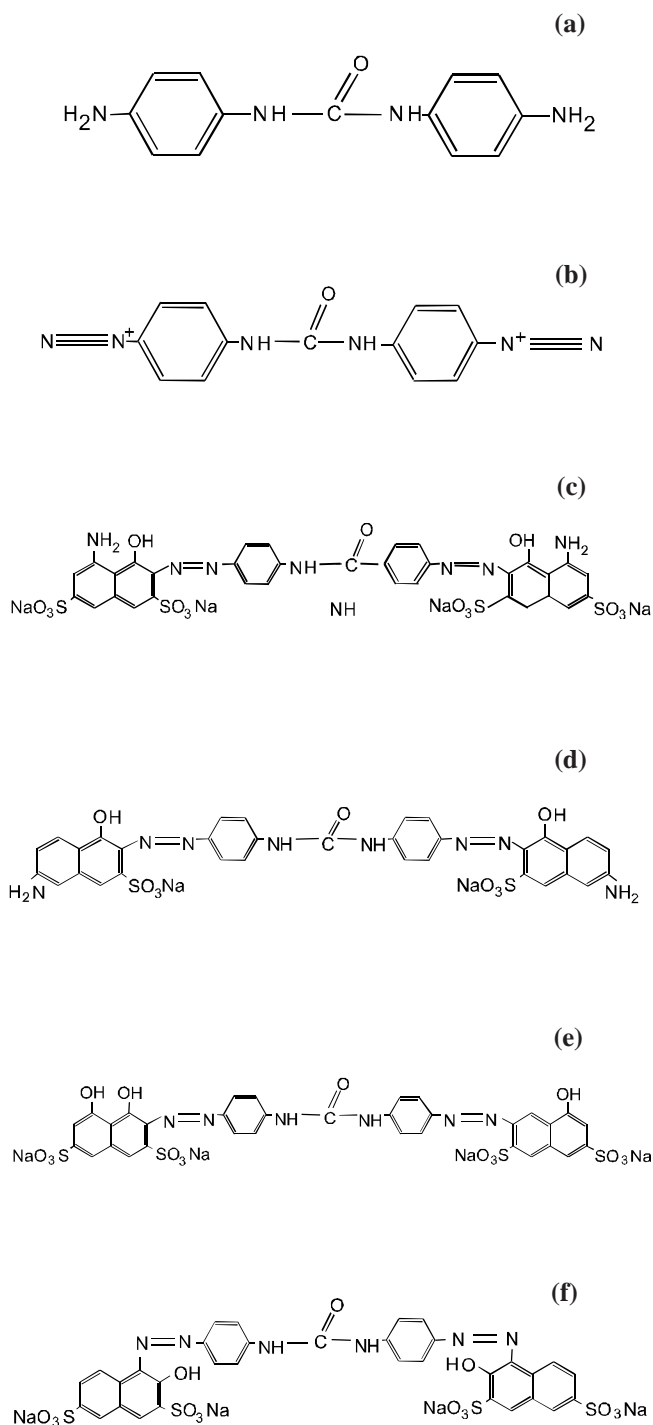
Catalyst	Appearance of DADPU	Yield (%)
CH ₃ COOH	colourless with very light mauve tinge	70.14
CH ₃ COOH + ZnCl ₂	mauve with bluish tinge	65.12
CH ₃ COOH + Zn	mauve with greyish tinge	63.17

Synthesis of dye-1. Tetrazotization step. DADPU (3.1 g), distilled water (30.0 ml) and 37% fuming HCl (6.7 ml) were transferred to a 250 ml beaker. The contents of the beaker were stirred vigorously and then cooled to 0 °C with the help of ice around the beaker. At 0 °C, 20% NaNO₂ (9.5 ml) was added dropwise for over 30 min by keeping the contents of the beaker in continuous stirring position. Stirring of the tetrazotized product was continued for further 20 min. Excess HNO₂ was neutralized using 10.0 ml of 20% urea solution. The tetrazotized product is shown in Fig. 1(b).

Coupling step. H-acid (1-amino-8-naphthol-3,6-disulfonic acid; 9.65 g) was stirred in 50.0 ml water and NaOH (20%) was added to it dropwise, with continuous stirring till all the H-acid dissolved. This solution was added dropwise over 2 h to the tetrazotized solution of DADPU and then the reaction mixture was stirred for further one h at 0-5 °C and pH 4-6. The pH of this solution was increased to 9.0-11.0, and the product was stirred vigorously for further 3 h. Dye was precipitated by the addition of NaCl. The paste so obtained was transferred to a china dish and the excess water was evaporated. The dye obtained was ground and stored in an air-tight container. The structure of the dye (**dye-1**) is shown in Fig. 1(c).

Synthesis of dye-2. Tetrazotization step. Tetrazotization of DADPU was conducted as described for **dye-1**.

Coupling step. J-acid (2-amino-5-naphthol-7-sulfonic acid; 6.8 g) was stirred in 50.0 ml water and NaOH (20%) was added to it dropwise with continuous stirring till all the J-acid

**Fig. 1.** (a) Chemical structure of 4,4'-diaminodiphenylurea (DADPU)- the parent compound for the synthesis of direct dyes; (b) the tetrazotized product of DADPU; (c) the chemical structure of **dye-1**; (d) the chemical structure of **dye-2**; (e) the chemical structure of **dye-3**; (f) the chemical structure of **dye-4**.

dissolved. This solution was added dropwise over 1.5 h to the tetrazotized solution of DADPU and then the reaction mixture was stirred for further one h at 0-5 °C and pH 4-6. The pH of this solution was increased to 9.5-11.5 and the product was stirred vigorously for further 4 h. The dye was precipitated by the addition of NaCl. The dye paste so obtained was transferred to a china dish and the excess water was evaporated. The dye obtained was (**dye-2**) ground and stored in an air-tight container. Structure of the dye (**dye-2**) is shown in Fig. 1(d).

Synthesis of dye-3. Tetrazotization step. This step was the same as described for **dye-1**.

Coupling step. Chromotropic acid (12.3 g) was stirred in 50.0 ml water and NaOH (20%) was added to it dropwise with continuous stirring till all the chromotropic acid dissolved. The resulting solution was added dropwise over 2.0 h to the tetrazotized solution of DADPU and the reaction mixture was then stirred for further two h at 0-5 °C and pH 3-5. The pH of this solution was increased to 6.0-8.0, and the product was stirred vigorously for further 4 h. The dye was precipitated by the addition of NaCl. The dye paste was transferred to a china dish and the excess water was evaporated. The dye (**dye-3**) obtained was ground and stored in an air-tight container. The structure of the (**dye-3**) is shown in Fig. 1(e).

Synthesis of dye-4. Tetrazotization step. Tetrazotization step was the same as described for **dye-1**.

Coupling step. R-acid (2-naphthol-3,6-disulfonic acid; 9.25 g) was stirred in 50.0 ml water and NaOH (20%) was added to it dropwise with continuous stirring till all the R-acid dissolved. The resulting solution was added dropwise, over 2 h, to the tetrazotized solution of DADPU and the reaction mixture was then stirred for further one h at 0-5 °C and pH 4-6. The pH of this solution was increased to 9.0-11.0, and the product was stirred vigorously for further 4 h. The dye was precipitated by the addition of NaCl. The dye paste so obtained was transferred into a china dish and the excess water was evaporated. The dye (**dye-4**) obtained was ground and stored in an air tight container. Structure of the dye (**dye-4**) is shown in Fig. 1(f).

Dyeing procedure. Dyeing of cotton. The following conditions were used: depth of shade 1%; dye concentration 1%; liquor ratio 1: 50.

Cotton fabric was immersed in a bath containing the dye solution (based on fabric weight). Bath was heated to 95 °C with continuous stirring of the contents of the bath. After 10 min, NaCl (7.0 g) was added to the dye-bath and stirring was continued. Bath was maintained at this temperature for 65 min,

then heated to boil and maintained at this temperature for further 10 min. Fabric was removed from the dye-bath and dried at room temperature. Absorption data and colour fastness properties of the dyes are shown in Table. 3.

Dyeing of leather. The synthesized dyes were used to dye buffalo split leather and sheep crust leather. A total of 5% was dyed on the weight of buffalo split and sheep crust leather (3.0% penetration followed by 2.0 % topping). Properties observed in both the cases are shown in Tables 4 and 5 for buffalo split leather and sheep crust leather, respectively.

Analytical measurements. Infra red (IR) spectrum (KBr) of DADPU was taken using IR spectrophotometer and is shown in Fig. 2. Analytical data for DADPU is shown in Table 6.

Results and Discussion

The use of NaHSO₃ (39%) as reducing agent. DADPU is oxidized under normal conditions. Therefore, the synthesis in prior studies of DADPU was carried out in deoxygenated conditions and required N₂ atmosphere (Spiewak, 1977). In the present work, NaHSO₃ was used as the reducing agent. It was observed that white DADPU can be obtained using a small amount of NaHSO₃, thus eliminating the need for the use of deaerated water and N₂ protection. Moreover, the residual NaHSO₃ can be easily removed from DADPU through washing the sample, as it is soluble in water.

The use of different catalysts. Different catalysts were used in the reaction for the synthesis of DADPU. It was observed that the appearance as well as the yield of DADPU changed when different catalysts were used. Best results were obtained when CH₃COOH was used as the catalyst. By using CH₃COOH, as the catalyst, better yield and appearance of the target compound was obtained as compared to other catalysts. Results obtained during the investigation are shown in Table 2.

Table 3. The dye absorption data and fastness properties* on cotton in respect of the dyes synthesized from 4,4'-diaminodiphenylurea (UADPU)

	Dyeing characteristics			
	Dye-1	Dye-2	Dye-3	Dye-4
λ_{max}	536	559	572	560
Washing (with soap)	4-5	4-5	4-5	3-4
Perspiration	4-5	4-5	4-5	4
Dry rubbing	4-5	4-5	4-5	4
Water	4-5	4	4	3-4
Sunlight	4-5	4-5	4	4

* Grey scale for assessing staining (ISO-105-A03)

Table 4. Dyeing characteristics of different dyes synthesized from 4,4'-diaminodiphenylurea (DADPU); material: buffalo split leather; thickness: 1.9-2.0 mm; article: buffalo garment leather

Parameters	Dye-1	Dye-2	Dye-3	Dye-4
Colour depth	excellent	good	good	fair
Rub fastness	poor	fair	good	good
Wash fastness	poor	poor	poor	poor
Light fastness	good	good	good	fair

Table 5. Dyeing characteristics of different dyes synthesized from 4,4'-diaminodiphenylurea (DADPU); material: sheep crust leather; thickness: 0.9-1.0 mm; article type: sheep garment leather

Parameters	Dye-1	Dye-2	Dye-3	Dye-4
Colour depth	good	poor	excellent	fair
Rub fastness	poor	fair	good	poor
Wash fastness	poor	poor	poor	poor
Light fastness	good	good	good	fair

Table 6. The infra red (IR) analytical (KBr) data for 4,4'-diaminodiphenylurea (DADPU)

Functional groups	IR (KBr) cm^{-1}
CO (carbonyl group)	1593, 1545
NH (amide group)	3262
CH (bending)	1506

It was observed that the yield of DADPU was improved by increasing the reaction time. Synthesis of DADPU was carried out at the reflux time of 24, 30, 36 and 40 h. Results obtained are shown in Table 1. It was observed that 59% yield was obtained after the reflux of 24 h. When the reaction time was increased from 24 to 30 h, 70% yield was obtained. After the reflux of 36 h, yield increased to 72%. By increasing the reaction time from 36 to 40 h, the increase was only 1%, making the 36 h reflux period as the optimal reaction time.

Conclusion

The different dyes synthesized from DADPU as the starting compound were used to dye cotton fabric and leather. It was concluded from the results obtained that dyes had good fastness properties for cotton fabric, whereas poor fastness properties were observed in the case of leather (Tables 3, 4, 5). Based on these observations, it can be concluded that the synthesized dyes had fair to good fastness properties for cotton.

References

- Calogero, F., Freeman, S.H., Esancy, J.F., Whaley, M.W., Dabney, B.J. 1987. Approach to the design of non-mutagenic azo dyes. Part-2. Potential replacements for the benzidine moiety of some mutagenic azo dyestuffs. *Dyes and Pigments* **8**: 431-447.
- Case, R.A.M., Hosker, M.E., McDonald, D.B., Pearson, J.T. 1954. Tumours of the urinary bladder in workmen engaged in the manufacture and use of certain dyestuff intermediates in the British Chemical Industry. Part-I. *Brit. J. Industrial Medicine* **11**: 75-104.
- Gong, G., Gao, X., Wang, J., Zhao, D., Freeman, S.H. 2002. Trisazo direct black dyes based on non-mutagenic 3,3'-

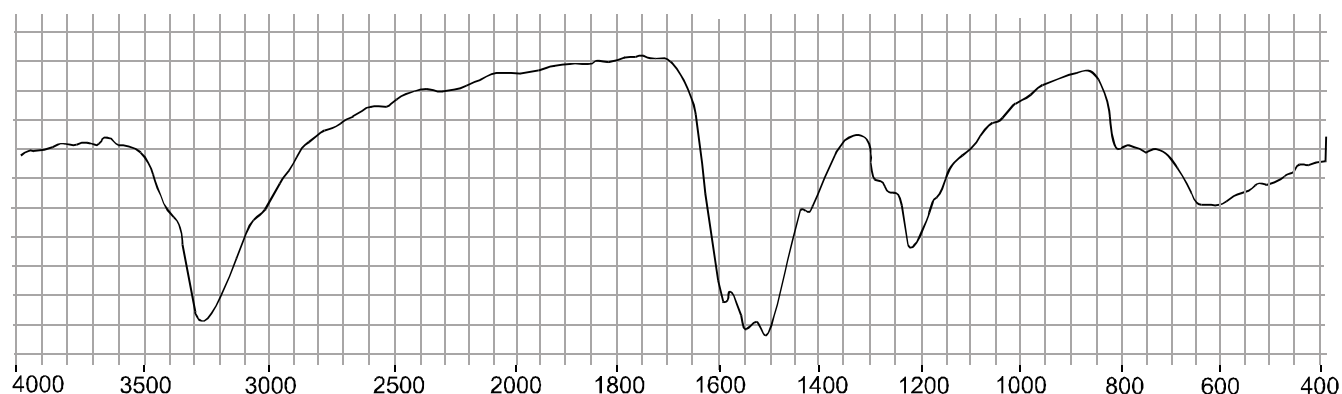


Fig. 2. Infra red spectrum (KBr) of 4,4'-diaminodiphenylurea (DADPU).

- disubstituted benzidines. *Dyes and Pigments* **53**: 109-117.
- IARC. 1975. *IARC Monographs on the Evaluation of Carcinogenic Risk Chemicals to Man*, International Agency for Research on Cancer, Lyon, France, **8**: 91, 151 and 267.
- Joachim, F., Burell, A., Andersen, J. 1985. Mutagenicity of azo dyes in the *Salmonella*/microsome assay using *in vitro* activation. *Mutation Res.* **156**: 134-138.
- Peng, X., Yu, H., Hang, Y., Wang, J. 1996. N,N'-phosgenation with triphosgene in the synthesis of direct dyes containing the ureylene group. *Dyes and Pigments* **32**: 193-198.
- Scott, T.S. 1952. The incidence of bladder tumors in a dye factory. *Brit. J. Industrial Medicine* **9**: 127-132.
- Shi, M., Chen, J., Yang, X., Wang, S. 1998. Preparation of triphosgene for azo dyes, Faming Zhuanli Shenqing Gong Kai Shuomingshu, Chinese Patent No. 1,224,704 (quoted from *Chemical Abstracts* **133**: 75329n, 2000).
- Spiewak, J.W. 1977. Ordered aromatic copolyamide urea polymer, U.S. Patent No. 40,35,344 (quoted from *Chemical Abstracts* **87**: 85789h, 1977).
- Wojciechowski, K., Gumulak, J. 2003. Benzidine-free direct dyes, amide derivatives of the iso- and terephthalic acids. *Dyes and Pigments* **56**: 195-202.
- Wojciechowski, K., Wyrebak, A., Gumulak, J. 2003. Direct dyes derived from iso- and terephthalic acids. *Dyes and Pigments* **56**: 99-109.
- Zhang, J. 1995. The substitute trend for the prohibited azo dyestuffs in the world. *Dye Ind.* **32**: 1.

Synthesis and Fungicidal Activity of Some Sulphide Derivatives of O-Ethyl-N-Substituted Phenylcarbamates

F. Adelowo-Imeokparia^{a*} and I. A. O. Ojo^b

^a Department of Pure and Applied Chemistry, Ladoké Akintola University of Technology, Ogbomoso, Nigeria

^b Department of Chemistry, Obafemi Awolowo University, Ile-Ife, Nigeria

(received March 14, 2006; revised September 12, 2006; accepted September 19, 2006)

Abstract. Monosulphides of O-ethyl-N-substituted phenylcarbamates were prepared by the reaction between O-ethyl-N-substituted phenylcarbamates and sulphur dichloride, while the corresponding disulphides were prepared by the reaction between O-ethyl-N-substituted phenylcarbamates and sulphur monochloride. The synthesized compounds were characterized by elemental analysis, thin layer chromatography (TLC), Fourier-transform infrared, and ¹H and ¹³C nuclear magnetic resonance spectroscopic techniques. *In vitro* fungicidal assay of these sulphides against *Fusarium oxysporum*, *Aspergillus niger*, *Aspergillus flavus* and *Rhizopus stolonifer* showed that they had greater fungicidal activity than their parent carbamates. The synthesized sulphides were more active towards *A. niger* and *A. flavus*. Unlike the parent carbamates, the type of substituents attached to the aromatic nucleus of these sulphides had little or no effect on their fungicidal activity as there was insignificant variation in the fungicidal activity of the monosulphide and the disulphide derivatives of O-ethyl-N-substituted phenylcarbamates.

Keywords: fungicidal activity, sulphide derivatives, O-ethyl-N-substituted phenylcarbamate, fungicides, organosulphur compounds

Introduction

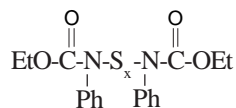
Countless sulphur compounds have been tested as fungicides, but only few of these have found worldwide applications (Ayodele, 2005; Lamberth, 2004; Tanaka *et al.*, 1978). Organosulphur compounds are economically important fungicides that play a significant role in the production of agricultural crops and in the preservation of industrial products (Lukens, 1971).

Stability of the metal-chelate formed between heavy metals present in fungal cells and the fungicide sulphur determines the fungicidal activity of these organosulphur compounds (Rich, 1960). Formation of such metal-chelates increases the hydrophobic property of metal ions, which enables them to pass through lipid layers of cellular membranes to inside the fungus cells, thereby leading to their poisoning (Eyring, 1966).

The toxicity of carbamates lies in their ability to inhibit the nervous system enzyme, acetylcholinesterase. Blockage of this enzyme results in a failure of the nervous system due to accumulation of acetylcholine in the nerve synapse. The inhibition of acetylcholinesterase in mammals (including man) leads to muscular spasm, headaches, diarrhoea, convulsion, respiratory failure and finally cardiac arrest (Kuhr and Dorough, 1976). The substitution of proton on the nitrogen atom of carbamates by a variety of functional groups results in derivatives that have lower anticholinesterase activity and

reduced mammalian toxicity when compared to their parent compounds (Fahmy and Fukuto, 1982). The possible attack of carbamates on the nervous system of humans involved in the fungicidal applications is reduced when derivatized carbamates are used in place of N-methylcarbamates (Fahmy *et al.*, 1970).

In continuation of the earlier research efforts (Ayodele *et al.*, 2000; Fahmy *et al.*, 1970) on the synthesis and structure-activity relationships of oligosulphides of the type PhCH₂-S_xCH₂CH₂OH (where x = 1-4), a consideration was given to the study of the following types of molecules.



x = 1 and 2 in the presently investigated molecules

Carbamates of this design were likely to cause less health hazards to the operators in particular as reported earlier (Fahmy *et al.*, 1982).

A wide variety of functional groups have been introduced into carbamates, which include sulfenyl, thiono, thiocarbonyl, acyl, sulfinyl, sulfonyl and phosphinothioyl (Szczepanski *et al.*, 1977; Field *et al.*, 1961; Grogan *et al.*, 1955). However, the most widely used functional group for derivatization of carbamates is the sulfenyl group (Black *et al.*, 1973; Kuhle, 1970; Kharasch, 1961; Reid, 1960). Several types of N-sulfenylated

*Author for correspondence; E-mail: funmiadelowo2000@yahoo.com

carbamates have shown lower mammalian toxicity than their corresponding parent compounds (Fahmy *et al.*, 1981; 1978; 1974).

The present report is concerned with the sulfonylation of some O-ethyl-N-substituted phenylcarbamates and the potential use of the derivatized products as fungicides.

Materials and Methods

Reagents and solvents. Solid reagents were recrystallized, while the solvents were redistilled. Toluene and diethyl ether were dried over sodium wire. Sulphur monochloride was redistilled over sulphur and collected at 138-139 °C. Similarly, sulphur dichloride was purified by distillation and the fraction was collected at 58-59 °C.

Synthesis of parent compounds. O-ethyl-N-substituted phenylcarbamates were prepared by the reaction between ethyl chloroformate and substituted aniline in the presence of pyridine, which was used for trapping the generated HCl. The general procedure for the synthesis of O-ethyl-N-substituted phenylcarbamates was as reported previously (Adelowo-Imeokparia *et al.*, 2005).

Synthesis of O-ethyl-N-(3-nitrophenyl) carbamate. Ethyl chloroformate (3.8 g, 3.3 cm³, 35 mmol) and 3-nitroaniline (4.8 g, 35 mmol) gave O-ethyl-N-(3-nitrophenyl) carbamate (6.0 g, 82%) as a yellow crystalline solid on recrystallization from methanol (found: C, 51.02; N, 13.08; calculated for C₉H₁₀N₂O₄: C, 51.43; N, 13.32%); m.p. 39-40 °C. The TLC (ethanol/DMSO, 3 : 1) gave a single spot, R_f = 0.83; ¹H (DMSO): 1.2 (CH₃CH₂, t, 3H), 4.1 (CH₃CH₂, q, 2H), 7.5 (Ar-H, m, 4H), 8.3 (N-H, b.s., 1H); ¹³C (DMSO): 15 (CH₃CH₂), 61 (CH₃CH₂), 112.5 (ArC-6), 117.5 (ArC-5), 124.5 (ArC-4), 130.5 (ArC-2), 141 (ArC-1), 149 (ArC-3), 154 (C=O).

Synthesis of O-ethyl-N-(4-nitrophenyl) carbamate. Ethyl chloroformate (5.4 g, 4.8 cm³, 50 mmol) and 4-nitroaniline (6.9 g, 50 mmol) gave O-ethyl-N-(4-nitrophenyl) carbamate (8.2 g, 78%) as a light yellow crystalline solid on recrystallization from methanol (found: C, 51.68; N, 13.50; calculated for C₉H₁₀N₂O₄: C, 51.43; N, 13.32%); m.p. 129-130 °C. The TLC (ethanol/DMSO, 3 : 1) gave a single spot R_f = 0.75; ¹H (C₃D₆O): 1.3 (CH₃CH₂, t, 3H), 4.2 (CH₃CH₂, q, 2H), 6.1 (N-H, b.s., 1H), 7.4 (Ar-H, d.d., 4H).

Synthesis of O-ethyl-N-(4-chlorophenyl) carbamate. Ethyl chloroformate (5.4 g, 4.8 cm³, 50 mmol) and 4-chloroaniline (6.4 g, 50 mmol) gave O-ethyl-N-(4-chlorophenyl) carbamate (7.2 g, 72%) as a light brown crystalline solid on recrystallization from methanol (found: C, 54.09; N, 6.92; calculated for

C₉H₁₀ClNO₂: C, 54.14; N, 7.01%); m.p. 40-41 °C. The TLC (ethanol/DMSO, 3 : 1) gave a single spot, R_f = 0.76; ¹H (DMSO): 1.2 (CH₃CH₂, t, 3H), 4.1 (CH₃CH₂, q, 2H), 7.35 (Ar-H, d.d., 4H), 9.7 (N-H, b.s., 1H); ¹³C (DMSO): 15 (CH₃CH₂), 61 (CH₃CH₂), 120 (ArC-2,6), 127 (ArC-3,5), 127 (ArC-1), 139 (ArC-4), 154 (C=O).

The infrared spectra of the synthesized carbamates showed strong carbonyl stretching bands between 1700 cm⁻¹ and 1705 cm⁻¹, while the secondary amide bands appeared between 3300 cm⁻¹ and 3350 cm⁻¹ for N-H stretching.

General procedure for the synthesis of monosulphides.

Synthesis of bis-[N-ethoxycarbonyl-N-(3-nitrophenyl)] monosulphide.

O-ethyl-N-(3-nitrophenyl) carbamate (1.05 g, 5 mmol) was dissolved in carbon tetrachloride (20 cm³). To the brown solution was added excess pyridine (10 cm³). Chilled sulphur dichloride, SCl₂ (0.52 g, 0.4 cm³, 5 mmol) dissolved in carbon tetrachloride (10 cm³) was added, dropwise, from a dropping funnel. The whole reaction mixture was set up in a 250 cm³ three-necked reaction flask fitted with a reflux condenser, a dropping funnel and a magnetic stirrer. The reaction mixture was stirred for 1 h at 20 °C in a fume cupboard. White fumes of hydrogen chloride, which disappeared with time were produced (Fig. 1). An equimolar quantity of O-ethyl-N-(3-nitrophenyl) carbamate (1.05 g, 5 mmol) dissolved in carbon tetrachloride (20 cm³) was added to the reaction mixture through a dropping funnel. Further evolution of white fumes was observed. The reaction mixture was stirred for another 1 h, and finally left to stir overnight at room temperature. The reaction mixture was washed with 10% hydrochloric acid (100 cm³) solution in a separatory funnel. The organic layer was separated and washed with distilled water (3 x 100 cm³). The brown organic layer was separated from the aqueous layer, dried with anhydrous sodium sulphate and filtered under suction. Volatile solvents were removed by means of a rotary evaporator to leave an oily residue, which solidified on cooling. The crude product was recrystallized from methanol to give the desired product, bis-[N-ethoxycarbonyl-N-(3-nitrophenyl)] monosulphide (**I**); yield: 1.80 g, 80%, brown crystals; m.p. 58-59 °C (found: C, 48.13; N, 12.24; S, 7.51; calculated for C₈H₁₈N₄O₈S: C, 47.99; N, 12.44; S, 7.12%). The TLC (ethanol/DMSO, 3 : 1) gave a single spot, R_f = 0.69; ¹H (DMSO): 1.2 (CH₃CH₂, t, 6H), 4.1 (CH₃CH₂, q, 4H), 7.5 (Ar-H, m, 8H); ¹³C (DMSO): 15 (CH₃CH₂), 61 (CH₃CH₂), 113 (ArC-6), 118 (ArC-5), 125 (ArC-4), 131 (ArC-2), 142 (ArC-1), 149 (ArC-3), 154 (C=O). The infrared spectrum of the synthesized compound showed a strong carbonyl absorption at 1715 cm⁻¹ and absence of amide band of N-H stretching.

Synthesis of bis-[N-ethoxycarbonyl-N-(4-nitrophenyl)] monosulphide. O-ethyl-N-(4-nitrophenyl) carbamate [2 x (1.05

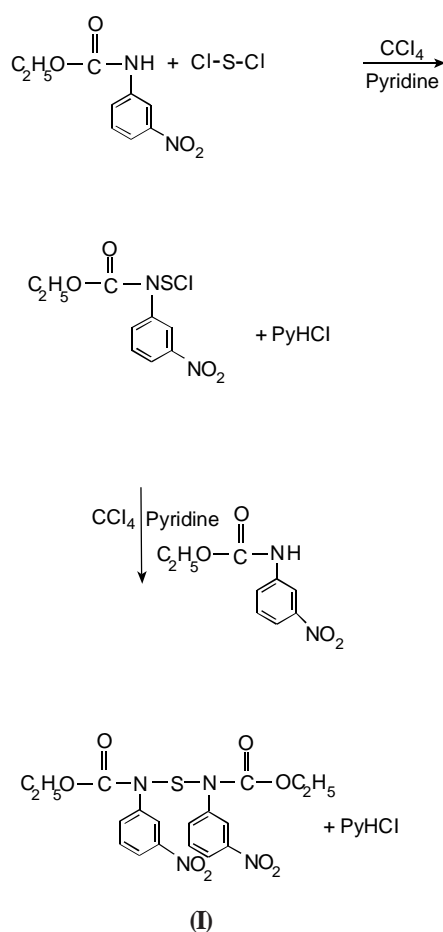


Fig. 1. Synthesis of bis-[N-ethoxycarbonyl-N-(3-nitrophenyl)] monosulphide.

g, 5 mmol)] and sulphur dichloride (0.52 g, 0.4 cm^3 , 5 mmol) gave the product bis-[N-ethoxycarbonyl-N-(4-nitrophenyl)] monosulphide; yield: 1.6 g, 71%; brown (shining) crystalline solid on recrystallization from methanol (found: C, 47.91; N, 11.98; S, 6.86; calculated for $\text{C}_{18}\text{H}_{18}\text{N}_4\text{O}_8\text{S}$: C, 47.99; N, 12.44; S, 7.12%); m.p. 101-102 °C. The TLC (ethanol/DMSO, 3 : 1) gave a single spot, $R_f = 0.69$; ^1H (DMSO): 1.3 (CH_3CH_2 , t, 6H), 4.2 (CH_3CH_2 , q, 4H), 7.4 (Ar-H, m, 8H).

Synthesis of bis-[N-ethoxycarbonyl-N-(4-chlorophenyl)] monosulphide. O-ethyl-N-(4-chlorophenyl) carbamate [2 x (1.03 g, 5 mmol)] and sulphur dichloride (0.52 g, 0.4 cm^3 , 5 mmol) gave the product, bis-[N-ethoxycarbonyl-N-(4-chlorophenyl)] monosulphide; yield: 1.82 g, 85%; brown crystalline solid on recrystallization from methanol (found: C, 49.99; N, 6.57; S, 6.31; calculated for $\text{C}_{18}\text{H}_{18}\text{Cl}_2\text{O}_4\text{S}$: C, 50.35; N, 6.53; S, 7.47%); m.p. 92-93 °C. The TLC (ethanol/DMSO, 3 : 1) gave a single spot, $R_f = 0.68$; ^1H (DMSO): 1.2 (CH_3CH_2 , t, 6H), 4.1 (CH_3CH_2 , q, 4H), 7.35 (Ar-H, m, 8H); ^{13}C (DMSO): 15 (CH_3CH_2), 61 (CH_3CH_2), 121 (ArC-2,6), 127 (ArC-3,5), 129 (ArC-1), 139

(ArC-4), 154 (C=O).

A general procedure for the synthesis of disulphides. *Synthesis of bis-[N-ethoxycarbonyl-N-(3-nitrophenyl)] disulphide.* To a solution of O-ethyl-N-(3-nitrophenyl) carbamate (1.05 g, 5 mmol) dissolved in carbon tetrachloride (20 cm^3) was added excess triethylamine, Et_3N (10 cm^3). Chilled sulphur monochloride, S_2Cl_2 (0.68 g, 0.4 cm^3 , 5 mmol), dissolved in carbon tetrachloride (10 cm^3), was added dropwise from a dropping funnel, whilst the reaction mixture was maintained below 10 °C by the addition of ice to the waterbath in which the reaction vessel stood. White fumes, which disappeared with time, were produced. The reaction mixture was kept stirred for another 30 min after the addition of sulphur monochloride was completed. Another equimolar quantity of O-ethyl-N-(3-nitrophenyl) carbamate, dissolved in carbon tetrachloride (20 cm^3) was added dropwise to the reaction mixture. Further evolution of white fumes was observed. The reaction mixture was allowed to stir at a temperature below 10 °C for an additional 30 min and finally left to stir overnight at room temperature (Fig. 2). The solid, triethylamine hydrochloride was re-

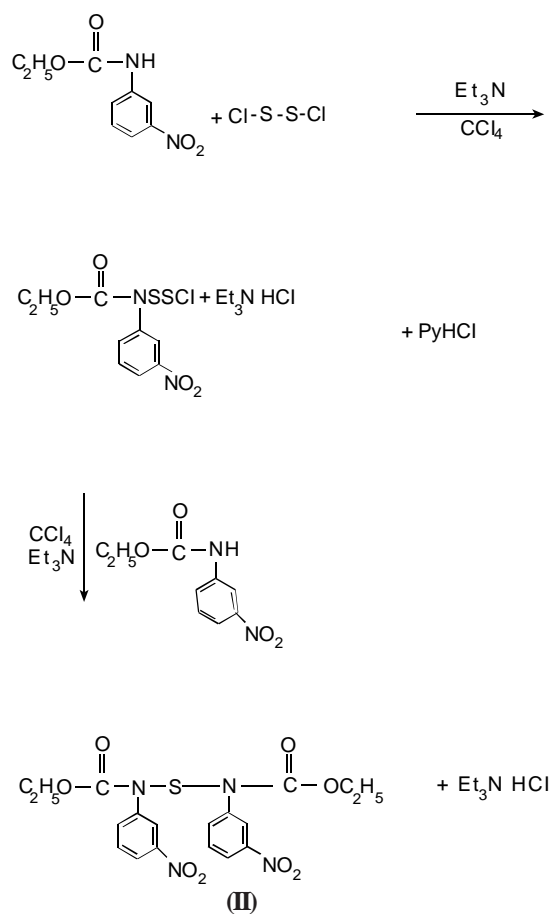


Fig. 2. Synthesis of bis-[N-ethoxycarbonyl-N-(3-nitrophenyl)] disulphide.

Table 1. Inhibitory effect of some synthesized compounds (sulphide derivatives of O-ethyl-N-substituted phenylcarbamates) on some fungal species through minimal inhibitory concentration (MIC) and inhibitory concentration at 50% inhibition (IC₅₀)

Synthesized compounds	<i>Aspergillus niger</i>		<i>Aspergillus flavus</i>		<i>Rhizopus stolonifer</i>		<i>Fusarium oxysporum</i>	
	MIC	IC ₅₀	MIC	IC ₅₀	MIC	IC ₅₀	MIC	IC ₅₀
O-ethyl-N-(3-nitrophenyl)carbamate	100	40	100	60	100	60	100	50
O-ethyl-N-(4-nitrophenyl)carbamate	250	80	250	80	250	100	250	100
O-ethyl-N-(4-chlorophenyl)carbamate	200	100	200	100	200	120	200	110
Bis-[(N-ethoxycarbonyl-N-(3-nitrophenyl)] monosulphide	50	10	50	10	50	18	50	21
Bis-[(N-ethoxycarbonyl-N-(4-nitrophenyl)] monosulphide	50	10	50	12	50	20	50	25
Bis-[N-ethoxycarbonyl-N(4-chlorophenyl)] monosulphide	50	11	50	10	50	20	50	22
Bis-[N-ethoxycarbonyl-N(3-nitrophenyl)] disulphide	50	08	50	10	50	20	50	24
Bis-[N-ethoxycarbonyl-N(4-nitrophenyl)] disulphide	50	12	50	15	50	23	50	25
Bis-[N-ethoxycarbonyl-N(4-chlorophenyl)] disulphide	50	10	50	12	50	25	50	25
Phenylmercury acetate (standard)	5	1	5	1	5	2	5	3
DMSO/H ₂ O (8:2) (control)	0	0	0	0	0	0	0	0

moved by filtration. The filtrate was washed with 10% hydrochloric acid (100 cm³) solution in a separatory funnel. The organic layer was washed with distilled water (3 x 100 cm³), dried with anhydrous sodium sulphate and filtered. Volatile solvents were removed from the filtrate by means of a rotary evaporator to leave oil, which solidified on standing. The crude product was recrystallized from methanol to give the desired product, bis-[N-ethoxycarbonyl-N-(3-nitrophenyl)] disulphide (**II**); yield: 1.9 g, 79%; brown crystalline solid; m.p. 120-121 °C (found: C, 43.98; N, 11.70; S, 10.62; calculated for C₁₈H₁₈N₄O₈S₂: C, 44.80; N, 11.61; S, 13.29%). The TLC (ethanol/DMSO 3 : 1) gave a single spot, R_f = 0.51; ¹H (DMSO): 1.2 (CH₃CH₂, t, 6H), 4.1 (CH₃CH₂, q, 4H), 7.6 (Ar-H, m, 8H); ¹³C (DMSO): 15 (CH₃CH₂), 61 (CH₃CH₂), 112 (ArC-6), 118 (ArC-5), 125 (ArC-4), 130 (ArC-2), 141 (ArC-1), 150 (ArC-3), 154 (C=O). The infrared spectrum of the synthesized compound showed strong carbonyl absorption at 1720 cm⁻¹ and absence of amide band of N-H stretching.

Synthesis of bis-[N-ethoxycarbonyl-N-(4-nitrophenyl)] disulphide. O-ethyl-N(4-nitrophenyl) carbamate [2 x (1.05 g, 5

mmol)] and sulphur monochloride (0.68 g, 0.4 cm³, 5 mmol) gave the product, bis-[N-ethoxycarbonyl-N-(4-nitrophenyl)] disulphide as a brown crystalline solid; yield: 1.9 g, 79%, m.p. 124-125 °C (found: C, 44.33; N, 10.84; S, 10.56; calculated for C₁₈H₁₈N₄O₈S₂: C, 44.80; N, 11.61; S, 13.29%). The TLC (ethanol/DMSO 3 : 1) gave a single spot, R_f = 0.54; ¹H (DMSO): 1.3 (CH₃CH₂, t, 6H), 4.2 (CH₃CH₂, q, 4H), 7.5 (Ar-H, m, 8H).

Synthesis of bis-[N-ethoxycarbonyl-N-(4-chlorophenyl)] disulphide. O-ethyl-N-(4-chlorophenyl) carbamate [2 x (0.99 g, 5 mmol)] and sulphur monochloride (0.68 g, 0.4 cm³, 5 mmol) gave the product, bis-[N-ethoxycarbonyl-N-(4-chlorophenyl)] disulphide as a reddish-wine coloured crystalline solid; yield: 1.6 g, 70%; m.p. 65-66 °C; (found: C, 47.11; N, 5.96; S, 11.64; calculated for C₁₈H₁₈Cl₂N₂O₄S₂: C, 46.85; N, 6.07; S, 13.89%). The TLC (ethanol/DMSO 3 : 1) gave a single spot, R_f = 0.54; ¹H (DMSO): 1.2 (CH₃CH₂, t, 6H), 4.1 (CH₃CH₂, q, 4H), 7.3 (Ar-H, m, 8H); ¹³C (DMSO): 15 (CH₃CH₂), 61 (CH₃CH₂), 120 (ArC-2,6), 127 (ArC-3,5), 129 (ArC-1), 139 (ArC-4), 154 (C=O).

Biological screening. Potato dextrose agar (PDA) plates were flooded with spore suspension of each fungus. About 6 mm

dia filter paper discs were sterilized in petri dishes at 160 °C for 2 h. With the aid of a sterilized pair of forceps, filter paper discs that had been soaked in solutions of various concentrations of each synthesized compound were put on the surface of inoculated PDA plates. Filter paper discs were also soaked in the standard (phenylmercury acetate) and the control (CDMSO/H₂O; 8 : 2), and then placed on the surface of the inoculated PDA plates. All the PDA plates were incubated at room temperature. The growth dia of the fungus colony was measured after every 24 h interval, until the control plate was complete covered with the growth of fungus. The minimum concentration of each synthesized compound, that gave 100% inhibition of fungus growth, was taken as the 'minimal inhibitory concentration (MIC) of the compound (Adelowo-Imeokparia *et al.*, 2005). The IC₅₀ (inhibitory concentration of the synthesized compound at 50% inhibition of the fungus colony) was extrapolated from the graph of percentage inhibition (1%) of fungus against concentration of the synthesized compound (Adelowo-Imeokparia *et al.*, 2005; Tabakova *et al.*, 1995).

Results and Discussion

A strongly basic tertiary amine was used in the synthesis of disulphides of O-ethyl-N-substituted phenylcarbamate so as to prevent any formation of their corresponding monosulphides (Fahmy *et al.*, 1974; Kuhle, 1970).

The values of the minimal inhibitory concentration (MIC) and the 50% inhibitory concentration (IC₅₀) of the synthesized compounds are presented in Table 1. The MIC value of the parent compounds (carbamates) were between 100 and 250 ppm, while their sulphides were 2- to 5-folds lower (50 ppm). Organic sulphur compounds move into the fungus cells and are able to take part in chemical reactions, such as chelation, oxidation-reduction and nucleophilic displacement (Lukens, 1971). Dithiocarbamates (disulphides of carbamate), such as thiram and ziram owe their fungicidal activity to their ability to chelate with heavy metals present in the cells of fungi (Metcalf, 1971). Ethylenebisdithiocarbamates (nabam, maneb and zineb), on the other hand, undergo oxidative decomposition. The ethylene diisothiocyanate so produced reacts with thiol compound within the fungal cell. This is responsible for the fungicidal activity of ethylenebisdithiocarbamates (Lukens, 1971). N-(trichloromethylthio)-4-cyclohexene-1,2-dicarboximide (a monosulphide) owe its fungicidal action to its involvement in nucleophilic displacement reaction with cellular thiols to produce thiophosgene as the toxicant (Cremlyn, 1979). It seems very appropriate, therefore, that the observed increase in fungicidal activity of the synthesized monosulphides and disulphides of O-ethyl-N-substituted phenylcarbamates (as shown by their MIC and IC₅₀

values), when compared with their parent compounds, could be ascribed to their involvement in any of the earlier mentioned reactions within the fungal cells.

The results of the MIC and IC₅₀ of the synthesized compounds showed that the monosulphides were as good as their disulphide analogues for the control of the four fungal species. The IC₅₀ values of the synthesized monosulphides and disulphides were about two-folds lower when tested against *Aspergillus* species. This shows that *Aspergillus* species were more susceptible to the synthesized mono- and disulphides than the remaining two fungal species. There was no evidence of dependence of activity on the benzene ring substituents since only electron withdrawing substituents were involved in this work.

The IC₅₀ of the standard, phenylmercury acetate (a well known fungicide), was about 4- to 12-folds lower than that for the monosulphides and disulphides, while it was about 20- to 60-folds lower than the carbamates. Since the level of activity of the monosulphides and disulphides was almost comparable to that of the standard, it may be concluded that the studied derivatives showed good promise as potential fungicides.

Conclusion

This work has demonstrated that the synthesized compounds have shown promising fungicidal activities against the selected fungi. The sulphide derivatives of phenylcarbamate precursors can probably improve on their fungicidal activity by the introduction of more sulphur atoms, replacing ethoxy group with phenoxy or naphthoxy group, and the use of electron donating substituents in the benzene ring.

References

- Adelowo-Imeokparia, F., Faboya, O.O.P., Ojo, I.A.O. 2005. Synthesis and fungicidal activity of some phenylcarbamates. *International J. Chem.* **15**: 101-111.
- Ayodele, E.T. 2005. Preparation and glass house screening of some substituted benzyl-2-hydroxyethyl oligosulfides. *International J. Biological and Physical Sci.* **10**: 56-62.
- Ayodele, E.T., Hudson, H.R., Ojo, I.A.O. 2002. Mass spectrometry of benzyl -2-hydroxyethyl oligosulphides, dibenzyl, di- and tri-sulfides, benzyl phthalimido disulphides and related compounds. *J. Phosphorus, Sulfur and Silicon, and Related Elements* **177**: 261-275.
- Ayodele, E.T., Hudson, H.R., Ojo, I.A.O., Pianka, M. 2000. Organosulfur compounds as potential fungicides: the preparation and properties of some substituted benzyl -2-hydroxyethyl oligosulfides. *J. Phosphorus, Sulfur and Silicon, and Related Elements* **159**: 123-142.

- Black, A.L., Chiu, Y.C., Fahmy, M.A.H., Fukuto, T.R. 1973. Selective toxicity of N-sulfonylated derivatives of insecticidal methylcarbamate esters. *J. Agric. Food Chem.* **21**: 747-751.
- Cremlyn, R., 1979. *Pesticides: Preparation and Mode of Action*, pp. 114-115, John Wiley and Sons Ltd., New York, USA.
- Eyring, H. 1966. Untangling biological reactions. *Science* **154**: 1609-1613.
- Fahmy, M.A.H., Fukuto, T.R. 1982. Rationale and chemistry of proinsecticidal methylcarbamates. *Pesticide Chemistry* **1**: 193-200.
- Fahmy, M.A.H., Fukuto, T.R. 1981. N-sulfonylated derivatives of methylcarbamate esters. *J. Agric. Food Chem.* **29**: 550-557
- Fahmy, M.A.H., Mallipudi, N.M., Fukuto, T.R. 1978. Selective toxicity of N,N-thiodicarbamates. *J. Agric. Food Chem.* **26**: 550-557.
- Fahmy, M.A.H., Chiu, Y.C., Fukuto, T.R., 1974. Selective toxicity of N-substituted biscarbamoyl sulphides. *J. Agric. Food Chem.* **22**: 59-62.
- Fahmy, M.A.H., Fukuto, T.R., Myers, R.O., March, R.B. 1970. The selective toxicity of new N-phosphorothioylcarbamate esters. *J. Agric. Food Chem.* **18**: 793-796.
- Field, L., Owen, T.C., Crenshaw, R.R., Bryan, A.W. 1961. Ornates and disulfides containing 2-aminoethyl moieties. *J. Am. Chem. Soc.* **83**: 4414-4417.
- Grogan, C.H., Rice, L.M., Reid, E.E. 1955. Dithiols and derivatives. *J. Org. Chem.* **20**: 50-58.
- Kharasch, N. 1961. *Organic Sulphur Compounds*, vol. 1, pp. 30-51, Pergamon Press, Headington Hill, Oxford, UK.
- Kuhle, E. 1970. One hundred years of sulfenic acid chemistry: sulfonyl halide synthesis. *Synthesis* **11**: 560-580.
- Kuhr, R.J., Dorough, H.W. 1976. *Carbamate Insecticides: Chemistry, Biochemistry and Toxicology*, pp. 103-124, CRC Press Inc., New York, USA.
- Lamberth, C. 2004. Sulfur chemistry in crop protection. *J. Sulfur Chem.* **25**: 39-62.
- Lukens, R.J. 1971. *Chemistry of Fungicidal Action*, pp. 1-138, Chapman and Hall Ltd., London, UK.
- Metcalf, R.L. 1971. Chemistry and biology of pesticides. In: *Pesticides in the Environment*, R. White-Stevens (ed.), R. Dekker Publishing, New York, USA.
- Reid, E.E. 1960. *Organic Chemistry of Bivalent Sulphur*, vol. **III**, pp. 363-367, Chemical Publishing Co., Inc., New York, USA.
- Rich, S. 1960. *Fungicidal Chemistry in Plant Pathology*, Academic Press Ltd., New York, USA.
- Szczepanski, C.V., Heindl, J., Hoyer, G.A., Schroder, E. 1977. Biologically active substances in plants. II. Synthesis and antimicrobial activity of some unsymmetrical oligosulphides. *Eur. J. Med. Chem. Chimica Therapeutica* **12**: 279-284.
- Tabakova, S., Dodoff, N. 1995. Effect of platinum(II) complexes of benzoic and 3-methoxybenzoic acid hydrazides on *Saccharomyces cerevisiae*. *Z. Naturforsch* **50C**: 732-743.
- Tanaka, S., Kato, T., Takahashi, K., Yamamoto, S. 1978. Fungicidal activities of 1,1-diisopropyl-2-(3-pyridyl)-3-p-ethoxy-phenylguanidine and its analogs. *Agric. Biol. Chem.* **42**: 803-807.

Isolation and Characterization of *Kappa*-Carrageenan from *Hypnea musciformis* (Red Alga) Collected from Karachi Coast, Pakistan

Fatima Bi*, Muhammad Arman, Mahmood-ul-Hassan and Seema Iqbal

Pharmaceutical Research Centre, PCSIR Laboratories Complex Karachi,

Sharah-e- Dr. Salimuzzaman Siddiqui, Karachi-75280, Pakistan

(received January 18, 2006; revised June 20, 2006; accepted June 27, 2006)

Abstract. *Hypnea musciformis*, collected from Karachi coast of Pakistan, was used for the isolation of a thickening and emulsifying agent, carrageenan. Various extraction procedures were employed and the yield of carrageenan obtained was in the range of 34-44%. Total sugar contents were found to be 31.8-55.4%. 3,6-Anhydrogalactose, a component of the total sugar, was present in the range of 19.9-27.6%. Sulphate and ash contents were high, 14.8-41% and 15.4-53%, respectively. The positive rotation of these polysaccharides indicated a predominance of α -D-glycosidic linkages in their structure. IR spectral studies showed *kappa*-carrageenan as the major phycocolloid, with a very small contamination of *iota*-type carrageenan, whereas *lambda*-type was not detected. Polysaccharides obtained showed a positive elicitor activity in garden peas (*Pisum sativum*). HPLC analysis indicated the presence of a single major component.

Keywords: carrageenan, Rhodophyta, polysaccharides, elicitor activity, *Hypnea musciformis*, phycocolloid

Introduction

Commercially important polysaccharides from red seaweeds (Rhodophyta) belong to the group of polydisperse, long chain, water-soluble galactans. Their building block is made up of alternating 3-linked β -galactopyranose and 4-linked β -galactopyranose, which can be variably modified and/or substituted. In carrageenans, the 4-linked units are in the D-configuration, whereas in agars they are in the L-configuration (Usov, 1992). The gelling and thickening properties, and the protein reactivity of these phycocolloids have led to their widespread commercial uses in the industry, including food and beverages, pharmaceuticals and cosmetics (Nishizawa, 2002). These are also used as biofertilizers in the agriculture sector. Because of the wide commercial applications of carrageenans, various extraction procedures to obtain this product from red algal plants have been reported in literature, while their structural determinations are done using spectroscopic techniques (Greer *et al.*, 1984). Karachi, Pakistan has a large coastal area yielding large quantities of marine algae. Unfortunately, these seaweeds are not utilized in Pakistan, either as marine vegetables or for extracting commercial compounds (Husain *et al.*, 2001), whereas huge amounts are spent on the import of seaweed products. The aim of the present study was to develop an effective procedure for the exploitation of these seaweeds so that carrageenans may be extracted in good quality and quantity from *Hypnea musciformis*. Another objective was to explore the nature of these polysaccharides as the inducers of hypersensitive response, characteristic of

resistance mechanism in plants against diseases, especially in terms of induced browning and production of phytoalexins (Nicholson and Wood, 2001). Garden peas (*Pisum sativum*) were used as the test plant for the elicitor activity experiments.

Materials and Methods

General method of extraction. *Hypnea musciformis* (red alga) was collected from Karachi coast, Pakistan in February and November 2003. The plant was cleaned of epiphytes, washed, dried, and ground to a fine powder. Representative material of the plant sample (25 g) was pretreated with HCl (0.1 N)/formaldehyde (20%), and extracted with water (tap/distilled) at 70-80 °C, with constant stirring for 6 h. Supernatant was collected and the residue was re-extracted twice under similar conditions. Experimental conditions were varied for optimizing the extraction procedures and carrageenans were obtained, as detailed below in different extraction protocols, by ethanol precipitation or by direct drying on a waterbath.

Extraction-1. Dry plant powder, pretreated with HCl (0.1 N), was stirred for 30 min in an icebath, washed extensively with tap water to remove traces of acid, followed by washing with distilled water. The supernatant was dried in a waterbath.

Extraction-2. Dry plant powder, pretreated with HCl (0.1 N), was washed, followed by extraction with distilled water. Supernatant was precipitated with 95% ethanol (three volumes of the extract), and the precipitate was dried.

Extraction-3. Dry plant material, pretreated with HCl (0.1 N), was washed and extracted with tapwater and dried in a waterbath.

*Author for correspondence; E-mail: klpcsir@khi.paknet.com.pk

Extraction-4. Dry plant material, pretreated with HCl (0.1 N), was washed and extracted with tapwater, precipitated with alcohol, and the precipitate was dried in a waterbath.

Extraction-5. Dry plant material, pretreated with HCl (0.1 N), was washed and extracted with distilled water. Supernatant was precipitated with 0.3 M KCl (solid) and the precipitate was dried in a waterbath.

Extraction-6. Dry plant material was mixed with formaldehyde (20%), left overnight, washed and extracted with distilled water. Supernatant was dried in a waterbath.

Analytical methods. Moisture, ash and total carbohydrate contents were determined. Acid hydrolysis was done for different time periods, 30, 90 and 180 min. Monosaccharide components were identified by paper chromatography, as described elsewhere (Bi and Iqbal, 1999). 3,6-Anhydrogalactose was determined colourimetrically using the modified resorcinol method (Yaphe and Arsenault, 1965). Sulphate content was determined in accordance with the method of Dodgson and Price (1962). Optical rotations of carrageenan solutions of known concentration (1% of **extracts-1, 2, 3, 4** and commercial carrageenans, and 0.1% of **extracts-5 and 6**) were determined with a digital polarimeter (Jas. Co. Dip. 360) using 50 mm tubes and sodium D line at 589 cm wavelength. Fourier transform infrared (FTIR) analyses were performed on a Nicolet Avatar 370 DTGS infrared fourier transform spectrometer.

Elicitor activity and extraction of induced secondary metabolites (ISM) from garden peas. A general method of elicitor application was employed (Whitehead *et al.*, 1982). Fresh garden peas (*Pisum sativum*), 100 g, were peeled and cotyledons were sterilized with 1% sodium hypochlorite solution, washed extensively with distilled water, followed by washing with sterilized water. The elicitor preparation (20 µl), made from **extract-5**, at a concentration of 100 µg glu eq/ml and sterilized water, were applied to the cut surface of cotyledons. The browning induced in the samples was recorded after 24 h of incubation, and the samples were dipped in distilled alcohol (95%) for the extraction of induced secondary metabolites.

Separation of ISM by HPLC. HPLC separation was accomplished on 4.6 mm x 25 cm reverse phase C₁₈ column (Perkin Elmer), with a variable UV-detector (254 nm) and isocratic solvent system. A guard column of pellicular C₁₈ hydrocarbon chemically bonded to glass beads was placed before the analytical column. Initially, 70 : 30 (acetonitrile : water), having 0.5% acetic acid, was run for 10 min and then acetonitrile (100%) was run for further 25 min.

Sample preparation for HPLC. Dry alcoholic extract of the treated and control samples were dissolved in 1 ml of the

initial solvent (70 : 30; acetonitrile : H₂O). This solution (100 µl) was further diluted with 2 ml of the same solvent and filtered with 0.45 µm filters, and 20 µl of the clear solution was applied on the column.

Results and Discussion

Various extraction procedures were applied during the present study to isolate and characterize carrageenans from *H. musciformis* (red alga). The average total recovery of galactans from hot water extractions was about 39% of the dry alga (Table 1), which was similar in range as described earlier (Knutsen *et al.*, 1995). Generally, yields were high in the extracts pretreated with mild acid (38-44%). Moisture and ash contents of the products were in the range of 3.1-7.7% and 15.4-18.4%, respectively, whereas **extract-5** had very low moisture (0.32%) and the highest ash content (53%). Total sugar contents were in the range of 31.8-55.4%. High sugar content in aqueous hot extract of *H. musciformis* has been also reported in a previous communication (Bi and Iqbal, 1999). It is documented that plants belonging to Rhodophyceae (red alga) commonly have sulphated galactan (Miller and Blunt, 2002). High sulphate contents (23.6-41.0%, except in **extract-5**) and 3,6-anhydrogalactose (20-27%), which were derived from the total sugar, confirm the earlier findings for these contents reported by Chiovitti *et al.* (1996).

Various characteristic properties of the phycolloids obtained using different extraction procedures are summarized in Table 2. After extraction and drying of samples, no odour was found in any extract. Most of the extracts were brown in colour. The alkali treatment of **extract-5** gave the sample a creamish white colour, close to the colour of commercial carrageenan.

Table 1. Yield and chemical composition of algal extracts of *Hypnea musciformis* (%; w/w)

Extracts*	Yield	Moisture	Ash	Sugar contents ^a	Sulphate
Extract-1	40.0	7.7	15.7	45.3 (20.9)	31.1
Extract-2	38.0	4.6	18.4	50.8 (21.8)	25.4
Extract-3	44.2	6.9	16.3	41.1 (23.1)	35.4
Extract-4	39.1	5.1	18.1	46.5 (27.6)	30.1
Extract-5	40.0	0.32	53.0	31.8 (25.9)	14.8
Extract-6	34.2	5.4	15.4	55.4 (22.3)	23.6
Carrageenan ^c	nd ^b	3.1	15.7	40.1 (19.9)	41.0

* = see Materials and Methods for the extraction procedures used for **extracts 1-6**; a = total sugar, within parenthesis is the value of 3,6-anhydrogalactose derived from the total sugar; b = not determined; c = commercial carrageenan used as the reference

Table 2. Characteristics of phycocolloids of *Hypnea musciformis*

	Extract-1	Extract-2	Extract-3	Extract-4	Extract-5	Extract-6	Commercial carrageenan
Colour	reddish-brown	light-brown	dark-brown	light-brown	creamish-white	brown	pinkish-white
Solubility in water (2%; w/v)	dissolved at 60-70 °C	dissolved at 60-70 °C	dissolved at 60-70 °C	dissolved at room temperature	dissolved at 60-70 °C	dissolved at 60-70 °C	dissolved at room temperature
Methylene blue test	ppt formed	ppt formed	ppt formed	ppt formed	ppt formed	ppt formed	ppt formed
Milk reactivity	positive	positive	positive	positive	positive	positive	positive
pH of aqueous solution (1%; w/v)	4.4	4.2	4.7	4.8	5.2	4.8	7.7
Aqueous gel strength (2%; w/v)	non-gelling	gel formed at 4 °C	non-gelling	non-gelling	gel formed at room temperature	gel formed at 4 °C	viscous solution at 4 °C
Optical rotation ($[\alpha]_D^{25}$)	+58.2°	+48.1°	+52.0°	+52.0°	+30.0°	+64.0°	+53.8°

Except **extract-4** and the commercial carrageenan, all other samples were soluble in water (2%) at 60-70 °C within 30 min, only a very small amount of insoluble material remained in some samples. Formation of precipitate, with methylene blue, and positive test with milk are the characteristic tests of carrageenans. pH of aqueous solution (1%) of **extracts 1-6** showed acidic nature (pH = 4-5), whereas the commercial carrageenan had slightly alkaline nature (pH = 7.7). The gelling strength of the aqueous solutions (2%) was recorded at room temperature and at 4 °C. Some of the **extracts-1, 3, 4** were non-gelling, but **extract-2, 6** formed thick and viscous gels at 4 °C. It has been reported that the presence of 3,6-anhydro sugar causes gelling, but if it is replaced by the 6-sulphate sugar, the gelling power is considerably lessened and the 2,6-disulphate in place of 3,6-anhydro sugar results in the complete loss of gelling power (Percival and McDowell, 1990). This suggests that gelling property not only depended on the anhydro sugar, but was also dependent on the sulphate content of the phycocolloids. It is also possible that acid treatment resulted in the hydrolysis of the linkage at 3,6-anhydro-galactose and made the samples totally non-gelling, whereas **extract-5** with low sulphate (14.8%) showed the highest gelling strength and thus formed thick and stable gel at room temperature. Some non-gelling polysaccharides obtained from marine algal plants have been also reported by Parekh *et al.* (1989). It was surprising that the commercial carrageenan only formed viscous solution at low temperature (4 °C), which may be due to its high sulphate content (41%). The marketed

carrageenan products are blended materials, which are used for different purposes, rather than as a pure product (Thomas, 1997). The positive optical rotation of these polysaccharides indicates a predominance of α -D-glycosidic linkages in their structure. The monosaccharide composition, as determined by acid hydrolysis and paper chromatography, showed galactose as the major sugar component of each extract and released as early as 30 min of hydrolysis. Regular increases were observed, which maximized at 3 h of hydrolysis. Xylose/arabinose and glucose along with minor amounts of fucoses, were also observed in the chromatogram. The intensity of spots was high in the extracts pretreated with mild acid, which may be due to some addition of glucose from starch as a contaminant.

Infra-red technique has been commonly used in the characterization of carrageenans (Estever *et al.*, 2002; Falshaw *et al.*, 1996). The IR spectra of the crude **extracts 1-6**, along with the commercial carrageenan, were recorded (Fig. 1). All the spectra displayed a broad absorption band at 1210-1220 cm^{-1} , corresponding to sulphate ester, which is common to all the sulphated polysaccharides and increased in size with the sulphate content. In the commercial carrageenan spectra, this band was fairly sharp and strong, which is in accordance with the high sulphate content of the sample (Table 1). The diagnostic region (940 cm^{-1} - 800 cm^{-1}) of the IR spectra of polysaccharides resembled that of *kappa*-carrageenans elaborated by the red algal plant, *H. musciformis* (Knutsen *et al.*, 1995). The characteristic bands at 930 cm^{-1} and 840 cm^{-1} represent the anhydrogalactose and galactose-4-sulphate, respectively. The

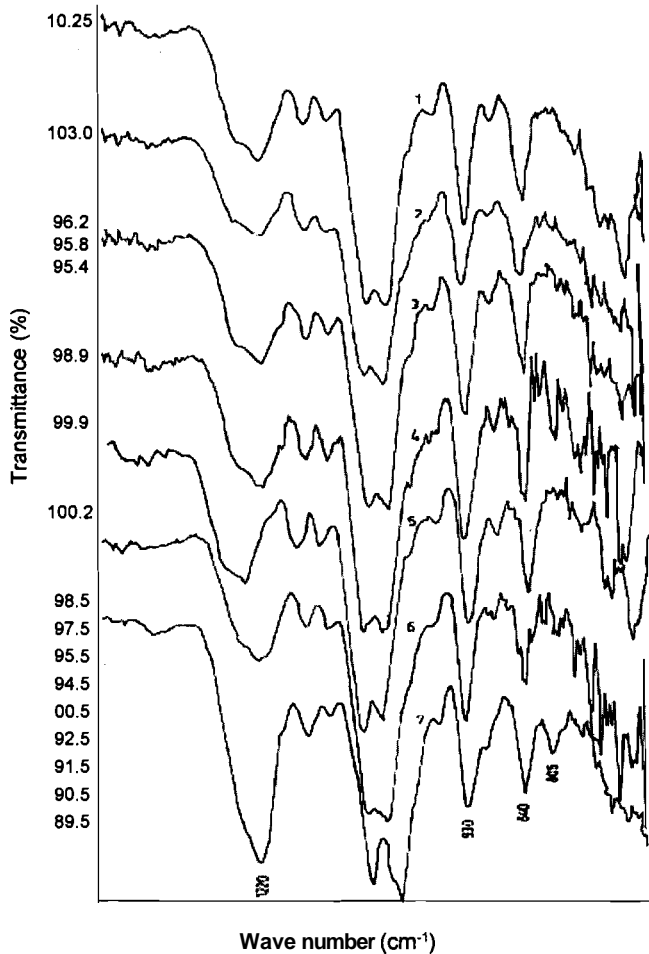


Fig. 1. Fourier transition infrared (FTIR) spectra of polysaccharide preparations from *Hypnea musciformis* (extracts 1-6) and a commercial sample of kappa-carrageenan (extracts-7); see Materials and Methods for the extraction procedures used for extracts 1-6.

lack of absorbencies at 820 and 830 cm^{-1} in all the spectra suggests that these samples were not galactans of only one common type. However, extracts-4, 5 and the commercial carrageenan had a small, but prominent, band at 805 cm^{-1} showing iota-carrageenan type structure present in these phycocolloids (Chiovitti et al., 1996), while other spectra displayed complete elimination of this absorption band. Greer et al. (1984) found that polysaccharides obtained from *H. musciformis* comprised of 73% of kappa-carrageenan and 17% of iota-carrageenan. Analysis of carrageenan from different algal sources has revealed hybrid nature of these polymers (Bellion et al., 1982). A careful examination of all the spectra leads to the conclusion that carrageenans derived from *H. musciformis* had features of both kappa- and very small portion of iota-carrageenan.

Seaweed polysaccharides have been reported as elicitors of plant defence mechanism in the tissues of chickpea in terms of induced browning and phytoalexin production (Bi and Iqbal, 2003). On the basis of chemical composition and IR spectral studies, Extract-5 was noted to be a close representative of kappa-carrageenan and was investigated for its elicitor activity in the tissues of garden peas (*Pisum sativum*). For this purpose, pea tissues were inoculated with $100\text{ }\mu\text{g glu eq/ml}$ preparation of elicitor (Extract-5). After 24 h of incubation, high intensity of browning was produced in the treated samples as compared to the control. Typical chromatogram (Fig. 2) showed the resolution of alcoholic extract of elicited tissues of peas using HPLC analysis. The prominent and sharp peak-A represents induced secondary metabolites eluted in the organic phase (100% acetonitrile). It is reported that the phytoalexin 6α -hydroxy pterocarpan and phenolic contents, as well as the enzyme activity, in peas was increased on fungal infection and elicitor treatment (Katoch et al., 2002; Banks and Dewick, 1982).

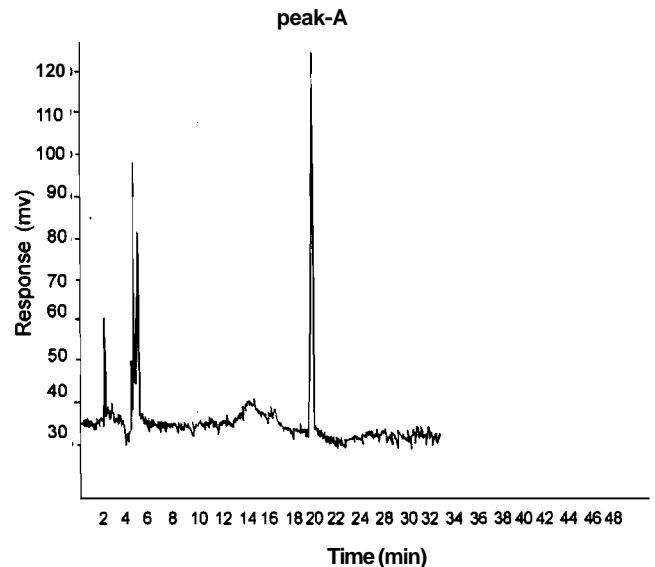


Fig. 2. HPLC separation of induced secondary metabolites (peak-A) in pea cotyledons treated with elicitor preparations (polysaccharide) of *Hypnea musciformis*.

The present studies indicated that seaweeds of Karachi coast can be utilised for the production of the commercially usable carrageenans, which have extensive application in various industrial sectors.

Acknowledgement

Authors are thankful to Mr. Muhammad Sadiq Ali, Junior Technical Officer and Mr. Muhammad Javaid, Senior Technician for their assistance in the laboratory work.

References

- AOAC. 2000. *Official Methods of Analysis of Association of Analytical Chemists*, Chapter 3, pp. 1-37, 17th edition, AOAC International, Gaithersburg, Maryland, USA.
- Banks, S.W., Dewick, P.M. 1982. Biosynthesis of the 6-hydroxy pterocarpan phytoalexin pisatin in *Pisum sativum*. *Phytochemistry* **21**: 2235-2242.
- Bellion, C., Hamer, G.K., Yaphe, W. 1982. The degradation of *Eucheuma spinosum* and *Eucheuma cottonii* carrageenans by *l*-carrageenases and *k*-carrageenases from marine bacteria. *Canad. J. Microbiol.* **28**: 874-880.
- Bi, F., Iqbal, S. 2003. Dose dependent and time course elicitor activity of *Codium elongatum* and *Ulva lactulus* (green algae) of Karachi coast. *Pak. J. Bot.* **35**: 511-518.
- Bi, F., Iqbal, S. 1999. Chemical investigation and elicitor activity of polysaccharides of red algae *Hypnea musciformis* and *Botryocladia leptopoda*. *Pak. J. Sci. Ind. Res.* **42**: 223-226.
- Chiovitti, A., Liao, M.-L., Kraft, G.T., Munro, S.L.A., Craik, D.J., Bacic, A. 1996. Cell wall polysaccharides from Australian red algae of the family Solieriaceae (Gigartinales, Rhodophyta): highly methylated carrageenans from the genus *Rhabdonia*. *Botanica Marina* **39**: 47-59.
- Dodgson, K.S., Price, R.G. 1962. A note on the determination of the ester sulphate content of sulphated polysaccharides. *Biochemical Journal* **84**: 106-110.
- Estevez, J.M., Ciancia, M., Cerezo, A.S. 2002. Carrageenans biosynthesized by carposporophytes of red seaweeds *Gigartina skottsbergii* (Gigartinaceae) and *Gymnogongrus torulosus* (Phylloporaceae). *J. Phycol.* **38**: 344-350.
- Falshaw, R., Furneaux, R.H., Wong, H., Liao, M.-L., Bacic, A., Chandkrachang, S. 1996. Structural analysis of carrageenans from Burmese and Thai samples of *Catenella nipae* Zanardini. *Carbohydrate Res.* **285**: 81-98.
- Georg, K., William, H.H. 1974. *Staining of Thin Layer of Paper Chromatograms for Sugar by Ag⁺/OH⁻*, *Hand Book of Micromethods for the Biological Sciences*, pp. 91-93, Van Nostrand Reinhold Company, New York, USA.
- Greer, C.W., Shomer, I., Goldstein, M.E., Yaphe, W. 1984. Analysis of carrageenan from *Hypnea musciformis* using *k*- and *l*-carrageenases and ¹³C-NMR spectroscopy. *Carbohydrate Res.* **129**: 189-196.
- Husain, S.A., Saeed, V.A., Masood, A. 2001. Economic seaweeds of Pakistan coast. *Pak. J. Mar. Biol.* **7**: 281-290.
- Katoch, R., Mann, A.P.S., Sohal, B.S. 2002. Elicitor watering influences the activity of defense related enzymes in pea. *Indian J. Plant Physiol.* **7**: 388-391.
- Knutsen, S.H., Murano, E., D'Amato, M., Toffanin, R., Rizzo, R., Paoletti, S. 1995. Modified procedures for extraction and analysis of carrageenan applied to the red alga *Hypnea musciformis*. *J. Appli. Phycol.* **7**: 565 - 576.
- Miller, I.J., Blunt, J.W. 2002. Mobility of sulphate ester during structural determination of red algal galactans. *Botanica Marina* **45**: 559-565.
- Nicholson, R.L., Wood, K.V. 2001. Phytoalexin and secondary products, where are they and how can we measure them. *Physiol. Mol. Plant Pathol.* **59**: 63-69.
- Nishizawa, M. 2002. Thickening stabilizer from seaweeds. *Shokuhin Eiseigaku Zasshi* **43**: J1- J6.
- Parekh, R.G., Doshi, Y.A., Chauhan, V.D. 1989. Polysaccharides from marine red algae *Acanthophora spicifera*, *Grateloupia indica* and *Halymenia porphyroides*. *Indian J. Marine Sci.* **18**: 139-140.
- Percival, E., McDowell, R.H. 1990. Algal polysaccharides. In: *Methods in Plant Biochemistry*, vol. **2**, *Carbohydrates*, P.M. Dey (ed.), pp. 523-547, Academic Press, London, UK.
- Thomas, W.R. 1997. Carrageenan. In: *Thickening and Gelling Agents for Food*, A. Imeson (ed.), pp. 45-59, 2nd edition, Blackie Academic and Professional, London, UK.
- Usov, A.I. 1992. Sulphated polysaccharides of the red seaweeds. *Food Hydrocolloids* **6**: 9-23.
- Whitehead, I.M., Dey, P.M., Dixon, R.A. 1982. Differential pattern of phytoalexin accumulation and enzyme induction in wounded and elicitor treated tissues of *Phaseolus vulgaris*. *Planta* **154**: 156-164.
- Yaphe, W., Arsenault, G.P. 1965. Improved resorcinol reagent for the determination of fructose and of 3,6-anhydrogalactose in polysaccharides. *Anal. Biochem.* **13**: 143 -148.

Comparative Studies on the Adsorption Properties of Powdered Activated Carbon and Propenoic Acid Modified Sawdust in the Treatment of Secondary Palm Oil Mill Effluent

M. O. Osuide^{a*}, C. M. A. Ademoroti^b, V. U. Okojie^a and F. E. Igbnavbiere^a

^aDepartment of Chemistry, Ambrose Alli University, Ekpoma, Nigeria

^bDepartment of Chemistry, University of Benin, Benin City, Nigeria

(received December 28, 2004; revised July 18, 2006; accepted July 22, 2006)

Abstract. Propenoic acid monomer was used to modify pulped cellulosic materials (sawdust). The sorption properties of the propenoic acid modified sawdust (PAMS) were compared with those of powdered activated carbon (PAC) in the tertiary treatment of palm oil mill effluent, previously clarified with iron(III) chloride plus lime (secondary effluent). The adsorption processes were effected in a fluidized bed reactor (FBR) at a pressure of 80 kiloNewton per meter square (kNm⁻²). Optimum amount of PAC and PAMS used for the fluidized adsorption of contaminants from the secondary palm oil mill effluent (POME) were 2.5 g/l and 4.0 g/l, respectively. These sorption processes were found to be optimum at 10 min and 50 min for PAC and PAMS, respectively. At optimum sorption conditions, removal differentials of 28.6%/g chemical oxygen demand, 19.1%/g suspended solids, and 19.3%/g colour in favour of PAC were established. The application of optimum conditions for adsorption, for both adsorbents, to the bulk treatment of the palm oil mill effluent yielded a clear effluent with wider reuse applicability.

Keywords: metal adsorption, palm oil mill effluent, propenoic acid treated sawdust, fluidized bed reactor, activated carbon, wastewater treatment

Introduction

Adsorption processes are becoming viable options for the removal of non-biodegradable substances from conventionally treated wastewaters (Osuide *et al.*, 2003; Lopez-Delgado *et al.*, 1998; Allen and Brown, 1995; Lo and Lin, 1989; AWTR-19, 1967). These substances exist as fine colloids or true solutes in these wastewaters, even after the wastewaters have been subjected to primary and secondary treatment processes.

Large-scale palm oil processing industries use waste stabilization ponds (WSPs) for the secondary treatment of their effluents. These ponds stabilize wastewaters through biodegradation processes. It has been observed that these pond systems, in typical cases, are quite elaborate in design and construction. The effluents so produced, do not fully meet the effluent discharge guidelines as stipulated by the Ministry of Environment, Nigeria (FEPA, 1988). With an average chemical oxygen demand (COD) value of 1096 mg/l, dissolved oxygen (DO) of 2.0 mg/l, and an oil and grease (O-G) value of 19,446 mg/l, in a typical study case, the usual treatment methods still leave a lot to be desired (Osuide, 2004).

Dependence on the natural purification schemes to continue the stabilization processes does not guarantee the protection of the environment owing to the large volume of wastewater

involved. It also does not provide for the extension of available water resources via the possibility of recycling.

Studies have generally shown the removal differentials of between 45% and 75% for most water quality parameters in favour of chemical treatment of industrial wastewaters as against treatment by waste stabilization pond systems (AWTR-19, 1967). Besides, chemical treatment provides for the possibility of recycling of industrial effluents.

Powdered activated carbon (PAC) is the most popular adsorbent for removing such recalcitrant pollutants from solutions in tertiary treatment steps (Lo and Lin, 1989; AWTR-19, 1967). However, the cost of preparing PAC is becoming quite prohibitive. In recent times, alternative materials are being sought to replace PAC in adsorption processes. Cellulosic materials available in the form of agricultural byproducts are now the choice. The capacity of these cellulosic materials to take up contaminants, particularly heavy metal ions from synthetic and natural standard solution have been examined variously by people working in this area (Saeed *et al.*, 2005; Saeed and Iqbal, 2003; Saeed *et al.*, 2002; Pelekani and Snoeyink, 1999; Lopez-Delgado *et al.*, 1998; Allen and Brown, 1995). The results show not much of a success story, though indicate the inherent potential. More recently, however, some workers have used active monomers and other reactive groups to modify cellulosic materials before application to sorption processes.

*Author for correspondence; E-mail: moosuide@yahoo.com

Such monomers include cyanoethene, 2-propenoic acid, and other monomers of acidic and basic formaldehyde or thioglycolic groups. These have been found to considerably enhance the uptake capacities of the cellulosic materials thus modified. By and large, the applications of these have been also extended to the treatment of standard synthetic metal ions solutions (Okieimen *et al.*, 1991; 1986; Randall *et al.*, 1978). Owing to the continuous enlargement of agricultural produce processing industries, there is a need to investigate for cheaper alternative sorption substrates that can be employed in the tertiary treatment of industrial effluents in anticipation for a wider range of effluent reuse, or at least for a safer discharge into the environment.

Sorption properties of propenoic acid modified sawdust (PAMS) and those of powdered activated carbon (PAC) were investigated for their comparative ability for the tertiary treatment of chemically clarified palm oil mill effluent (POME).

Materials and Methods

The wastewater material. Palm oil mill processing effluent (POME) obtained from a palm oil mill industry in Benin City, Nigeria, was treated using experimentally determined optimum conditions in a preliminary study. The preliminary study included: determination of optimum time of sedimentation for POME over a time range of 10-100 min at 10 min intervals (60 min was found optimum); determination of the amount of FeCl_3 required as coagulant over a concentration range of 200-700 mg/l at 50 mg/l interval (350 mg/l FeCl_3 was found to be optimum at pH 4.6); and the amount of CaO (lime) required as flocculant over a range of 25-150 mg/l at 25 mg/l interval, in constant mixture with 350 mg/l FeCl_3 (75 mg/l CaO was found to be optimum at a mixture pH of 5.2). These optimum conditions were then applied in the treatment of raw POME via integrated physicochemical unit treatment processes. The unit treatment processes included sieving and sedimentation (primary treatment), coagulation and flocculation using 350 mg/l FeCl_3 plus 75 mg/l CaO (lime) (secondary treatment) (Osuide, 2004; AWWA, 1989; Ademoroti, 1985). This effluent was sand-filtered to yield the secondary effluent used in the present study.

Preparation of the sorbent. The powdered activated carbon (PAC; Nentech product) was reactivated at 110 °C for 24 h before use. Sawdust, obtained from a local sawmill in Ekpoma town, Nigeria, was modified using 2-propenoic acid. The modification process was as follows: the raw sawdust was dried in the sun to constant weight. Methanol was used to extract excretory and fatty materials from the dried sawdust. 50.0 g portions of the extracted cellulose material was pulped for 1 h in 800 ml hot water using 18.0 ml ethanoic acid and 22.5 g sodium chlorite, which were added in three portions

of 6.0 + 7.5 g, respectively, in a well ventilated hood (fume cupboard). The pulped sawdust (holocellulose) was filtered and air-dried, and then placed in a three-necked round bottom flask containing 36.0 ml of 0.1% (v/v) nitric acid. The flask was placed in a waterbath maintained at 40 °C. Ceric ammonium sulphate (0.674 g; equivalent to 0.26 g ceric ion, Ce^{4+}) was dissolved in 6.0 ml of 0.1% (v/v) nitric acid, which acted as the initiator, and added to the contents of the flask. The flask was shaken to ensure good dispersion. 2.0 g propenoic acid monomer was added to the flask, stoppered and shaken continuously for 5 min, and then shaken briefly at 10 min intervals for a total period of 1 h. After 1 h, the pulp was washed, filtered and air-dried at room temperature. The copolymer or homopolymer was later extracted using dimethylformamide over a period of 24 h, after which it was filtered and air-dried at room temperature to constant weight (Okieimen *et al.*, 1986). This yielded the propenoic acid modified sawdust (PAMS) used in the present studies.

Fluidized bed reactor. A portable laboratory model of a fluidized bed reactor (FBR) was designed and built using Perspex sheets, following the Pillai procedure described in detail elsewhere with (Ademoroti, 1979), as shown in Fig 1. The main compartment of the FBR is divided into two parts: the lower and the upper chambers. The lower chamber is fitted with a funnel through which enters the compressed air into the system, then passing into the upper chamber through perforated partition. The upper chamber is the fluidization compartment where the chemically treated effluent and sorbents are mixed and fluidized by the compressed air from a compressor. The optimum fluidization pressure was earlier determined as 80 kilo Newton per meter square (kNm^{-2}) from trial runs (Osuide, 2004).

Sand filtration bed. Loose fine sand of aggregates of 0.5-1.0

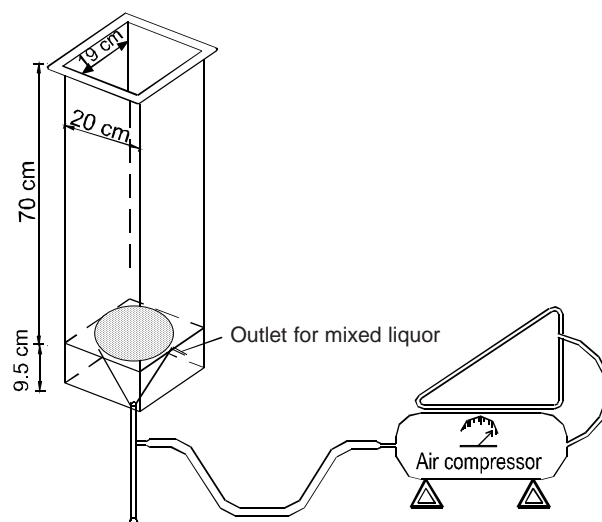


Fig. 1. Fluidized bed reactor (FBR) developed for the treatment of secondary palm oil mill effluent.

mm gradings was obtained from river dredgings. It was thoroughly washed with water and rinsed several times with distilled water. The washed sand was further leached with 1% (v/v) of hydrochloric acid at a rate of 1 ml per min using 300 ml of the acid in a glass column. It was then rinsed with distilled-deionised water until it became free of acid, after which it was sun-dried. The leached sand was packed into glass column of internal dia 6.71 cm. An optimum height of the sand column for the filtration of the sorptively fluidized palm oil mill effluent was obtained from test run as 90.0 cm. The total length of the glass column from tip of the tap to top was 81.0 cm. Two glass columns were used to accommodate the required 90.0 cm of sand column for filtration, by allowing each of the glass column to accommodate 45.0 cm height of the sand column. The total filtered liquid was passed through the two glass columns in series.

Batch procedure. Batch tests were carried out on one litre each of the secondary palm oil mill effluent to establish the optimum time (min) and the amount of adsorbents required for sorption fluidization in the FBR. Three important and quickly determinable parameters were used to ascertain optimum conditions for adsorption, which included: chemical oxygen demand (COD), suspended solids (SS), and colour (as absorbance at 465 nm). The optimal removal levels were based on percentage levels of the parameters. Four readings were taken in each case and the average value was calculated.

Optimum time for sorption fluidization in the FBR. With moderate amount of PAC or PAMS (2.0 g) the sample was fluidized

for a given time (5, 10, 20, 30, 40, 50 and 60 min), at an optimum pressure of 80 kNm², for both the adsorbents. Following the sorption pattern observed for PAMS, sorption time for this sorbent was extended to 80 min (Ademoroti, 1979).

Optimum amounts of adsorbents for fluidization in the FBR.

Different amounts of the adsorbents, PAC or PAMS, were used at the constant pressure of 80 kNm², at the optimum condition of time for the respective adsorbents.

Analysis. The analytical procedures used for this study were as described by APHA (1989). Typical analysis of the secondary effluent (FeCl₃ + lime pre-treated and sand filtered palm oil mill effluents is shown in Table 1.

Abbreviations used: TS (total solids), DS (dissolved solids), SS (suspended solids), DO (dissolved oxygen), BOD₅ (5-day biochemical oxygen demand), COD (chemical oxygen demand), NO₃⁻-N (nitrate-nitrogen), SO₄⁻² (sulphate), Cl⁻ (chloride), PO₄⁻³ (phosphate), O and G (oil and grease), TBC (total bacterial count).

Results and Discussion

The secondary POME FeCl₃ (coagulated + lime treated) had a light orange colour and could only manifest minimal sediments when left to stand overnight. The data shown in Table 1 depict a better quality effluent in comparison with what the processing industries usually let out into the environment. This, however, still falls short of the guidelines set out by the Ministry of Environments, Nigeria (Table 1). The reuse possibility of

Table 1. Analysis of the FeCl₃ + lime pre-treated and sand filtered palm oil mill effluent (secondary effluent)

Parameters	Range of values	Mean	SD	SE	FEPA limits*
Colour (nm)	0.199-0.26	0.202	0.060	0.027	-
Odour	slightly rancid, oily odour	-	-	-	-
Temperature (°C)	23-28	25.75	2.217	0.992	-
pH	5.0-5.9	5.6	22.236	9.944	6.9
Turbidity (NTU)	41.6-59.2	51.28	7.352	3.288	-
Conductivity (µS/cm)	(0.5-0.7)x10 ³	0.61 x10 ³	0.098	0.044	-
Total solids (mg/l)	360-520	440.00	67.330	30.111	2000
Suspended solids (mg/l)	306-501	367.7	52.009	23.259	30
Dissolved solids (mg/l)	153-189	172.25	15.435	6.903	2000
Dissolved oxygen (mg/l)	2.8-3.4	3.08	0.250	0.112	-
BOD ₅ (mg/l)	72-101	89.50	13.429	6.006	30
COD (mg/l)	300-306	305.00	15.055	6.733	50
Nitrate-N (mg/l)	1.09-1.25	1.193	0.071	0.032	10
Sulphate (mg/l)	0.3-1.32	0.780	0.435	0.195	500
Chloride (mg/l)	120-150	136.75	13.841	6.190	600
Phosphates (mg/l)	1.3-1.32	1.318	0.024	0.011	5.0
Oil and grease (mg/l)	600-620	611.75	20.156	9.014	10
TBC (per 100 ml)	(0.60-1.60) x 10 ⁷	1.100 x 10 ⁷	4.761x 10 ⁶	5.214 x 10 ⁶	-

* = FEPA (1988); TBC = total bacterial count; SD = standard deviation; SE = standard error; NTU = nephelometric turbidity unit

this effluent are still limited, hence the necessity for tertiary treatment. The values of SS (367.7 mg/l), BOD₅ (89.50 mg/l), COD (305 mg/l), and O-G (611.0 mg/l), are above the mandatory limits (FEPA, 1988). All the other values, however, fall below the guideline limits for the respective parameters.

The TBC test was aimed at highlighting the presence of bacterial load, which may be involved in the accompanying biodegradation processes which could be occurring along with chemical/adsorption treatment processes.

The variation of sorption levels with time, using PAC and PAMS, respectively, are shown in Fig. 2 and Fig. 3.

Optimum removal of contaminants was observed to be at 10 min fluidization for PAC adsorption. The rapid rise in uptake level

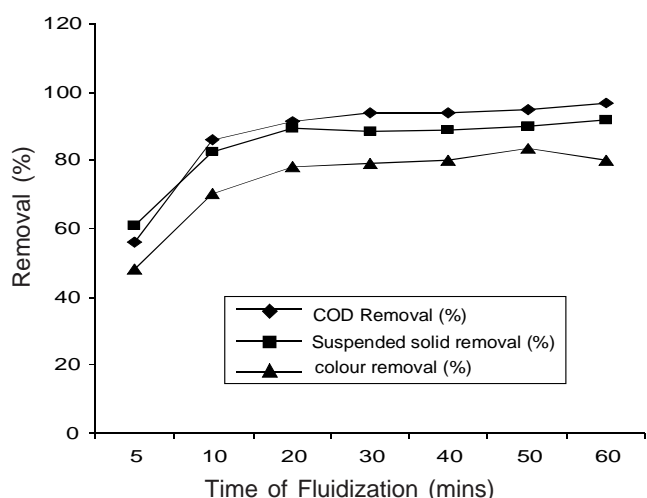


Fig. 2. Effect of variation of time of contact between 2.0 g powdered activated carbon (PAC) and the secondary palm oil mill effluent per liter during fluidization at 80 kNm⁻² pressure.

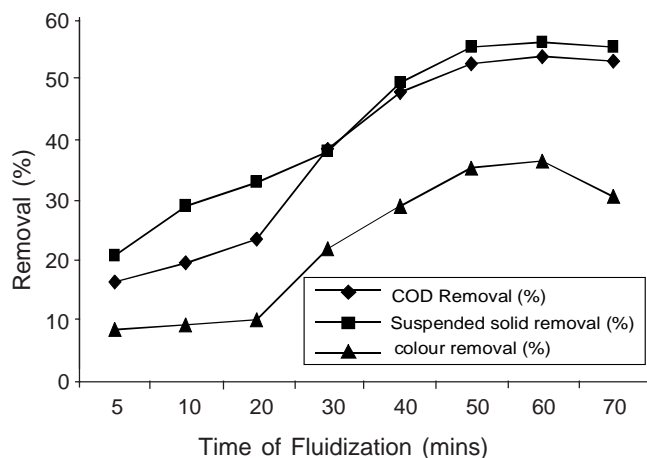


Fig. 3. Effect of variation of time of contact between 2.0 g propenoic acid modified sawdust (PAMS) and the secondary palm oil mill effluent per litre during fluidization at 80 kNm⁻² pressure.

between 5 and 10 min typically depicts a physical process, which also suggests saturation of adsorption surface beyond 10 min.

The uptake of materials from solution by PAMS was more gradual, and the curves rose steadily from 5 min through 10 min and attained peaks at 50 min (Fig. 4). Beyond 60 min, no significant rise in the curves was noticed even up to 80 min. The differences in the uptake pattern (Fig. 2, Fig. 3), suggest different uptake mechanisms for the two adsorbents. Chemisorption is more probable with PAMS. Fig. 4 and 5 illustrate, respectively, the optimum amount of PAC and PAMS required for the sorption clarification of the secondary effluent.

These show narrower range of variation for the amount of PAC required than is needed for PAMS. Preliminary studies indicate an optimum range for PAC between 2 and 3 g; 2.5 g PAC yielded optimum removal for COD, SS and colour from the effluent. But with PAMS, 4.0 g was required for even lower level percentage removal.

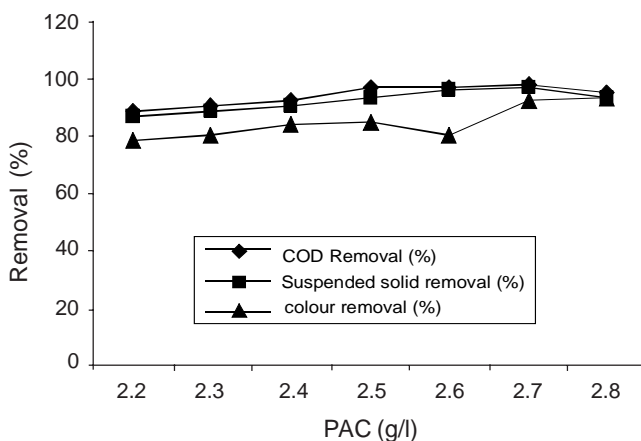


Fig. 4. Optimum amount of powdered activated carbon (PAC) required for the fluidization of secondary palm oil mill effluent at 10 min.

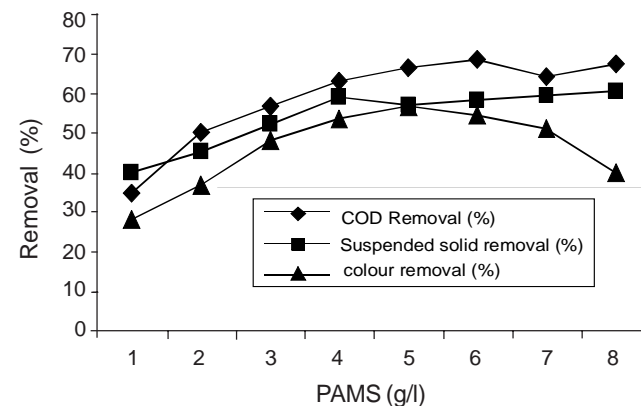


Fig. 5. Optimum amount of propenoic acid modified sawdust (PAMS) required for the fluidization of secondary palm oil mill effluent at 50 min.

Tables 2 and 3 show the level of clarification by PAC and PAMS, respectively, against the initial values as shown in Table 1.

It has been shown that during the sorption process, the non-biodegradable substances, which could inhibit biodegrading processes (enzyme inhibition), are more favourably removed by adsorption from the effluent medium, leaving the effluent

medium more favourable for microbial breakdown of the contaminant materials (Suidan *et al.*, 1996) This dual clarification process leaves the effluent clearer than only the adsorption process would have achieved.

The sorption patterns obtained in the present studies suggest different sorption mechanisms for PAC and PAMS. The high

Table 2. Analysis of the powdered activated carbon (PAC) fluidized secondary palm oil mill effluent at 10 minutes

Parameters	Range of values	Mean	SD	SE	Reduction (%)
Colour (nm)	0.016-0.022	0.01925	0.002754	0.001377	92.5
Odour	slightly rancid oily odour				-
Temperature (°C)	23-27	24.75	2.061553	1.030776	-
pH	6.1-6.5	6.325;7.0 ^a	0.170783	0.085391	-
Turbidity (NTU)	20-28	24.5	3.696846	1.848423	53.5
Conductivity (µS/cm)	(0.13-0.39) x 10 ³	0.28	0.119164	0.059582	63.3
Total solids (mg/l)	105.3-162.4	135.925	23.70758	11.85379	81.1
Suspended solids (mg/l)	45.3-95.3	70.45	21.48309	10.74155	70.9
Dissolved solids (mg/l)	60.0-67.1	63.3	2.947315	1.473658	84
Dissolved oxygen (mg/l)	5.2-6.0	5.605	0.408289	0.204145	75.8*
BOD ₅ (mg/l)	6.0-7.8	6.8975	0.805828	0.402914	92.7
COD (mg/l)	28-33	30.525	2.214159	1.107079	89
Nitrate-N (mg/l)	0.1-0.6	0.4375	0.203695	0.101848	65.8
Sulphates (mg/l)	0.01-0.04	0.025	0.01291	0.006455	85.7
Chlorides (mg/l)	0.21-0.29	0.2525	0.038622	0.019311	78.5
Phosphates (mg/l)	0.61-0.73	0.675	0.051962	0.025981	46.6
Oil and grease (mg/l)	86-90	88.25	1.666333	0.833167	85.5
TBC (per 100 ml)	(0.09-0.15)x10 ⁶	1.250 x 10 ⁵	26457.51	2.646 x 10 ⁴	99.1

* = increase %; ^a = adjusted pH; TBC = total bacterial count; NTU = nephelometric turbidity unit

Table 3. Analysis of the propenoic acid modified sawdust (PAMS) fluidized secondary palm oil mill effluent at 50 minutes

Parameters	Range of values	Mean	SD	SE	Reduction (%)
Colour (nm)	0.066-0.071	0.06875	0.002217	0.000573	70.8
Odour	slightly rancid oily odour	-	-	-	-
Temperature (°C)	25-28	26.225	1.265899	0.326854	-
pH	5.99-6.3	6.1225;7.0 ^a	0.152834	0.039462	-
Turbidity (NTU)	38-46.4	42.025	3.720551	0.960642	15
Conductivity (µS/cm)	(0.38-0.44) x 10 ³	0.41	0.02582	0.006667	33.3
Total solids (mg/l)	250-360	295.75	46.20516	11.93012	48.5
Suspended solids (mg/l)	61-106	91.25	20.83867	5.38052	37.2
Dissolved solids (mg/l)	189-254	220.5	31.39533	8.106239	49.4
Dissolved oxygen (mg/l)	3.80-4.0	3.915	0.086987	0.02246	18.5*
BOD ₅ (mg/l)	80-112	95.175	13.97053	3.607176	9.6
COD (mg/l)	200-260	229.25	29.22756	7.546522	21.3
Nitrate-N (mg/l)	1.0-1.20	1.135	0.091469	0.023617	1.7
Sulphates (mg/l)	0.08-0.12	0.0975	0.017078	0.00441	47.6
Chlorides (mg/l)	0.51-0.72	0.6275	0.096047	0.024799	52.4
Phosphates (mg/l)	0.80-1.0	0.91	0.088694	0.022901	29
Oil and grease (mg/l)	99.5-268	184.475	71.69009	18.5103	57.5
TBC (per 100 ml)	(0.10-1.2)x10 ⁷	5.03 x 10 ⁶	3.229 x 10 ⁵	3.33 x 10 ⁶	91.5

* = increase %; ^a = adjusted pH; TBC = total bacterial count; NTU = nephelometric turbidity

amount of the required PAC might have been caused by the size of the colloidal and aqueous contaminants, most of which at this stage exist as contaminant coagulant complexes. These large molecular moieties and the oily macromolecular structures may have sizes that are too large for the micropores of the PAC. It follows that possibly only the surface adsorption occurs. Therefore, if surface unimolecular coverage is the uptake mechanism, then quite reasonable quantity of PAC would be required to achieve a clear solution. The initial rapid uptake at 0-10 min suggests a physical process that can be interpreted using the Freundlich isotherms model, however, the heterogenous nature of the effluent makes uniform interpretation difficult.

Cellulosic materials have been shown to be a repository of some reactive groups such as $>C=O$, $-CHO$, $-HS$, $-OH$, etc. Some of these might still remain after treatment of the cellulosic material to provide sites for contaminant uptake via a formal bond (Lopez-Delgado *et al.*, 1998). Besides, the grafted moiety presents a hydrophobic portion and hydrophilic functional group: $(-CH_2-CH_2-COOH)$. Hence, it is proposed here that H^+ ion likely destabilizes the electrical colloidal and aqueous states of the contaminants. These become more disposed to be chemisorbed on active sites and physisorbed on hydrophobic matrices on the PAMS. At the optimum sorption time and amount of adsorbents, a comparison between the adsorptive capacities of PAC and PAMS shows a removal differential of 28.6%/g COD, 19.1%/g SS and 19.3%/g colour in favour of PAC. That less than 30% removal differential per gram adsorbent was observed between the adsorbents suggests that modified cellulosic materials could be used as substrates for tertiary clarification of secondary effluents. It is obvious that a follow-up disinfection step to eliminate the microbial community, will precipitate left-over contaminants and "shelf" the effluent. This will result in enhance the effluent quality and increase its reuse applicability.

Conclusion

Modified cellulosic materials are capable of yielding sorbents with uptake capacities comparable with those of powdered activated carbon. With an uptake differential of less than 30% per gram, 2-propenoic acid modified sawdust portends a viable alternative to PAC.

References

- Ademoroti, C.M.A. 1985. Integrated biological/chemical wastewater treatment. *Effluent and Water Treatment Journal* **25**: 237-241.
- Ademoroti, C.M.A. 1979. Studies on Physicochemical Methods of Wastewater Treatments. *Ph.D Thesis*, pp. 302-225, University of London, London, UK.
- Allen, S.P., Brown, P.A. 1995. Isotherm analysis for single component and multi-component metal sorption onto lignite. *J. Chem. Technol. Biotechnol.* **62**: 17-24.
- APHA. 1985. *Standard Methods for the Examination of Water and Wastewater*, American Public Health Association, Washington DC, USA.
- AWTR-19. 1967. *Advanced Waste Treatment Research Summary Report; The Water Pollution Control Research Series*, July 1964-July 1967, WP-20-AWTR-19, pp. 4-7, Advanced Waste Treatment Research, Summary Report, The Department of Interior, Federal Water Pollution Control Administration, Washington DC, USA.
- AWWA. 1989. Coagulation as an integrated water treatment process. In: *Coagulation Committee Report*, J. American Water Works Assoc. **18**: 72-78.
- FEPA. 1988. *National Interim Guidelines and Standards for Industrial Wastes Management in Nigeria*, pp. 46-55, Federal Environmental Protection Agency, Ministry of Environment, Abuja, Nigeria.
- Lo, S.L., Lin, C.Y. 1989. Adsorption of heavy metals from wastewater with activated sludge. *J. Chin. Inst. Engg.* **12**: 451-456.
- Lopez-Delgado, A., Perez, C., Lopez, F.A. 1998. Sorption of heavy metals on blast furnace sludge. *Water Res.* **32**: 989-996.
- Okieimen, F.E., Okundia, E.U., Ogbefun, D.E. 1991. Sorption of cadmium and lead ions on modified groundnut (*Arachis hypogaea*) husks. *J. Chem. Technol. Biotechnol.* **51**: 97-103.
- Okieimen, F.E., Ebhodaghe, F., Ebhoaye, J. 1986. Grafting acrylonitrile and acrylic acid monomers on cellulosic materials. *J. Appl. Polymer Sci.* **31**: 1275-1280.
- Osuide, M.O. 2004. Studies on the Application of Chemical Clarification/Adsorption Techniques to Industrial Effluent Treatment. *Ph.D Thesis*, pp. 81-83, 109-110, University of Benin, Benin City, Nigeria.
- Osuide, M.O., Ademoroti, C.M.A., Okogie, V.U. 2003. Integrated physico-chemical and fluidized sorptive treatment of palm oil mill processing wastewater. *Adv. Nat. Appl. Sci. Res.* **1**: 99-119.
- Pelekani, C., Snoeyink, V.L. 1999. Competitive adsorption in natural water: role of activated carbon pore size. *Water Res.* **33**: 1209-1219.
- Randall, J.M., Hautala, E., McDonald, G. 1978. Binding of heavy metal ions by formaldehyde-polymerised peanut skins. *J. Appl. Polymer Sci.* **22**: 379-387.
- Saeed, A., Iqbal, M. 2003. Bioremoval of cadmium from aqueous solution by black gram husk (*Cicer arietinum*). *Water Research* **37**: 3472-3480.
- Saeed, A., Akhter, M.W., Iqbal, M. 2005. Removal and recovery of heavy metals from aqueous solution using papaya wood as new biosorbent. *Separation and Purification Technology* **45**: 25-31.
- Saeed, A., Iqbal, M., Akhtar, M.W. 2002. Application of biowaste materials for the sorption of heavy metals in contaminated aqueous medium. *Pak. J. Sci. Ind. Res.* **45**: 206-211.
- Suidan, M.T., Flora, J.R.V., Boyer, T.K., Wuellner, A.M., Narayanan, B. 1996. Anaerobic dechlorination using a fluidized-bed GAC reactor. *Water Res.* **30**: 160-170.

Short Communication

Some Studies on the Changes in the Composition of Coal Ash and Bottom/Fly Ash Produced in Atmospheric Fluidized Bed Combustor

Ismat Ali* and M. Mohsin Ali

Fuel Research Centre, PCSIR, Shahrah-e-Dr. Salimuzzman Siddiqui, Karachi-75280, Pakistan

(received October 26, 2004; revised November 16, 2005; accepted November 19, 2005)

Abstract. A study on the ash of Lakhra lignite coal and the bottom/fly ash, obtained from combustion of Lakhra lignites in atmospheric fluidized bed combustor (AFBC) was carried out. It has been observed that the absence of alkali metals was of significant importance, as alkali metals were responsible for agglomeration in the AFBC.

Keywords: atmospheric fluidized bed combustion, coal energy, environmental pollution, coal, Lakhra lignites

The role of mineral coal in the energy consumption of Pakistan is insignificant (Table 1). This needs to be given urgent attention. Annual mining of coal in Pakistan is less than three million ton (Ali, 1995), whereas coal deposits in the country have been estimated to be 185 billion ton (ESP, 1999). The Thar coal-fields are the largest coal deposits in the country, but these have yet to be developed. The Lakhra coal-fields are considered to be the largest fields from the point of view of coal mining. According to a survey report, about 91% of the mined coal is used for burning in brick kilns, while the remainder is used for power generation (ESP, 2000). Based on the indigenous source of coal, only one coal-fired power plant is operating in the country. The analyses of Lakhra coal used in the plant are given in Tables 2 and 3. The three coal-fired power plant units of 50 MW each, situated at Khanot, Sindh, Pakistan, which were based on the Lakhra lignite atmospheric fluidized bed combustion (AFBC), and the 15 MW Sor-Range coal-based power plant at Quetta have since been scrapped.

This paper reports a study carried out on the ash of Lakhra lignites and bottom/fly ash, obtained from atmospheric fluidized bed combustion (AFBC), which are burnt along with limestone to trap sulphur. These studies were aimed at determining the alkali metals present, the extent of sulphur fixed, and the utilization of ash for some useful purposes such as insulation bricks, road construction and as a soil conditioner.

The commercial power plants, based on atmospheric fluidized bed combustion of coal, have the necessary quality control facilities to routinely analyse coal and limestone, as supplies of these materials vary considerably in their compositions from lot to lot. The analyses of coal ash and

bottom/fly ash, therefore, also show wide variations. The results reported in the present studies represent only one batch of the supplies obtained from a testing atmospheric fluidized bed combustor. Analyses of these supplies were carried out on standard analytical computerized equipment.

Table 1. The percentage contribution of various fuels in Pakistan*

Fuels	1996-97	1997-98	1998-99
Oil	48.0	46.8	47.7
Natural gas	29.4	31.3	31.0
Electric	15.4	15.5	14.6
Coal	6.3	5.4	5.7
LPG	0.9	1.0	1.1

* = ESP (2000; 1999); LPG = liquified petroleum gas

Table 2. Ultimate analysis of Lakhra lignites (dry; ash-free basis)

Elements	Percentage
Carbon	58.5 - 72.4
Hydrogen	4.5 - 5.8
Nitrogen	0.9 - 1.4
Sulphur	2.4 - 16.7
Oxygen	14.4 - 22.3

Table 3. Proximate analysis of Lakhra lignites

Constituents	Percentage
Moisture (%)	13.01 - 20.12
Volatile matter (%)	17.49 - 42.8
Ash (%)	28.82 - 37.37
Fixed carbon (%)	12.68 - 31.07
Heating value (MJ/kg)	14.31 - 21.05

*Author for correspondence

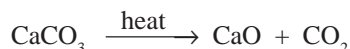
The ultimate (elemental) analyses of coal were carried out on CHN-600 (LECO, USA), which have been shown in Table 2. The proximate analysis of coal was done on Mac-400 (LECO, USA), which is shown in Table 3. The sulphur content of coal was determined on sulphur determinator SC-132 (LECO, USA) as shown in Table 2. The heating (calorific) value was determined on the Parr oxygen adiabatic bomb calorimeter (Table 3). Analysis of ash and bottom/fly ash has been given in Table 4.

Table 4. Comparison of ash of Lakhra coal and bottom/fly ash obtained from atmospheric fluidized bed combustion plant

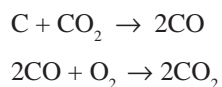
Constituents	Lakhra coal ash (%)	Bottom ash (%)	Fly ash (%)
Silica	32.76	40.30	45.20
Alumina	20.18	25.85	22.30
Iron oxide	30.23	10.00	14.85
Calcium oxide	4.55	10.52	7.33
Magnesium oxide	2.28	2.53	3.03
Sodium oxide	1.18	0.66	0.53
Potassium oxide	0.62	0.10	0.30
Sulphur trioxide	16.9	3.85	3.49

The ultimate (elemental) and proximate analyses of the Lakhra lignite coal showed that sulphur and ash were higher, as compared to good quality coals, such as bituminous, anthracite, and even lignites found in the USA and China. The Pakistani lignites, in general, and the Lakhra lignites in particular, have been noted to be high in sulphur and ash.

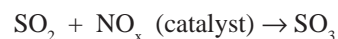
During the combustion of coal in the atmospheric fluidized bed combustor (AFBC), sulphur changes to SO_2 or SO_3 , which is absorbed/fixed in CaCO_3 (calcinated in AFBC):



The carbon dioxide (CO_2) produced also reacts with carbon of coal to form carbon monoxide (CO), which oxidizes to CO_2 in excess air in the AFBC as below:



During the combustion of coal in the AFBC, NO_x forms from the oxidation of nitrogen compounds present in the coal (Ali, 1997). The NO_x acts beneficially as a catalyst for the oxidation of sulphur dioxide (SO_2) to sulphur trioxide (SO_3). It may also be observed that NO_x is not formed in the AFBC from the oxidation of air nitrogen (N_2), as the temperature of the bed is maintained around 800°C .



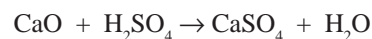
Sulphur trioxide (SO_3) reacts with lime or limestone as shown below:



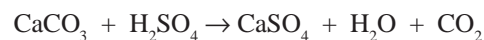
Sulphur trioxide (SO_3) may also react with the water vapours, produced during combustion, forming sulphuric acid (H_2SO_4):



The CaO produced in the AFBC, due to calcination of limestone, reacts with sulphuric acid (H_2SO_4) and produces calcium sulphate (CaSO_4):



Sulphuric acid (H_2SO_4) also reacts with limestone (CaCO_3) forming CaSO_4 and CO_2 :



It has been observed that coals from the same field, even from the same seam in general, and particularly in the case of Lakhra coal, yield different analytical results, as no two samples of the same coal have the same composition. This is quite expected since mineral coal is a very complex mixture of organic and inorganic constituents. Only pure compounds have fixed ratio and the same composition of their constituents. It is, therefore, a range of constituents in the Lakhra coal that have been recorded in Tables 2 and 3. Even at the coal-fired power plant, the exact composition of coal is not maintained as it is practically not possible. Similar is the case with limestone or other materials used in power plants. Large commercial power plants are operated using commercial grade raw materials, after the necessary sizing, etc. Therefore, the ash obtained from Lakhra coal and the bottom/fly ash obtained from the AFBC power plant had no fixed/constant composition. The ash of coal and the ash obtained from AFBC (bottom and fly ash) were compared to the best approximations, so as to assess the fixation of sulphur in limestone in the form of calcium sulphate.

As shown in the Table 4, the percentage of silica in the Lakhra coal increased from 32.76 to 40.30 and 45.20 and alumina from 20.18 to 25.85 and 22.30, respectively, in bottom ash and fly ash, whereas iron content was reduced from 30.23 to 10.00 and 14.85. Calcium oxide increased from 4.55 to 10.52 and 7.33. The percentage of calcium oxide was increased because limestone was added to coal for the fixation of sulphur. Two interpretations can be offered for the decrease of sulphur trioxide from 16.9 to 3.85 and 3.49, namely the escape of SO_3 to the atmosphere along with the flue gases, or SO_3 may get fixed as

calcium sulphate. Gravimetric analysis may indicate the quantity of calcium sulphate formed. Exact quantity of the sulphur fixed in calcium sulphate is yet to be ascertained. However, the negligible quantity of oxides of sodium and potassium present indicated little chances of agglomeration. The deposition of ash on the boiler tube and on the inner walls of the combustion chamber would be least problematic. One of the advantages of the fluidized bed combustion was that the bed temperature is maintained around 800 °C to avoid ash fusion and agglomeration in the AFBC (Gray, 1986).

A detailed study of the fixation of sulphur in limestone is also emphasized from the environmental impact point of view by incorporating monitoring equipment for the flue gases and ash produced in the AFBC. Based on the experience, large-scale combustion of Pakistani lignite for power generation may prove worthwhile. Calcium sulphate produced in the AFBC appears in the bottom/fly ash as shown in the analysis of ash (Table 4). The combustion of Lakhra lignite was problematic as it contained sulphur in the range 2.4-16.7% (Table 2). Samples of ash were, therefore, obtained when good quality of limestone of the coal-feed was used for the maximum trapping of sulphur of coal. It was expected that the ash of the AFBC would be mostly CaSO_4 , which may be directly applied to soil as soil conditioner.

Application of fertilizer to the soil should be according to the deficiencies of the acidic or basic ingredients. Similar is the case with calcium sulphate. Therefore, it is imperative that calcium sulphate be applied to soils on the recommendation of soil analysts/experts or agriculturists. Soil may be damaged due to unnecessary/over-feeding of fertilizers. Dosage of fertilizers is also important. Therefore, it is recommended that proper and appropriate dose of fertilizer be applied to soils.

The quality control of ash from the AFBC is also very important, as composition of this ash changes from batch to batch as the feed (both coal and limestone) is not of uniform composition. Coal, after mining, also undergoes spontaneous combustion and hence the composition of coal, if not used in a day or two, varies. Similar is the case of limestone composition (purity), which varies from quarry to quarry.

Ash from the AFBC can also be used for brick-making by using high pressure press for moulding. These bricks can be used for insulation as the conductivity of these bricks is very low. Ash from the AFBC can also be used with other materials for building of roads and streets or plastering of roads and streets and pavements. Quality of the calcium sulphate also needs to be checked, otherwise cracks may appear and damage the roads. Since the sorbents (limestone, dolomite, etc.) are used to trap sulphur of the coal, their physical or chemical properties may need to be changed by subjecting to high temperature reactions. The baked broken bricks, if crushed and remoulded, will not give the same results as the originally baked bricks. Their binding property would thus be inevitably damaged.

References

- Ali, I. 1997. NO_x in AFBC, *Engineering Horizons* **112**: 24.
- Ali, I. 1995. Some studies on combustion of Lakhra coal in AFBC. *Karachi Univ. J. Sci.* **23**: 73-80.
- ESP. 2000. *Economic Survey, 1999-2000*, p. 216, Government of Pakistan, Islamabad, Pakistan.
- ESP. 1999. *Economic Survey, 1998-99*, p. 173, Government of Pakistan, Islamabad, Pakistan.
- Gray, V.R. 1986. Retention of sulphur by laboratory prepared ash from low-rank coal. *Fuel* **65**: 1618-1619.

High Frequency *In vitro* Propagation of *Polianthes tuberosa*

Muhammad Saeed Ahmad, Tauqeer Ahmad, Nasreen Zaidi* and Idrees Ahmad Nasir
Plant Biotechnology Laboratory, Food and Biotechnology Research Centre, PCSIR Laboratories Complex,
Ferozepure Road, Lahore-54600, Pakistan

(received February 7, 2006; revised September 9, 2006; accepted September 19, 2006)

Abstract. Calli induced on MS medium supplemented with 10 μM α -naphthaleneacetic acid (NAA) grew extensively when cultured on MS medium modified with 4 μM 2,4-dichlorophenoxyacetic acid (2,4-D), producing on an average four shoots per callus culture. The addition of 1 mM L-arginine in the culture media enhanced the induction rate upto 10 shoots per callus culture in 12 weeks. When 2-3 cm long regenerated shoots were replanted on MS medium with 20 μM 6-benzyladenine (BA) and 4 μM 2,4-D, shoots proliferated at the cut ends. Floral axis buds produced 3-4 cm long multiple shoots on NAA and BA. New shoots regenerated from the calli produced at the base of shoots subcultured on 10 μM NAA. Repetition of shoot development, callus formation, and again shoot formation on 10 μM NAA and 2 μM BA greatly increased the number of plants from single shoots. Eighty five percent bulb explants produced 290 shoots in 12 weeks directly on 15 μM BA and 5 μM NAA. The somatic psuedoembryos formed in the calli were dormant.

Keywords: L-arginine, clonal propagation, *Polianthes tuberosa*, tuberose plant

Abbreviations: IAA = indol-3-acetic acid; IBA = indole-3-butyric acid; BA = N⁶-benzyladenine; CH = casein hydrolysate; CW = coconut water; 2,4-D = 2,4-dichlorophenoxyacetic acids; Kin = kinetin; NAA = naphthalene acetic acid; MS = Murashige and Skoog medium

Introduction

Polianthes tuberosa (family: Amaryllidaceae) is one of the important cut flower. Its fragrance particularly makes it second to none. It is widely used for the extraction of essential oils and aromatic compounds, used as raw material in the fast growing perfume industry. Attention has been, therefore, focused on developing new techniques for the genetic manipulation of this species, requiring the *in vitro* culture of tuberose tissues from which whole plant can be propagated.

Very few studies have been reported on the *in vitro* culture of this species. Amongst these the work of Narayanaswami and Prabhudesai (1979) was the foremost on the culture of the tuberose *in vitro*, which reported direct and indirect regenerations from its meristematic tissue explants. Gi and Tsay (1989) reported studies on anther culture, and induced somaclonal variations in *P. tuberosa*. Later on, Nisar *et al.* (1989) reported regeneration multiple shoots from callus cultures, which was followed by studies on multiple shoots from quiescent nodal buds of floral stalk, plantlets from nodal segments, and the evidence of formation of protocorm-like bodies from anther stalk calli (Zaidi *et al.*, 1994). Regenera-

tive potential of bulb, leaf and scale of the tuberose were also investigated by Khan *et al.* (2000). Krishnamurthy *et al.* (2001) reported micropropagation of the 'single' and 'double' types of tuberose.

In an effort to explore further, *in vitro* cultural features about the enhancement in shoot multiplication rate, were investigated. The present study reports findings on shoot differentiation from bud explants and the calli, and somatically regenerated pseudoembryos.

Materials and Methods

Stock plant. *Polianthes tuberosa* plants, commonly called as tuberose, were obtained from local nurseries. Bulbs, inflorescence axis and floral buds of the plant were used as the source material. The floral stalks were separated from the bulbs at their bases. Leafless floral stalks and bulbs were scrubbed clean with detergent and treated individually for sterilization. Hot water and fungicide treatment of the bulbs preceded the surface sterilization process for bulb explants. The bulbs were treated with hot water at 58 °C for 30 min, and dried on filter paper at room temperature for one day. Roots were then removed, the tunica dried, and the bulbs submerged in 3 g/l solution of Diathane M-45 (AgrEvo Chemical Company, Berlin, Germany) for 30 min prior to explant preparation. Bulb explants (3-5 mm³) were removed from the inner core of the peeled off bulbs. For axillary bud explants, 1 cm³ lump of the bulb, with at least one bud near the basal plate, were obtained. Axillary bud and storage tissue explants of the bulb were surface sterilized in 0.1% (w/v) mercuric chloride solution with

*Author for correspondence; E-mail: imtauqeer@yahoo.com

1-2 drops of Tween-20 for 15 min and rinsed with sterile distilled water, 5 times prior to inoculation. Nodal and internodal explants (1 cm segments) were obtained from the non-flower bearing portion of the floral axis. The explants were sterilized in 0.1% (w/v) mercuric chloride solution with 1-2 drops of Tween-20 for 10 min. The explants were finally rinsed 5 times with sterile distilled water in aseptic environment. Prior to inoculation, floral shoot explants were trimmed at both ends.

Culture medium preparation. A number of modifications to the MS medium (Murashige and Skoog, 1962) were tried during the studies. The culture medium was supplemented with the following organic addenda: 100 mg/l myoinositol, 10 mg/l thiamin HCl, 50 mg/l glycine, 3% sucrose, 0.8% agar or 0.3% phytigel, auxins, cytokinins and reduced nitrogen sources, such as casein hydrolysate (CH) and 15% (v/v) coconut water (CW) in combination and concentrations as necessary. The plant growth regulators used were N⁶-benzyladenine (BA), kinetin (Kin), naphthalene acetic acid (NAA), indole-3-acetic acid (IAA), indole-3-butyric acid (IBA), 2,4-dichlorophenoxy acetic acid (2,4-D) and picloram. The pH of the medium was adjusted to 5.8 with 0.1 N NaOH HCl prior to the addition of agar and autoclaved at 121 °C for 30 min at 138 kpa.

Cultural conditions. The explants were cultured in 100 × 15 mm petri plates (25 ml culture medium per plate), 150 × 18 mm test tubes (15 ml culture medium per tube), and magentas (50 ml culture medium per magenta), whose covers were wrapped with parafilm to avoid contamination. Cultures were kept in a growth room at 25 ± 2 °C and relative humidity of 50-60%. The cultures were exposed to illumination of 2000 lux light intensity, 16 h photoperiod. Callus cultures were kept in the dark. Each treatment consisted of 10 replicates.

Transplantation. As the plantlets developed to 10-15 cm in height and 4-5 number of roots, the plantlets were transferred to pots. The roots were washed with luke warm water to remove the medium and dipped in the fungicide solution (3 g/l Dithane M-45) to protect the plantlets from soil born diseases. The potting compost consisted of sterilized soil, sand and peat moss in 1 : 1 : 1, ratio supplemented with Hogland's solution to meet the nutrient requirements of the plants. Pots were covered with transparent polythene bags, placed in the growth room at 25 ± 2 °C for 4-6 weeks, until the plants were established in the pots and gained appropriate size for transplanting in field.

Results and Discussion

Multiple shoots from callus. Callus induction was tried with bulb tissue explants. Calli were induced on MS medium

supplemented with 5, 10, 15 and 20 µM NAA. Greenish-white friable calli formed in 3-4 weeks. Preliminary studies with the freshly induced callus indicated that hormonal requirement for the growth of tuberosa was specific. Extensive callus growth occurred with 4 µM 2,4-D, which 20 µM was primarily obtained with 10 µM NAA. Several attempts were made to induce redifferentiation in the bulb calli, using MS medium supplemented with different combinations and concentrations of 2,4-D and BA (Table 1). Calli were cultured on regeneration media and subcultured after every 4-week period. After second subculture on the same medium, visible morphogenetic changes were observed in the calli. Most of the calli turned green and the signs of shoot proliferation were evident in eight weeks. Within 10-14 weeks after first subculture from each callus, on an average four shoots were produced. The number of shoots per callus increased with the passage of time, without subculturing and inspite of necrosis of the parent calli. However, the addition of 1 mM L-arginine to the culture medium reduced the time for shoot production. The number of shoots per callus increased up to 10 shoots per callus within 12 weeks (Fig. 1). Sabapathi and Nair (1992) also reported improvement in the rate of shoot proliferation in the case of *Colocasia esculenta* on modified Linsmaier and Skoog medium (Linsmaier and Skoog, 1965) supplemented with L-arginine and ornithine in addition to NAA and Kin. Todd and Gifford (2003) observed that application of exogenous L-arginine to cotyledons of the seedlings of *Pinus taeda* germinated in the absence of megagametophyte resulted in an increase in the total shoot pole argenase activity. These findings are suggestive of the positive physiological role of L-arginine in enhancing shoot multiplication *in vitro*. The 2-3 cm long regenerated shoots were removed from the calli and replanted on the same MS medium supplemented with 20 µM BA and 4 µM 2,4-D. Shoots were observed to resume growth. In addition, shoot proliferation also occurred from the basal part of the detached shoots. The successive shoot proliferations, one after the other, resulted in the formation of small clumps of rootless shoots (Fig. 2). For callus induction, NAA

Table 1. The effect of 2,4-D and BA on callus growth from the bulbs of *Polianthes tuberosa* and shoot development after 14 weeks

Concentration of 2,4-D (µM)	Concentration of BA (µM)					
	1	5	10	15	20	25
2	-	-	++	sh	sh	sh
4	++	++	sh	sh	sh	sh

-- = no effect; ++ = callus growth; sh = shoot formation

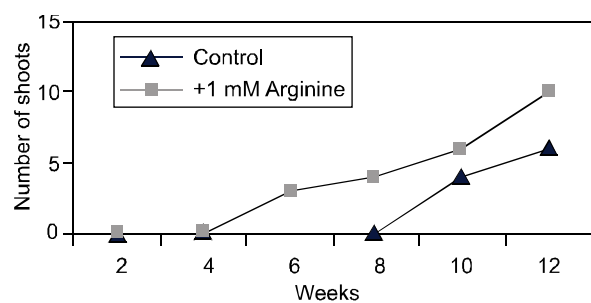


Fig. 1. The effect of addition of L-arginine to MS medium on the calli of *Polianthes tuberosa* to form shoots, as compared to the control calli cultured on MS medium alone after 12 weeks of culture.

appears to be a key factor for bulb tissue. In previous studies, Narayanaswami and Prabhudesai (1979) found that explanted tissue of the bulb required a high concentration of 2,4-D in conjunction with 15% CW (v/v) and a longer incubation period to elicit callus induction. Both NAA and 2,4-D are very strong auxins. According to studies reported earlier, NAA should be used occasionally and the use of 2,4-D should be avoided for callus induction as they may cause rapid increase in ploidy in cultures from a wide range of plant tissues (Wilmer and Hellendoorn, 1968; Sunderland, 1973). However, these results indicated that tuberose requires a higher exogenous level of auxins for callus induction. Extensive callus growth occurred on MS medium when 4 μM 2,4-D was used. Though 2,4-D is also regarded as a strong auxin, which causes cell elongation and proliferation, yet its behaviour is modified in combination with BA favouring shoot growth and proliferation. Marin and Rubluo (1995) also experienced unexpected morphogenetic responses induced by auxins alone in *Mammillaria sanangelensis*, a severely endangered cactus, suggesting that it is the genetic constitution of the plant that modifies the expected morphogenetic behaviours of phytohormones in *in vitro* conditions.

Multiple shoots from floral axis buds. The nodal explants of floral axis carrying quiescent buds cultured on modified MS media with different combinations of 5 μM NAA, 15 μM



Fig. 2. The axillary shoot proliferation of *Polianthes tuberosa* resulted in the formation of a small clump of rootless shoots after 12 weeks.

BA and/or 15 μM Kin produced multiple shoots (Table 2). Visible morphogenetic changes were observed just after four weeks. Shoots were formed on M1 and M2 media, while on M3 and M4 media explants turned brown (Table 2). The shoot proliferation depended on the presence of NAA with BA, irrespective whether Kin was present or not. Twenty five percent explants produced 20 shoots in 8 weeks, while the remaining 75% produced less than that. The reason for this may be that the bud explants derived from the nodes close to the subterrestrial zone of the floral axis would have lost their meristematic activity due to ageing. Following induction, shoot growth continued without subculturing and attained 3-4 cm height in 11-12 weeks. At that stage, the shoots were excised and subcultured on fresh media. Subsequent development of the excised shoots was determined by the hormonal content of the medium. As compared to induction medium, callus pro-

Table 2. The effect of combination of auxins and cytokinins on the floral axis shoot buds of *Polianthes tuberosa*

Media code	Growth regulators (μM)			Observations
	NAA	BA	Kin	
M1	5	15	15	Shoot proliferation
M2	5	15	-	Shoot proliferation
M3	5	-	15	Senescence of explants
M4	-	15	15	Senescence of explants

M1-M4 = basal MS medium + mentioned growth regulators

liferation occurred around the base of excised shoots on the media containing 10 μM NAA. The calli were highly caulogenic, giving rise to new shoots within 4 weeks. In turn, when recultured on media supplemented with 10 μM NAA + 2 μM BA, these produced more callus leading to further shoot production. The alternate concurrence of shoot development, callus formation, and adventive shoot formation were repeated several times, which greatly increased the number of plants from single shoots. The multiple shoots rooted well on MS medium containing 10 μM IBA in the medium varied in expression in contrast to tuberose cultures, depending on the concentration and genetic constitution of the explants as in *Lilium japonicum*. BA and NAA.

The effect of combination of BA and NAA in the medium varied in expression in contrast to tuberose cultures, depending on the concentration and genetic constitution of the explants as in *Lilium japonicum*. BA and NAA also caused bulbet regeneration from mother scale callus (Mizuguchi and Ohkawa, 1994) and active biomass production in *Cattleya aurantiaca* shoot explants reported by Mauro *et al* (1994).

Multiple shoot formation from bulb explants. Bulb explants carrying dormant buds cultured on MS medium supplemented with 15 μM BA and 5 μM NAA produced multiple shoots directly. Efficiency of shoot production obtained from 100 such explants is shown in Fig. 3, on an average 30 shoots appeared in 10% of the explants in 6 weeks. After 12 weeks, 85% of the explants produced a total number of 290 shoots, while average shoot count was 4 per explant. The shoots normally gained a height of 8-10 cm in 6 weeks. Similar high frequency direct shoot regeneration from corm axillary buds and the rapid clonal propagation of *Colocasia esculenta* is

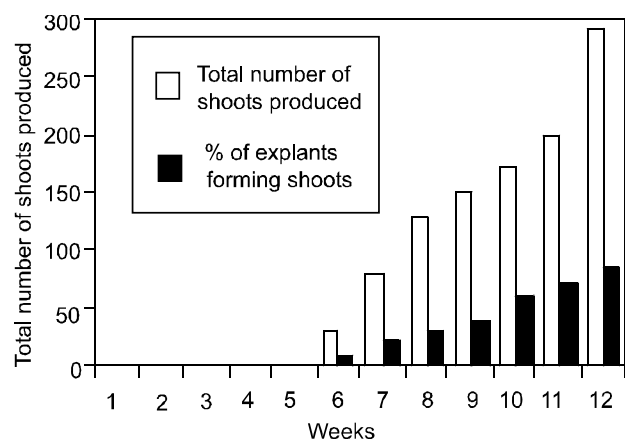


Fig. 3. Efficiency and rate of axillary shoot formation from bulb explants of *Polianthes tuberosa* after 12 weeks of culture.

reported by Chng and Goh (1994), indicating that axillary buds on the underground modified stems, whether a corm or bulb, actively responded to hormonal stimulus in *in vitro* condition, giving rise to multiple shoots.

Pseudosomatic embryogenesis. Extensive callus growth occurred on MS medium supplemented with 4 μM 2,4-D. The shifting of 2-week-old calli on basal MS medium induced characteristic changes in its appearance. Nodular overgrowths resembling embryoid-like structures were produced in quick successions (Fig. 4). Such overgrowths retained their independent identity, not resembling with meristematic nodules. The tadpolelike embryoids showed root like appendages at one end and presumptive shoot apex at the other end, apparently resembled proembryos of zygotic origin. The somatic redifferentiation was obtained only in those calli, which were incubated on media supplemented with 4 μM 2,4-D. On prolonged incubation in nutrient medium upto 8 weeks, the nodular bodies were somewhat elongated. In order to promote their further growth and differentiation, isolated embryos were transferred to MS liquid medium containing twice the concentration of ammonium nitrate and 15% CW (v/v), and shakern at 50-60 rpm at 25 °C. Within 3 weeks of culture, elongation of ovoid structures was observed, which resembled typical embryoids of somatic origin. To regenerate the embryoids, or to succeed in breaking down their dormancy, they were cultured on different hormonal compositions, with complex addenda which, however did not yield the desired result, showing browning and senescence of the cultures.

Attempts to induce the embryoids to develop into normal plantlets on a basal medium under the influence of natural adjuvant such as water extract of bulb, malt extract, casein

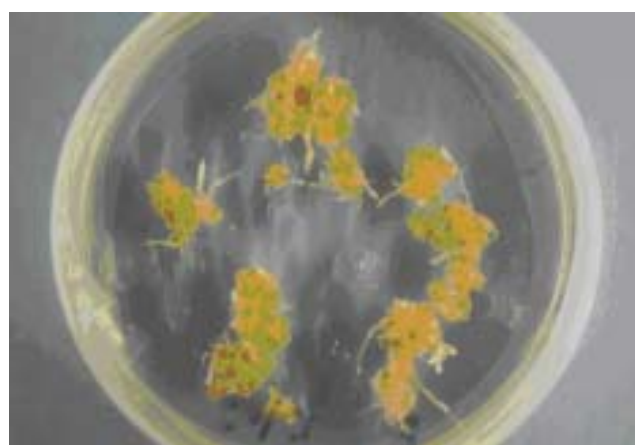


Fig. 4. Pseudoembryogenic clumps developed in calli on growth regulator free medium showing out growth of root like structure.

hydrolysate or change of carbon source, and increasing the concentration of sucrose (upto15%) were of no avail. Physical factors, such as exposure to high intensity light or continuous chilling at 4 °C prior to incubation also proved ineffective in inducing the embryoids to undergo normal differentiation except rhizogenesis. On prolonged incubation, the embryoids, which were imperfect, accumulated starch grains in their cells and remained quiescent indefinitely. Eventually, all attempts to regenerate plantlets from somatic embryos were not successful. The embryo-like structures induced in the tuberose calli were of the nature of shootless embryoids. This is comparable to the occurrence of rootless shoots, prevalent in some cultures of Pergularia (Prabhudesai and Nayranaswamy, 1974) and many other plants in the *in vitro* condition. This has its parallel in the species *Escholtia californica*, where embryoids, although produced in abundance, failed to develop into normal plantlets. On differentiating medium, the primary root was well developed representing growth of the axial structures in continuity with the shoot region and was never adventitious in origin from a callus mass. However, owing to lack of typical organization of shoot apex it could not initiate leaf primordia and thereby was arrested in development. Nayranaswamy and Prabhudesai (1979) and Zaidi *et al.* (1994) also obtained elongated embryoids of *Polianthes tuberosa*. However, none of the innumerable embryoid-like structures grew into plantlets cultured even under aforesaid variety of nutrients and hormonal conditions, such structure were not embryoids but psuedoembryoids. Interpretations of Tian and Yang (1984) are fully applicable to these abortive regenerants. They observed similar situation in gynogenetic embryoids and callus in ovary culture of *Oryza sativa*. Chang *et al.* (1986) have reasoned that abnormality occurred due to the absence of nurse tissue-like endosperm and some inadequacy in the culture medium.

References

- Chang, Z., Hongyuan, Y., Huiqiaq, T., Zhonglai, L. 1986. *In vitro* unpollinated ovaries in *Oryza sativa* L. In: *Haploids of Higher Plants in vitro*, H. Han, Y. Hongyuan (eds.), pp. 165- 181, Academic Publishers, Beijing, China.
- Chng, R.C.O., Goh, C.J. 1994. High frequency direct shoot regeneration from corm axillary buds and rapid clonal propagation of taro, *Colocasia esculenta* var. *esculenta* (L.) Schott (Araceae). *Plant Sci. Limerick* **104**: 93-100.
- Gi, H.S., Tsay, H.S. 1989. Anther culture and somaclonal variation of tuberose (*Polianthes tuberosa* L.). *J. Agric. Res. China* **38**: 346-352.
- Khan, N.H., Zaidi, N., Shah, F.H.2000. Micropropagation potential of *Polianthes tuberosa* L. bulbs, scales and leaves. *Pak. J. Sci. Ind. Res.* **43**: 118-122.
- Krishnamurthy, K.B., Mythili, J.B., Srinivas, M. 2001. Micropropagation studies in “single” vs. “double” types of tuberose (*Polianthes tuberosa* L.). *J. Appl. Hort.* **3**: 82-84.
- Linsmaier, E.M., Skoog, F.1965. Organic growth factor requirements of tobacco tissue cultures. *Physiol. Plant.* **18**:100-127.
- Marin, T., Rubluo, A. 1995. Unexpected morphogenetic responses induced by auxins alone in *Mammillaria san-angelensis*, severely endangered cacti. *In Vitro Cell Dev. Biol.* **31**: 74A(Abstract).
- Mauro, M., Sabapathi, D., Smith, R.A. 1994. Influence of benzylaminopurine and alpha-nephtaleneacetic acid on multiplication and biomass production of *Cattleya aurantiaca* shoot explants. *Lindleyana* **9**: 169-173.
- Mizuguchi, S., Ohkawa, M. 1994. Effects of nephtaleneacetic acid and benzyladenine on growth of bulblets regenerated from white callus of mother scale of *Lilium japonicum* Thunb. *J. Japan Soc. Hort. Sci.* **63**: 429-437.
- Murashige, T., Skoog, F. 1962. A revised medium for rapid growth and bioassays with tobacco tissue cultures. *Physiol. Plant* **15**: 473-497.
- Narayanaswamy, S., Prabhudesai, V.R. 1979. Somatic psuedoembryogeny in tissue culture of tuberose (*Polianthes tuberosa*). *Indian J. Experimental Biol.* **17**: 873-875.
- Nisar, R., Khan, N.H., Zaidi, N., Shah, F.H. 1989. The growth of *Polianthes tuberosa* *in vitro*. *Sci. Int.* **1**: 257-261.
- Prabhudesai, V.R., Narayanaswamy, S. 1974. Organogenesis in tissue cultures of certain asclepiads. *Z.P flanzeng-physiolog.* **71**: 181-185.
- Sabapathi, S., Nair, H. 1992. *In vitro* propagation of taro, with spermine, arginine, and ornithine. I. Plantlet regeneration from primary shoot apices and axillary buds. *Plant Cell Reports* **11**: 290-296.
- Sunderland, N. 1973. Nuclear cytology. In: *Plant Tissue and Cell Culture*, H.E. Street (ed.), pp.161-190, Blackwell Publishers, Oxford, UK.
- Tian, H.O., Yang, H.Y. 1984. Morphogenetic aspects of gynogenetic embryoids and callus in ovary culture of *Oryza sativa* L. *Acta Bot.* **26**: 372-375.
- Todd, C.D., Gifford, D.J. 2003. Loblolly pine arginase responds to arginine *in vitro*. *Planta* **217**: 610-615.
- Wilmer, C., Hellendoorn, M.H. 1968. Growth and morphogenesis of *Asparagus* cultures *in vitro*. *Nature* **217**: 369-370.
- Zaidi, N., Khan, N.H., Shah, F.H. 1994. Regeneration of plantlets and protocorms from *Polianthes tuberosa*. *Pak. J. Agric. Res.* **15**: 43-48.

Morphological Changes in Cotton Roots in Relation to Soil Mechanical Impedance and Matric Potential

Ghulam Nabi^{a*} and C. E. Mullins^b

^aLand Resources Research Programme, National Agricultural Research Centre, Islamabad-45500, Pakistan

^bDepartment of Plant and Soil Science, Cruickshank Building, University of Aberdeen, AB24 3UU, UK

(received July 15, 2005; revised August 12, 2006; accepted September 5, 2006)

Abstract. Soil mechanical impedance (MI) and matric potential can both cause reduction in the root growth rate, modify rooting pattern and root diameter. Cotton seedlings are sensitive to the soil physical environment, particularly during early stages of growth. Soil matric potential and MI effect on root biomass, axial root length and diameter, and the number and length of lateral roots in soil packed to penetration resistances (PR) of 0.1, 1.0, 1.1 and 1.2 MPa (megaPascal = 10^6 Pascal), each at three matric potentials of -10 , -100 and -500 kPa (kiloPascal = 10^3 Pascal), were determined. Total root lengths were reduced by 29, 50 and 53% at impedance of 1.0, 1.1 and 1.2 MPa, respectively, as compared to the control, whereas MI of 1.2 MPa resulted in 60% reduction in axial root length. A similar increase in diameter was caused by increasing mechanical impedance, while decreasing matric potential had little effect. Roots that were water stressed did not change their diameter but had a shorter axis and longer lateral length. In contrast, the impeded roots (PR = 1.0, 1.1 and 1.2 MPa) had both a shorter axis and a smaller total length, but had increased diameter. These results not only illustrate the plasticity of root response to stress but also demonstrate how the response differs between different types of stresses.

Keywords: soil mechanical impedance, soil matric potential, root plasticity, root length, penetration resistance, soil physical environment

Introduction

Plants require networks of roots to absorb water and nutrients from the soil. Soil factors, which influence the distribution of plant root system, often limit plant productivity by modifying the extent of plant root exploration and by reducing the efficiency of water absorption. Soil physical factors, such as soil matric potential and mechanical impedance, affect the root growth. Mechanical impedance is the resisting pressure encountered by growing roots. It is ubiquitous within the root environment. Penetration resistance of 0.5-1.0 MPa (megaPascal = 10^6 Pascal), and greater, are commonly experienced in soils that can reduce root elongation rates considerably (Martino and Shaykewich, 1994). It increases with increase in soil bulk density. It also usually increases as the soil matric potential decreases during soil drying. Unless roots are able to exploit soil structural features to bypass the bulk of soil, their growth rate reduces as mechanical impedance is increased (Bengough and Mullins, 1990). Indeed, drying soils can become strong enough to affect root growth at matric potential as high as -0.1 MPa (Mullins *et al.*, 1992). Water potential of -0.1 MPa appears to have little direct effect on root elongation, or root growth pressure (Whalley *et al.*, 1998). Under controlled conditions, root growth rate varies in

approximately inverse proportion to mechanical impedance. This is in consequence of both a reduction in the rate of cell division in the meristem and a decrease in the length of fully expanded cells (Smucker and Atwell, 1988; Eavis, 1967). Wilson *et al.* (1977) reported that under impeding conditions, cell length and the volume of inner cortical cells decreased but the diameter and volume of the outer cortical and epidermal cells was considerably increased. The epical meristem and zone of cell expansion of impeded roots is short and the cells on the surface of the tips may slough off (Bengough and McKenzie, 1997). In barley, initiation of lateral roots and growth of root hair took place nearer the tip under impeded conditions (Goss and Russell, 1980). In roots that bent after an encounter with an obstacle, lateral roots predominated on the concave side of the bent while root hairs dominated on the convex side.

Under field conditions, plant root systems encounter considerable spatial variations in mechanical impedance. Even in compact soils, areas of lower mechanical impedance will occur due to shrinkage cracks and channels formed by earthworms or roots of previous crops (Tardieu, 1988). Furthermore, dense compact layers frequently underline the loosened top soil in cultivated soils. Under these conditions, a root system encountering hard compact zones of soils has

*Author for correspondence; E-mail: drgnabi@yahoo.co.uk

the opportunity to proliferate in zones of looser soil. Such plasticity in root system development, in response to heterogeneous soil conditions, has been reported in both pot (Garcia *et al.*, 1988) and field experiments (Bengough *et al.*, 2006; Pietola, 2005; Clark *et al.*, 2003; Montagu *et al.*, 1998). However, a common consensus on the root morphology changes is lacking.

Increased mechanical impedance has been associated with decreased root elongation rates in many plant species including maize (Veen, 1982), cotton (Nabi *et al.*, 2001; Taylor and Ratiliff, 1969), wheat (Nabi and Mullins, 2001; Masle, 1992), peas (Tsegaye and Mullins, 1994), grasses (Cook *et al.*, 1996), and radiata pine (Zou *et al.*, 2001). With increased mechanical impedance, the above-ground plant growth is also affected. Reduced root growth has often been associated with reduced shoot growth (Kirby and Bengough, 2002; Cook *et al.*, 1996; Blaikie and Mason, 1993). Young *et al.* (1997) observed 36.2% and 22.6% reduced leaf elongation rates in barley and wheat, respectively. Reduced transpiration rates (Masle, 1992) and stomatal conductance (Masle, 1998) have also been associated with increased mechanical impedance sensed by plant roots. Decreased nutrient uptake (total P and N) has been reported with increased soil mechanical impedance (Pietola and Tanni, 2003; Chassot and Richner, 2002; Habib, 2002).

The present study was conducted to determine the effect of mechanical impedance and matric potential on morphology of cotton roots and to demonstrate how the root growth responses differ between different types of stresses.

Materials and Methods

Experimental work was conducted during 1998 at the Department of Plant and Soil Science, University of Aberdeen, UK, in a growth cabinet in packed soil wetted to three matric potentials, i.e., -10, -100 and -500 kPa (kiloPascal = 10^3 Pascal). The soil was packed in perplex cylinders (300 mm long, with 50 mm internal dia) to dry bulk density equivalent to the mechanical impedance of 0.1, 1.0, 1.1 and 1.2 MPa. Pregerminated seedlings of cotton (variety MNH 147) were grown for 72 h at 32 °C in the dark. Each treatment had three replications with two seedlings in each of the cylinders.

A sandy clay loam (Carpow Series) topsoil (0-10 cm) was sieved and aggregates between 1 and 3.35 mm dia were retained. The prepared soil contained 0.21% organic matter with particle size distribution of 20.6% clay, 18.0% silt and 61.4% sand. Water retention curve of the soil was developed following standard procedures of tension table and pressure plate apparatus (Klute, 1986). According to the water reten-

tion curve, the soil was wetted to the required matric potentials and packed into cylinders in layers of 20 mm increments up to 200 mm depths, separately, at different bulk densities. The packed cylinders were then incubated at 32 °C for 24 h. The incubation was intended to attain a homogeneous temperature and consequently moisture distribution inside the cylinders, and to avoid heat shock of seedlings at transplanting. After incubation, two germinated seedlings of 5 mm length were transplanted, 5 mm apart, in each cylinder and rest of the packing was completed with more soil accordingly. Finally, the cylinders were shifted inside the phytotron cabinet maintained at 32 °C in the dark. Temperature within cylinders was recorded hourly with a bead thermistor attached to a data logger (Skye Instruments Data Hog, Skye Ltd., Ddole Industrial State, Llandrindod, Wells, UK).

After 72 h of transplanting, the cylinders were removed from the phytotron. The seedlings were excavated from the cylinders along with the soil, and soil was separated from the seedlings with gentle washing. After washing and blotting, the root weight, root length, root diameter and the number of root laterals were recorded. The roots were then dried in an oven at 80 °C for 72 h to record their dry weights. Total root length was measured using DIAS image analyzer with the root measurement system software (Root Measurement System Software, version 1.6, Delta-T Devices Ltd., Burwell, Cambridge, UK). High quality photocopies of the stained roots were used for length measurement. Each image was measured three times to check for reproducibility and mean of these was used for further data analyses.

Analysis of variance (ANOVA) was computed for each parameter using four mechanical impedance and three matric potentials with four replications in a 4 x 3 factorial design using Minitab Statistical Software, Minitab for windows version 10.5 (Minitab Corporation, Inc., USA). Least significant difference (LSD) test was used to compare the treatment means.

Results and Discussion

The mechanical impedance and matric potential were noted to reduce significantly the axial and total root length ($p < 0.05$). Interactions between matric potential and mechanical impedance were also significant. Axial root length decreased with increasing mechanical impedance (Fig. 1). A reduction of 52% and 56% was observed at mechanical impedance of 1.2 MPa as compared to control (0.10 MPa) in seedlings grown at -10 and -500 kPa, respectively. With a decrease of matric potential from -10 kPa to -100 and -500 kPa, the axial lengths were also reduced significantly. At the three matric potentials studied, significant higher reductions were observed in the impeded treatments of pen-

etration resistance 1.0, 1.1 and 1.2 MPa. These results were expected, as the mechanical impedance has been reported to reduce elongation of roots (Nabi and Mullins, 2001; Bennie, 1996; Verpraskas, 1994). However, a single line drawn through all the points (to within the limits of experimental error) indicated a unique relationship between penetration resistance and root growth rate, independent of matric potentials down to -500 kPa (Fig. 2). This line suggested that any apparent effect of matric potentials on the rate of root growth was no longer significant if the undesirable effects of matric potential on penetration resistance were taken into account.

Total root lengths were also decreased with increased mechanical impedance (Fig. 3). A reduction of about 50% was observed at all the matric potentials at 1.2 MPa relative to the control. In contrast to the reduction in axial root lengths with decrease in matric potential, total root lengths tended to increase with decreasing matric potential. In 1.0 and 1.1 MPa treatment, 25% and 3% longer roots were recorded at -500 kPa than at -10 kPa matric potential. These longer roots at the lower matric potential may either be due to increase in the number of root laterals or lengths of individual laterals in response to decreased matric potential.

The number of root laterals was reduced by impedance, but the overall effect of matric potential on the lateral root number was non-significant (Table 1). The interactions between matric potential and mechanical impedance were also non-significant. Only in the 0.1 MPa treatments, the number of root laterals decreased significantly with decrease in matric potential. A reduction of 20, 39 and 54% was noted when mechanical impedance increased to 1.0, 1.1 and 1.2 MPa, respectively, over the unimpeded treatment. This was in line with the earlier findings that root branching of plants grown in mechanically impeded soil is restricted but does not necessarily mean that spacing of laterals has changed (Misra and Gibbons, 1996; Boone and Veen, 1982).

Total length of root laterals was reduced significantly ($p < 0.05$) by increased mechanical impedance (Table 1). On the average, a reduction of 29, 50 and 53% was observed at impedance of 1.0, 1.1 and 1.2 MPa, respectively, as compared to the control. Matric potential also reduced the length of laterals, though it was statistically non-significant. In treatments with higher mechanical impedance, longer laterals were observed in response to a decrease in matric potential. This was in contrast to the control treatment where laterals were shorter at -500 kPa than at -10 and -100 kPa. Neither matric potential, nor mechanical impedance, affected lateral spacing at all impedance levels.

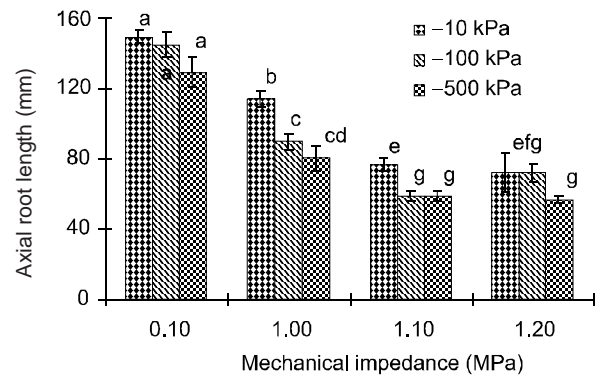


Fig. 1. Effect of mechanical impedance and matric potentials on axial root length of cotton seedlings (values are mean \pm SE; single SED value computed from ANOVA = 5.77; bars with similar letters do not differ significantly at $p > 0.05$).

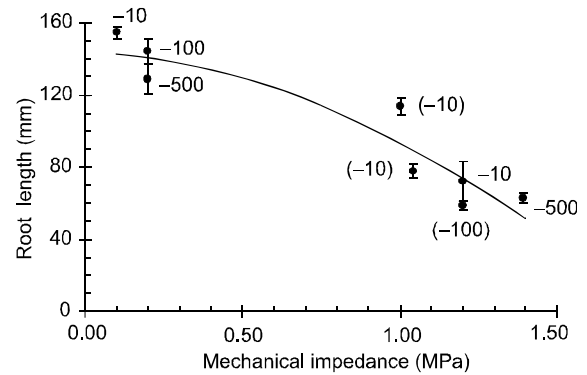


Fig. 2. Effect of mechanical impedance and matric potentials on root length of cotton; a single penetration resistance value at any matric potential of -10 kPa, for which data at -100 and -500 kPa at respective mechanical impedance was not available appear in parenthesis.

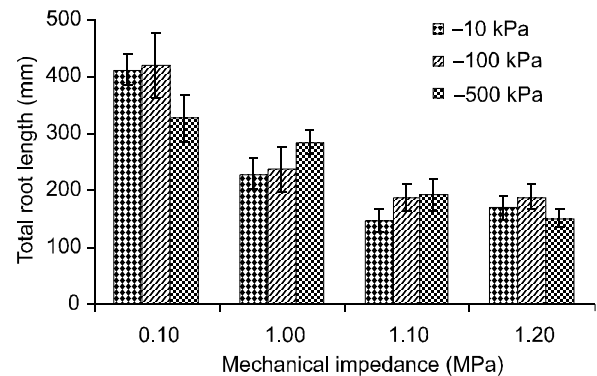


Fig. 3. Effect of mechanical impedance and matric potentials on total root length of cotton seedlings (values are mean \pm SE; single SED value computed from ANOVA = 43.7).

Table 1. Effect of mechanical impedance and matric potentials on the number and length of root laterals of cotton seedlings

Mechanical impedance (MPa)	Number of root laterals*			Length of root laterals (mm)**		
	-10 kPa	-100 kPa	-500 kPa	-10 kPa	-100 kPa	-500 kPa
0.1	34	32	28	265	273	192
1.0	24	26	27	113	148	205
1.1	20	20	19	70	130	134
1.2	14	17	12	104	118	95

* = for comparison of number of root laterals: LSD ($p < 0.05$) for mechanical impedance 3.21, LSD ($p < 0.05$) for matric potential 2.76, penetration resistance-mechanical impedance: non-significant; ** = for comparison of length of root laterals: LSD ($p < 0.05$) for mechanical impedance 49, LSD ($p < 0.05$) for matric potential 43, penetration resistance-mechanical impedance: non-significant

Root diameter was significantly increased with increase in soil mechanical impedance (Table 2), but did not change significantly with matric potential. Higher mechanical impedance have been reported to result in thicker roots of maize (Shierlaw and Alston, 1984; Boone and Veen, 1982), wheat (Collis-George and Yoganathan, 1985; Bennie, 1979), Cotton (Bennie, 1979), and potatoes (Boone *et al.*, 1985).

Mechanical impedance and matric potential significantly affected ($p < 0.05$) dry root biomass (Fig. 4). However, their interactions were non-significant. The root biomass was decreased with increase in mechanical impedance. Fresh weights were reduced in the order of 19, 42 and 49% at penetration resistance of 1.0, 1.1 and 1.2 MPa, respectively. Higher fresh weights were observed at -100 kPa matric potential than at -10 or at -500 kPa.

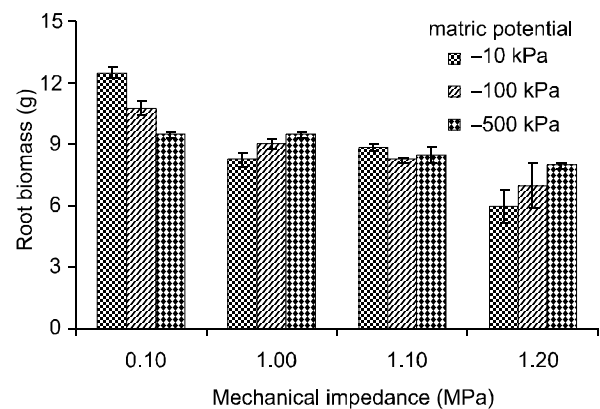
The number of root laterals and the total length of root laterals was reduced with increase in mechanical impedance, while spacing of root laterals was not affected, as was also observed by Tsegaye and Mullins (1994) for peas, indicating some kind of overall plant control to maintain lateral spacing. Reduction in number of root laterals with increased soil compaction has been observed in maize by Sauerbeck and Helal (1986). Stress in soil physical environment imposes contrasting effects on the root system, some of which the plants were able to compensate for, for example, through increase in lateral lengths in cotton with decrease in matric potential. But other stresses imposed constraints which the plants were unable to compensate for, for example, reduced root length with increased mechanical impedance.

It is interesting to note that the overall root biomass was affected very little, implying that seedlings tended to unload/release metabolites at a rate which is not strongly dependent on soil physical conditions. However, there was a clear and interesting contrast between root response to

Table 2. Effect of mechanical impedance and matric potentials on the number of root laterals, spacing of root laterals, length and root diameter (values in parenthesis indicate percentage reduction over control)

Mechanical impedance (MPa)	Number of root laterals	Length of root laterals (mm)	Spacing of root laterals (mm)	Root diameter (mm)
0.1	31 ^a (-)	244 ^a (-)	2.64 ^a	0.93 ^c
1.0	26 ^{ab} (16)	155 ^b (36)	2.29 ^a	0.95 ^b
1.1	19 ^b (39)	111 ^b (53)	2.42 ^a	1.10 ^a
1.2	14 ^c (54)	106 ^b (56)	3.46 ^a	1.00 ^a
LSD ($p < 0.05$)	3.21	49	ns*	0.15

ns* = non-significant; values in columns with similar letters do not differ significantly ($p > 0.05$)

**Fig. 4.** Effect of mechanical impedance and matric potential on root biomass of cotton seedlings (values are mean \pm SE; single SED value computed from ANOVA = 2.74).

water stress (decreasing matric potential) and to mechanical impedance. Roots that were water stressed did not change their diameter but had a shorter axis and longer total lateral length. In contrast, the mechanically impeded roots had both a shorter axis and a smaller total root length but increased root diameter.

Since decreasing matric potential resulted in shorter axis with same lateral spacing but with greater total lateral length, the smaller number of laterals must have been considerably longer. Increasing mechanical impedance also resulted in a shorter axis, with the same lateral spacing, giving ultimately less number of laterals, but also decreased total lateral lengths. Visual observations of roots supported the conclusion that average lateral lengths were greater in water stressed plants. This suggested the plastic behaviour of the root system to cope with stressed conditions.

A contrasting behaviour of the cotton lateral roots in response to water stress was observed. Roots that were water stressed did not change their diameter but had a shorter axis and longer laterals. In contrast, mechanically impeded roots had both a shorter axis and a smaller total root length, but increased root diameter. A plastic nature of the root system to cope with stressed environment has been thus indicated.

Changes of water content in the soil immediately surrounding a root causes changes in the root cell osmotic and turgor pressures. A decline in soil water content, and associated decrease in soil matric potential, results in a reduction in water uptake, a decrease in root cell osmotic potential, a reduction in cell wall extension and decrease in the ability of roots to overcome the mechanical constraints of the soil (Taylor, 1983). The osmotic adjustment will allow growth to continue as if sufficient water were available, but the other changes tended to reduce growth rates. The above explanation emphasizes the hydraulic response of the roots to water shortage. However, chemical changes occur too. Increasing evidence suggests that abscisic acid has a particularly important role in regulating many of these responses (Hartung and Davies, 1991). Root growth at low water potentials appears to be dependent upon abscisic acid accumulation

References

- Bengough, A.G., Bransby, M.F., Hans, J., Stephen, J.M., Roberts, T.J., Valentine, T.A. 2006. Root responses to soil physical conditions; growth dynamics from field to cell. *J. Exptl. Botany* **57**: 437-447.
- Bengough, A.G., McKenzie, C.J. 1997. Sloughing of root cap cells decreases the fractional resistance to maize (*Zea mays* L.) root growth. *J. Exptl. Botany* **48**: 885-893.
- Bengough, A.G., Mullins, C.E. 1990. Penetrometer resistance and root elongation rate in two sandy loam soils. *Plant and Soil* **131**: 59-66.
- Bennie, A.T.P. 1996. Growth and mechanical impedance. In: *Plant Roots: The Hidden Half*, Y. Waisel, A. Eshel, U. Kafkafi (eds.), pp. 453-470, Marcel Dekker, Inc., New York, USA.
- Bennie, A.T.P. 1979. The Influence of Soil Compaction on Soil-Plant System. *Ph.D. Thesis*, University of Orange Free State, Bloemfontein, South Africa.
- Blaikie, S.J., Mason, W.K. 1993. Restriction to root growth limit the yield of shoots of irrigated white clover. *Aust. J. Agric. Res.* **44**: 12-35.
- Boone, F.R., Veen, B.W. 1982. The influence of mechanical resistance and phosphate supply on morphology and functions of maize-roots. *Netherlands J. Agric. Sci.* **30**: 179-192.
- Boone, F.R., deSmet, L., VoonLoon, C.D. 1985. The effects of soil compaction on potato growth in a loamy sand soil. I. Physical measurements and rooting patterns. *Potato Res.* **28**: 295-314.
- Chassot, A., Richner, W. 2002. Root characteristics and phosphorus uptake of maize seedlings in a bi-layered soil. *Agron. Journal* **94**: 118-127.
- Clark, L.J., Whalley, W.R., Barraclough, P.B. 2003. How do roots penetrate strong soils? *Plant and Soil* **255**: 93-104.
- Collis-George, N., Yoganathan, P. 1985. The influence of soil strength on germination and emergence of wheat. I. Low shear strength conditions. *Aust. J. Soil Res.* **23**: 577-588.
- Cook, A., Marriott, C.A., Seel, W., Mullins, C.E. 1996. Effects of soil mechanical impedance on root and shoot growth of *Lolium perene* L., *Agrostis capillaris* and *Trifolium repens* L. *J. Exptl. Botany* **47**: 1075-1084.
- Eavis, B.W. 1967. Mechanical impedance to root growth. In: *Agricultural Engineering Symposium*, paper 4/F/30, 1-11, Silsoe.
- Garcia, F., Cruse, R.M., Blackmer, A.M. 1988. Compaction and nitrogen placement effect on root growth, water depletion and nitrogen uptake. *Agron. Journal* **52**: 792-798.
- Goss, M.J., Russell, R.S. 1980. Effect of mechanical impedance on root growth in barley (*Hordeum vulgare* L.). III. Observation on mechanism of response. *J. Exptl. Botany* **31**: 577-588.
- Habib, N. 2002. Mechanical impedance to root growth and phosphorus uptake. In: *17th World Congress of Soil Science*, Symposium No. 22, paper No. 1052, pp. 1-7, August 14-21, 2002, International Union of Soil Science, Bangkok, Thailand.
- Hartung, W., Davies, W.J. 1991. Drought induced changes in

- physiology and ABA. In: *Abscisic Acid Physiology and Biochemistry*, W.J. Davies, H.G. Jones (eds.), pp. 227-243, Bios Scientific Publishers, Oxford, UK.
- Kirby, J.M., Bengough, A.G. 2002. Influence of soil strength on root growth: experiments and analysis using a critical state model. *Euro. J. Soil Sci.* **53**:119-128.
- Klute, A. 1986. Water retention: laboratory methods. In: *Methods of Soil Analysis, Part-I, Physical and Mineralogical Methods*, S.S.S.A. Book Series, Chapter 26, pp. 635-660, Soil Science Society of America, Inc., Madison, Wisconsin, USA.
- Martino, D.L., Shaykewich, C.F. 1994. Root penetration profiles of wheat and barley as affected by soil penetration resistance in field conditions. *Can. J. Soil Sci.* **74**: 193-200.
- Masle, J. 1998. Growth and stomatal response of wheat seedlings to spatial and temporal variation in soil strength of bi-layered soils. *J. Exptl. Botany* **49**: 1245-1257.
- Masle, J. 1992. Genetic variations in the effects of root impedance on growth and transpiration rates of wheat and barley. *Aust. J. Plant Physiol.* **19**: 109-125.
- Misra, R.K., Gibbons, A.K. 1996. Growth and morphology of eucalyptus (*Eucalyptus niters*) seedling roots in relation to soil strength arising from compaction. *Plant and Soil* **182**: 1-11.
- Montagu, K.D., Conroy, J.P., Francis, G.S. 1998. Root and shoot response of field grown lettuce and broccoli to compact subsoil. *Aust. J. Agric. Res.* **49**: 89-97.
- Mullins, C.E., Blackwell, P.S., Tisdall, J.M. 1992. Strength development during drying of a cultivated flood-irrigated hard-setting soil. 1. Comparison with structurally stable soil. *Soil Tillage Res.* **25**: 113-128.
- Nabi, G., Mullins, C.E. 2001. Elongation rates of root and shoot of wheat during emergence as affected by mechanical impedance and matric potential of the growth medium. *Pak. J. Soil Sci.* **19**: 92-99.
- Nabi, G., Mullins, C.E., Montemayor, M.B., Akhtar, M.S. 2001. Germination and emergence of irrigated cotton in Pakistan in relation to sowing depth and physical properties of the seed bed. *Soil Tillage Res.* **59**: 33-44.
- Pietola, L. 2005. Root growth dynamics of spring cereals with discontinuation of mould-board ploughing. *Soil Tillage Res.* **80**: 103-114.
- Pietola, L., Tanni, R. 2003. Response of seedbed physical properties, soil N and cereal growth to peat application during transition to conservation tillage. *Soil Tillage Res.* **74**: 65-79.
- Sauerbeck, D.R., Helal, H.H. 1986. Plant root development and phosphate consumption depending on soil compaction. In: *Transactions of the 13th Congress of the International Soil Science Society*, August 13-20, 1986, pp. 948-949, Hamburg, Germany.
- Shierlaw, J., Alston, A.M. 1984. Effect of soil compaction on root growth and uptake of phosphorus. *Plant and Soil* **77**: 15-28.
- Smucker, A.M.J., Atwell, B.J. 1988. Soil compaction modification of root functions. In: *Proceedings of the Symposium on Plant Roots and their Environment*, B.L. McMichael, H. Persson (eds.), August 21-26, 1988, Uppsala, Sweden, Elsevier Publishing, New York, USA.
- Tardieu, F. 1988. Analysis of the spatial variability of maize root density. 1. Effect of wheel compaction on the spatial arrangement of roots. *Plant and Soil* **107**: 269-266.
- Taylor, H.M. 1983. Managing root systems for efficient water use: an overview. In: *Limitations to Efficient Water Use in Crop Production*, H.M. Taylor, W.R. Jordan, T.R. Sinclair (eds.), pp. 87-113, American Society of Agronomy, Crop Society of America, Soil Science Society of America, Madison, Wisconsin, USA.
- Taylor, H.M., Ratliff, L.F. 1969. Root elongation rates of cotton and peanut as a function of soil strength and soil water content. *Soil Sci.* **108**: 113-119.
- Tsegaye, T., Mullins, C.E. 1994. Effect of mechanical impedance on root growth and morphology of two varieties of pea. *New Phytologist* **6**: 707-713.
- Veen, B.W. 1982. The influence of mechanical impedance on the growth of maize roots. *Plant and Soil* **6**: 101-109.
- Verpraskas, M.J. 1994. Plant response mechanisms to soil compactions. In: *Plant-Environment Interactions*, R.E. Wilkinsons (ed.), pp. 263-287, Marcel Dekker, Inc., New York, USA.
- Whalley, W.R., Bengough, A.G., Dexter, A.R. 1998. Water stress induced by PEG decreases the maximum growth pressure of pea seedlings. *J. Exptl. Botany* **49**: 1689-1694.
- Wilson, A.J., Robards, A.W., Goss, M.J. 1977. Effect of mechanical impedance on root growth in barley (*Hordeum vulgare* L.). II. Effects on the development in seminal roots. *J. Exptl. Botany* **28**: 126-1227.
- Young, I., Montagu, M.K., Conroy, J., Bengough, A.G. 1997. Mechanical impedance of root growth directly reduces leaf elongation rates of cereals. *New Phytologist* **135**: 613-619.
- Zou, C., Penfold, C., Sands, R., Misra, R.K., Hudson, I. 2001. Effects of soil air field porosity, soil matric potential and soil strength on primary root growth of radiata pine seedlings. *Plant and Soil* **236**: 105-115.

Multiple Parameters for Ascertaining Yield Stability of Upland Cotton Varieties Tested Over Number of Environments

Muhammed Jurial Baloch* and Nasreen Fatima Veesar

Department of Plant Breeding and Genetics, Sindh Agriculture University,
Tandojam, Sindh, Pakistan

(received October 5, 2005; revised August 16, 2006; accepted August 29, 2006)

Abstract. Thirteen upland cotton varieties were evaluated in 12 different environments of the Sindh province, Pakistan, so as to arbitrate their stability in yield performance. The regression coefficient (**b**) parameter was used as a measure of varietal adaptability, whereas the sum of squared deviations from regression (**s²d**) and coefficient of determination (**r²**) were implied as the measure of stability. The regression coefficients (**b**) of all the varieties, though did not deviate significantly from a unit slope (**b** = 1.0), yet varieties FH-1000, VH-142, BH-147 and FH-945 exhibited (**b**) values very close to a unit slope suggesting their better adaptation to the test environments. Varieties CRIS-467, DNH-57 and FH-945 displayed lower **s²d** and higher **r²** values implying that these varieties were relatively more stable in yield performance than others in the test environments. Generally, not all the stability and adaptability parameters simultaneously favoured the same variety except FH-945, which was thus considered more stable, based on majority of the parameters. Principal component analysis (**PCA**) revealed that latent vectors of first two components, i.e., **PCA-1** and **PCA-2** accounted for about 91.24 % of the total variation. The eigen vectors of first **PCA-1** were smaller and all were positive, which further suggested that the test varieties were quite adaptive to all the test sites. However, in **PCA-2**, some varieties gave positive and some negative eigen values, yet varieties FH-1000, CIM-499, CRIS-467 and FH-945 expressed smaller and positive **PCA-2** scores suggesting less genotype-environment interactions for these particular varieties.

Keywords: stability and AMMI analysis, genotype-environment interaction, upland cotton varieties, environmental index, multivariate analysis

Introduction

Cotton breeders are always tempted to assess the magnitude of genotype-environment interactions and their pattern. These attributes, of course, help plant breeders to decide whether the newly evolved varieties are suitable for multiple environments or for specific environments. To answer this complicated question, a broad range of multivariate statistical procedures has long been used. The most common and earlier approach was the regression analysis (Eberhart and Russell, 1966; Finlay and Wilkson, 1963). However, several researchers have pointed out some limitations of the regression method (Crossa, 1988). Lin and Binns (1988) concluded that the ten most commonly used parameters, representing stability and adaptability of genotypes are actually different approaches of statistics that measure the same attribute. Thus, among the ten parameters of stability analysis, the similar ones were grouped together. As a consequence, only three major groups, namely, deviation of average performance of genotypes, the genotype-environment interaction (**G x E**), and regression of environmental index were arbitrated. Lin *et al.* (1986) used multivariate analysis (**MA**), so as to ensure thorough elucidation of the response of cultivars within the scope of three new classifications representing the stability of genotypes. By regressing each variety over environmental index, Bilbro and

Ray (1976) demonstrated regression coefficient (**b**) as a measure of adaptability, whereas coefficient of determination (**r²**) and the sum of squared deviation (**s²d**) were shown as a measure of stability. It is still, however, questionable whether these parameters are completely reliable in describing the stability and adaptability response of genotypes tested in both favourable and unfavourable environments. By using multivariate analysis, nevertheless, Lin *et al.* (1986) succeeded to a large extent, in explaining the most complicated situation of genotype-environment interaction pattern. To further overcome the limitations of the previously used statistics, the additive main effects and multiplicative interaction (**AMMI**) as proposed by Gauch (1992) has been incorporated in the present studies. The important feature of the **AMMI** model is that it integrates the analysis of variance and principal component analysis (**PCA**) into a unified approach (Gauch, 1992; Crossa *et al.*, 1990), which better explains the genotype-environmental interaction pattern. However, Dos Santos Dias and Krzanowski (2006) compared **AMMI** models as proposed by Gabriel (2002), Cornelius and Crossa (1999), Eastment and Krzanowski (1982), and Gollob (1968) for the detection of interaction patterns between genotypes and environments. The authors observed that all the four statistical methods adopted by these researchers produced different results for the same set of data and yielded a rather mixed picture. They

*Author for correspondence; E-mail: dr_mjr@hotmail.com

also noted that the method of Eastment and Krzanowski (1982) was more stable and behaved appropriately when a small number of components was considered. The Gabriel model (Gabriel, 2002) was very volatile and tended to choose many components, whereas the method of Cornelius and Crossa (1999) was more suitable for more important components, but was less stable than the Eastment-Krzanowski method. The Gollob version was broadly similar to the Cornelius-Crossa model, yet slightly poor in stability. However, authors (Santos Dias and Krzanowski, 2006) concluded that Eastment-Krzanowski model produced better results for AMMI analysis. Thus, in the present studies, multiple parameters have been used to determine the yield stability of thirteen newly evolved varieties tested in twelve different environments of the Sindh province of Pakistan.

Materials and Methods

Thirteen cotton varieties (all hirsutum type), of which three belonged to the Sindh province (CRIS-168, CRIS-467, CRIS-468), while the other ten varieties were evolved in the Punjab (DNH-57, FH-1000, NIBGE-1, VH-142, CIM-499, BH-147, MNH-635, CIM-473, SLH-257, FH-945), were compared for their adaptation to a series of environments. The varieties were sown in six districts of Sindh for two consecutive years (2001-2002). The experiments at each site/location were carried out in a randomized complete block design (RCBD) and consisted of four repeats. The same plot size of 10 x 47 feet was kept at all the test sites. The usual inputs like fertilizer, irrigations and insecticides were given as and when required. The recommended distance of 2.5 feet between row to row and 9.0 inches between plant to plant was given for healthy plant growth and development. The seed cotton yield was recorded in kg/ha of two picks. In the first instance, individual site analysis of variance was carried out for determining homogeneity of error mean squares. This parameter was declared similar, which allowed to conduct combined analysis of variance over locations. The terms environments, locations and test sites, hereafter, will be used interchangeably. The years and locations were combined and treated as environments with random effects.

The combined ANOVA over environments was performed according to Steel and Torrie (1980). When the genotype x environment interaction mean squares were declared significant, stability and adaptability parameters were determined according to Eberhart and Russell (1966), and the principal component analysis by Zobel *et al.* (1988). Linear regression coefficient (**b**) and the sum of squared deviations from regression (**s²d**) were calculated as suggested by Bilbro and Ray (1976). In addition to these statistics, principal component

analysis (**PCA-1**, **PCA-2**, latent roots and latent vectors), means, and grand means were also calculated as supporting statistics for measuring the varietal stability.

Results and Discussion

In a combined ANOVA (Table 1), the variety x environment source of variation was declared significant, which allowed further partitioning of this term into: (i) environment linear, (ii) variety x environment linear, and (iii) pooled deviations. The main effects due to the variety and environments were also found significant, which suggested that varieties performed differently over test locations.

These results further implied that genotypes should be thoroughly tested before they could be cultivated to wider or specific areas. For this purpose, regression analysis as suggested by Zobel *et al.* (1988), Bilbro and Ray (1976) and Eberhart and Russell (1966), were carried out. In the ANOVA,

Table 1. Mean squares from stability and adaptability analysis for seed cotton yield in upland cotton varieties tested in twelve environments

Source of variation	Degrees of freedom	Mean squares
Total	155	
Variety	12	235138.73**
Environment + variety x environment	143	540345.77**
Environment linear	1	278552.52
Variety x environment linear	12	2520821.34**
Pooled deviations	130	74388.29
Deviations from regression of each variety		
CRIS-168	10	88595.29
DNH-57	10	31064.99
FH-1000	10	47272.65
CRIS-468	10	51405.46
NIBGE-1	10	113695.27
VH-142	10	132472.35
CIM-499	10	64990.31
CRIS-467	10	10493.47
BH-147	10	102698.36
MNH-635	10	78624.35
CIM-473	10	143994.65*
SLH-257	10	62701.59
FH-945	10	39038.75
Pooled error	144	75714.61

** , * = significant at 1% and 5% probability levels, respectively

the term, pooled deviation, was tested against pooled error, which was declared non-significant, suggesting linear response of varieties in the test environments. However, the significance of the term, variety x environment linear, when tested against pooled deviations implied the existence of genetic differences among genotypes for their regression on the environmental index and regression coefficient (**b**). The deviation of each variety from regression was significant to only variety CIM-473, implying its more genotype-environment interaction.

The results presented in Table 2 show the stability and adaptability parameters of all the thirteen genotypes. The regression coefficient (**b**) accounted for the measure of adaptability, whereas the sum of squared deviations and coefficient of determination gave a measure of stability. The mean of varieties compared to grand mean was also used as the supporting statistics of varietal stability. A variety with regression coefficient (**b**) not significantly different from a unit slope (**b** = 1.0) could be considered adaptive to all types of environments, that is both the favourable and unfavourable ones.

The varieties with the (**b**) values higher than 1.0 means the varieties were more suitable to only highly favourable environments and the (**b**) values significantly less than 1.0 suggested that varieties performed well in less favourable environments. In the present studies, the values of regression coefficients (**b**) shown in Table 2 for all the test varieties evaluated, were not significantly different from the unit slope, hence, generally suggesting that the varieties were fairly adaptive to all the test sites. Nevertheless, the varieties FH-1000 (**b** = 1.059), VH-142 (**b** = 1.087), BH-147 (**b** = 1.078) and FH-945 (**b** = 1.065) gave the (**b**) values near to a unity, and were thus regarded as varieties with wider adaptability. The mean yields of these varieties were also higher or closer to the grand mean except VH-142, which also supported the wider adaptation of the above varieties. The mean yield of VH-142 was far below (1889.3 kg/ha) the grand mean (2001.42 kg/ha), but still displayed the (**b**) value near to unity (**b** = 1.087), which suggested that regression coefficient and mean yields were independent attributes for ascertaining yield stability of varieties. Variety CRIS-168 with regression coefficient **b** = 1.133 also gave mean yields (2251.3 kg/ha), which was higher than the grand mean indicating that this variety was adaptive to highly favourable environments. Nonetheless, varieties CRIS-467 (**b** = 0.766) and SLH-257 (**b** = 0.774) displayed (**b**) values lower than the unity and gave mean yields lower than the grand means, which suggested that both the varieties may perform well in less favourable environments.

The stability indicators, such as the minimum sum of squared deviations (s^2d) and values of coefficient of determination (r^2)

presented in Table 2 demonstrated that the varieties CRIS-467 and DNH-57 with minimum s^2d and higher r^2 were well stable in less favourable environments, whereas CIM-473 and NIBGE-1 varieties with maximum s^2d and less r^2 values were less stable in test environments. Though not all the stability and adaptability parameters discussed so far simultaneously favoured one variety over the others, yet on the basis of majority of the parameters, it is concluded that FH-945 is well adaptive to all types of environments, whether favourable or unfavourable, CRIS-168 to only highly favourable environments, and CRIS-467 to only less favourable environments. Similar to the present findings, Baloch (2003; 2001) and Geng *et al.* (1987) have also reported that not all the stability and adaptability parameters simultaneously favoured the same variety. The (s^2d) and (**b**) for the most part were not correlated in the present studies, which is also in consonance with the results obtained by Baloch (2003) and Gutierrez *et al.* (1994). However, a negative correlation between (s^2d) and (r^2) in the present studies is a sort of an indication of wider stability, which was noted in the case of varieties DNH-57, CRIS-467 and FH-945. Coefficient of determination (r^2) being significantly higher for all the varieties also coincided with the regression coefficient (**b**) values, which further indicated that all the varieties were fairly stable in yield performance in the test environments.

In addition to stability and adaptability parameters, a principal component analysis (PCA), a part of AMMI model, has

Table 2. Stability and adaptability parameters of thirteen upland cotton varieties tested in twelve different environments

Variety	Variety means	Regression coefficient (b)	Sum of squared deviations (s^2d)	Coefficient of determination (r^2)
CRIS-168	2251.3	1.133	885952.9	0.870
DNH-57	2138.0	0.866	310649.9	0.924
FH-1000	1978.1	1.059	472726.5	0.937
CRIS-468	1976.9	1.152	514054.6	0.929
NIBGE-1	1984.7	1.108	1136952.7	0.846
VH-142	1889.3	1.087	1324723.5	0.821
CIM-499	1981.2	0.976	649903.1	0.884
CRIS-467	1846.3	0.766	104934.7	0.966
BH-147	2217.4	1.078	1026983.6	0.852
MNH-635	1765.2	0.834	786243.5	0.819
CIM-473	2027.9	1.102	1439946.5	0.812
SLH-257	1905.0	0.774	627015.9	0.835
FH-945	2057.2	1.065	390387.5	0.933
Grand mean 2001.42				

been worked out to further determine the pattern of interaction. The results shown in Table 3 indicate that latent vectors of the first two principal components (**PCA-1** and **PCA-2**) accounted for about 91.242% of the total variation. El-Shaarawy (2000) using multiplicative principal component analysis recorded 87.77 % of total variation in lint yield attributable to first three **PCAs**. The eigen values of first principal component analysis (**PCA-1**) of all the varieties were smaller and positive, hence suggesting that test varieties were highly stable in the test environments. While some varieties gave positive and others negative eigen values for **PCA-2**, smaller positive values were expressed by varieties FH-1000, CIM-499, CRIS-467 and FH-945, suggesting that these varieties had shown relatively less genotype-environment interaction, and were thus suitable to all the test environments. Palomo and Godoy (1996) also reported that varieties showing smaller **PCA** scores were more stable in their yield performance.

It may be generally concluded from the overall results, that variety CRIS-168 is suitable to highly favourable environments, CRIS-467 to less favourable environments, and FH-945 to all types of environments.

The AMMI biplot illustrates a significant portion of the genotype-environment interaction in a more comprehensible manner. Genotypes that appeared almost on a perpendicular or horizontal line have similar pattern of interaction. Genotypes with large **PCA-2** scores, either positive or negative, showed high interaction in test environments, whereas genotypes with **PCA-2** scores near to zero have small interactions. Varieties with a **PCA-2** score smaller or near to zero indicate their adaptability to all types of environments, while those with large **PCA-2** scores showed a specific adaptability in the environments. Four groups of genotypes are evident from the biplot (Fig. 1). In fact, all the **PCA-2** scores (Table 3) were multiplied with a common figure of 100, making the figures larger, hence easier to plot (Fig. 1).

Group-1 includes genotypes VH-142 and CRIS-468. These varieties showed a similar mean yield response (yields below the grand mean) and had also similar large negative interactions. **Group-2** consists of genotypes NIBGE-1, CIM-499 and FH-1000. The mean yields of these varieties were similar, but their interactions with the environments were quite different. The interaction **PCA-2** score of variety FH-1000 was smaller and positive, whereas positive and larger for variety NIBGE-1. The **Group-3** represents varieties MNH-635, CIM-499 and FH-945. These varieties had similar and smaller positive **PCA-2** scores, but were very different in mean yields. Variety CIM-499 has both the desirable attributes, that is, the **PCA-2** score and the mean yield. Hence, in the biplot (Fig. 1) it falls just at

the junction of horizontal and vertical lines of the x and y axes. The variety had the mean yield near the grand mean and **PCA-2** score was near zero. Variety MNH-635, though gave smaller **PCA** score hence showing less genotype-environment interaction, yet its mean yield was far below the grand mean. The third variety of the group is FH-945, which gave smaller and positive **PCA** scores and also gave mean yields

Table 3. The eigen values, latent vectors (**PCA-1** and **PCA-2**) of varieties and percent variance determined by the principal component analysis

Order*	Variety ⁺	Latent roots (eigen values)	Percent variance	Latent vectors (eigen vectors)	
				PCA-1	PCA-2
1	CRIS-168	6026132.52	87.484	0.315	-0.354
2	DNH-57	258903.25	3.759	0.241	-0.002
3	FH-1000	208248.42	3.023	0.255	0.091
4	CRIS-468	158050.43	2.294	0.321	-0.232
5	NIBGE-1	88059.72	1.278	0.307	0.433
6	VH-142	67971.88	0.987	0.302	-0.138
7	CIM-499	46842.76	0.680	0.269	0.044
8	CRIS-467	16957.69	0.246	0.212	0.057
9	BH-147	10699.82	0.155	0.300	0.364
10	MNH-635	4518.93	0.066	0.230	0.322
	CIM-473			0.309	-0.577
	SLH-257			0.214	0.175
	FH-945			0.296	0.020

* = corresponds to latent roots and percent variance; + = corresponds to latent vectors only

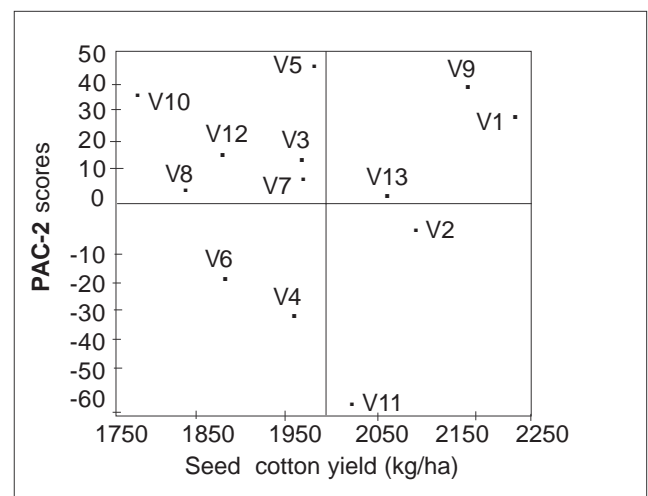


Fig. 1. Biplot of seed cotton yield and **PCA-2** scores for thirteen cotton varieties tested in twelve different environments (V1 to V13 represent the variety numbers).

higher than the grand mean showing high level of stability in test environments. **Group-4** includes varieties CRIS-168 and CIM-473 with high positive and negative **PCA** scores, respectively, but had similar mean yields. Variety CRIS-467 gave mean yields near the grand mean, whereas CRIS-168 produced mean yields higher than the grand mean. Hence, both the varieties are suitable for specific environments as explained in previous paragraphs.

References

- Baloch, M.J. 2003. Measuring yield performance of upland cotton varieties using adaptability, stability and principal component analysis. *Proceedings Pakistan Acad. Sci.* **4**: 147-150.
- Baloch, M.J. 2001. Stability and adaptability analysis of some quantitative traits in upland cotton varieties. *Pak. J. Sci. Ind. Res.* **44**: 105-108.
- Bilbro, J.D., Ray, L.L. 1976. Environmental stability and adaptation of several cotton cultivars. *Crop Sci.* **16**: 821-824.
- Cornelius, P.L., Crossa, J. 1999. Prediction assessment of shrinkage estimators of multiplicative model for multi-environment cultivar trials. *Crop Sci.* **39**: 998-1009.
- Crossa, J. 1988. A comparison of results obtained with two methods for assessing yield stability. *Theor. Appl. Genet.* **75**: 460-467.
- Crossa, J., Gauch Jr., H.G., Zobel, R.W. 1990. Additive main effects and multiplicative interaction analysis of two international maize cultivar trials. *Crop Sci.* **30**: 493-500.
- Dos Santos Dias, C.T., Krzanowski, W.J. 2006. Choosing components in the additive main effect and multiplicative interaction (AMMI) models. *Scientia Agricola* **63**: 169-175.
- Eastment, H.T., Krzanowski, W.J. 1982. Cross-validatory choice of the number of components from a principal component analysis. *Technometrics* **24**: 73-77.
- Eberhart, S.A., Russell, W.A. 1966. Stability parameters for comparing varieties. *Crop Sci.* **6**: 36-40.
- El-Shaarawy, S.A. 2000. Modified AMMI for measuring performance stability for different genotypes over different environments. In: *2000 Proceedings of the Beltwide Cotton Conferences*, Memphis, Tennessee, USA, **2000**: 550-553.
- Finlay, K.W., Wilkinson, G.N. 1963. The analysis of adaptation in plant breeding programmes. *Aust. J. Agric. Res.* **14**: 742-754.
- Gabriel, K.R. 2002. Le biplot-outil d'exploration de données multidimensionnelles. *Journal de la Société Française de Statistique* **143**: 5-55.
- Gauch, H.G. 1992. *Statistical Analysis of Regional Yield Trials: AMMI Analysis of Factorial Designs*, Elsevier Science Publishers B.V., Amsterdam-London, The Netherlands, UK.
- Geng, Shu, Quifa Zhang, Basset, W.M. 1987. Stability in yield and fibre quality of California cotton. *Crop Sci.* **27**: 1004-1010.
- Gollob, H.F. 1968. A statistical model which combines features of factor analytic and analysis of variance techniques. *Psychometrika* **33**: 73-115.
- Gutierrez, J.C., Lopez, M., El-Zik, K.M. 1994. Adaptation of upland cotton genotypes to the Guadalquivir valley in Spain. In: *Proceedings of the Beltwide Cotton Conferences*, January 5-8, San Diego, California, USA, **2**: 670-673.
- Lin, C.S., Binns, M.R. 1988. A superiority measure of cultivar performance for cultivar x location data. *Can. J. Pl. Sci.* **68**: 193-198.
- Lin, C.S., Binns, M.R., Lefkovich, L.P. 1986. Stability analysis. Where do we stand? *Crop Sci.* **29**: 894-900.
- Palomo, A., Godoy, S. 1996. Yield stability of nine cotton genotypes. In: *Proceedings of the Beltwide Cotton Conferences*, Memphis, Tennessee, USA, **1**: 592-598.
- Steel, R.G.D., Torrie, J.H. 1980. *Principles and Procedures of Statistics*, pp. 195-215, 2nd edition, McGraw-Hill Book Company, New York, USA.
- Zobel, R.W., Wright, M.J., Gauch Jr., H.G. 1988. Statistical analysis of a yield trial. *Agron. Journal* **80**: 388-393.

Isolation and Stabilization of Dark Red Food Dye from *Beta vulgaris*

Alim-un-Nisa*, Shamma Firdous and Nusrat Ijaz

Food and Biotechnology Research Centre, PCSIR Laboratories Complex, Ferozpur Road, Lahore-54600, Pakistan

(received August 25, 2005; revised June 30, 2006; accepted July 6, 2006)

Abstract. Natural highly coloured dark red pigment was isolated from *Beta vulgaris*, in paste and powdered form. Total colouring matter of the concentrated colour was 1.86% and 4.5%, respectively, for the paste and powdered forms, calculated as betanine. Sodium benzoate (0.01%) was used as the stabilizer for paste, while silicon dioxide (2%) was added in addition to sodium benzoate (0.01%) for storage of the red colour in powdered form. Other parameters that may influence the stability of the colour, such as pH, temperature and relative humidity, were studied. Toxicity evaluation, and lead and arsenic levels were determined. The addition of stabilizers, like citric acid, ascorbic acid, EDTA and sodium chloride, were also investigated, none of which showed useful effect.

Keywords: food colour, betanine, beetroot colour, *Beta vulgaris* red colour, food colour isolation, food colour stabilization

Introduction

Beetroot contains betanin ($C_{24}H_{26}N_2O_{13}$) as the principal pigment, which is the D-glucopyranoside of betanidin (FAO, 1984). It is obtained from the roots of red beet (*Beta vulgaris*). The red colour of beetroot is suitable for products having relatively short shelf-lives and where the food stuff has not to undergo high or prolonged heat treatment (Coulson, 1980). Stability is higher in the pH range of 4-5, though the stability is reasonable in the pH range of 3-7. Adding colour, after the heating process has ceased, can be successfully done for the colouration of foods that have to undergo heat treatment. Adding small amount of benzoate, sorbate or EDTA can enhance stability of the colour. Beetroot red colour may be used, with the addition of a suitable stabilizer, in soft drinks, ice cream, meat and soyabean protein products, and in dry mixes such as gelatin desserts (Coulson, 1980).

Various laboratory techniques have been reported for the isolation of colour from beetroot (Krasnikova *et al.*, 1996). The rich red dye in powdered form has been obtained by heating beetroots at 100 °C for 5 min. The peroxide present can be inactivated, and the colour extracted with aqueous citric acid (Lozano *et al.*, 1993). The red dye has been also obtained by the aqueous extraction of colour from beetroots (Kutsakova *et al.*, 1997). Red dye from beet was earlier obtained by pre-heating beet slices with 0.125% citric acid at 100 °C for 20 min and the average recovery was reported as 63.3% (Liu, 1981).

The presently developed procedure involves the extraction of red food dye from beetroots with salicylic acid (0.125%),

which was then concentrated by freeze drying. The purpose of the present study was to produce natural red dye in powdered as well as in paste form, to enhance the stability of colour at different pH values and temperatures, to study any toxicological effect of the extracted red food dye, and to determine the usefulness of the obtained colour in different foodstuffs. The principal objective of the present study was to produce natural food dye that is non-toxic and harmless to human health, since it has been claimed that several artificial colours and flavours used in foods may lead to hyperactivity and learning disability in children (Feingold, 1975). It was estimated that 50% of the hyperactive children could be completely cured by a diet, totally devoid of these chemicals.

Materials and Methods

Instruments used. Freeze dryer (Eyela; FD 550), vacuum oven (Hitachi Yamato; DP 41), hotplate blender (Waring), spectrophotometer (Hitachi; U-1100), atomic absorption spectrometer (Hitachi, 170-10).

Chemicals. Sodium benzoate (Win Laboratories); citric acid, salicylic acid, silicon dioxide, ascorbic acid, disodium hydrogen phosphate (E. Merck, Germany); EDTA (BDH).

Extraction of the colour. The red colour was extracted with 0.125% solution of salicylic acid by blending fine slices of beetroots in a Waring blender at medium speed for 5 min. The extract was filtered through Whatman filter paper# 1. Residues were washed thrice with salicylic acid solution.

Drying techniques. Various drying techniques were used to concentrate the fresh colour extracted from the beetroots, such as waterbath drying, hotplate drying, sun-drying, vacuum oven-

*Author for correspondence; E-mail: izaancheema@yahoo.com

drying, and freeze drying. Maximum betanine contents (the colouring matter of beetroots) were obtained when the freeze drying method was used. The colour dried with other techniques resulted in the product having lesser colour content, which turned reddish brown. Therefore, the freeze drying technique was used to concentrate the extracted red colour.

Freeze drying technique. The extracted colour was dried in a freeze dryer in two steps. In the first step, the extracted red colour was frozen and the temperature of the freeze dryer was set according to the quantity of the extract (if volume of the sample was less, then it was frozen at - 20 °C; if the quantity of the sample was greater, then the temperature was lowered down, according to the requirement). In the second step, sublimation was initiated, and the dry mass was obtained within 6 to 8 h.

Measurement of colour contents. The total colour contents were measured spectrophotometrically in McIlvaine's citric acid buffer (pH 5) by measuring absorbance at 535 nm (FAO, 1984). The colour intensity was calculated on the basis of maximum absorption. All the red colouring matter is betanine, which was calculated as below (FAO, 1984):

$$\text{absorbance} \times 100 / \text{concentration} \times A [1\%, 1\text{cm}]$$

Metallic impurities. The extracted colour was digested in a mixture of sulphuric acid, nitric acid and perchloric acid. The digested metals were determined by atomic absorption spectroscopy according to the method of FAO (1984).

Results and Discussion

Percentage of colour contents. The colour obtained after freeze drying was stored in the paste and powdered forms. Total colour contents were 4.5% in the powdered form and 1.86% in the paste form. Higher percentage of betanine was obtained due to the lesser degradation of betanine in the selected drying technique.

Effect of relative humidity. Relative humidity was noted to influence colour contents, as well as appearance of the colour, during storage (Table 1). It is evident from these results that the powdered form exists only upto 40% relative humidity and colour contents were also higher at this relative humidity. However, with increase in relative humidity (60%), the colour intensity slightly decreased and the extracted red colour was converted to a hard mass. At 70% relative humidity and above, the colour contents decreased to 1.86% and the colour was converted to the paste form. Stringent control of conditions, like humidity and temperature, is required to maintain colour in powdered form. Silicon dioxide was also added in the extracted red colour to avoid settling of the colour, which was also observed to

Table 1. Effect of relative humidity on the stability and appearance of the red colour extracted from beetroots, when stored at 25 °C for a period of six months

Relative humidity (%)	Colour* contents (%)	Appearance of the colour
30	4.5	powder
40	4.3	setteled powder
60	4.0	hard Mass
70	2.0	paste
80	1.86	paste

* = measured as betanine

enhance shelf-life of the colour and for maintaining it in the powdered form for a longer period of time.

Effect of stabilizers. The effect of different stabilizers on the stability of the extracted colour is shown in Table 2. Stabilizers were used individually and in different combinations. It was found that intensity of the colour, without any stabilizing chemical, decreased within few weeks. It was observed that addition of sodium benzoate (0.01%) to the colour extracted with salicylic acid (0.125%) significantly enhanced the stability as well as shelf-life of the colour, and the assayable content as betanine remained constant for upto one year. Intensity and stability of the colour has been reported to be enhanced on the addition of ascorbic acid (0.125%) with sodium benzoate (0.01%), and citric acid (0.125%) with sodium benzoate (0.1%) (Krasnikova *et al.*, 1996). Similar observation was made by Chorbanov *et al.* (1988) and Zhrebina *et al.* (1991). However, it was concluded that shelf-life and total colouring matter decreased when sodium benzoate was added to the extracted colour as stabilizer. Colour with sodium chloride as the stabilizer, absorbs moisture and turned to liquid form even after 24 h of drying. EDTA (0.1%) also increased the stability, but sodium benzoate was noted to be a better stabilizer than EDTA. It was also concluded that the colour stored in powdered form settled into a hard mass after few months. Silicon dioxide (2%) was added to overcome this problem.

Effect of pH. The colour isolated from beetroots showed maximum stability in the pH range of 4.5-7.5 (Fig. 1). At the lower pH (2.5) level, reduction in the colour contents was noted as the colour turned to light red. At pH values higher than 7.0, the colour changed from dark red to reddish violet, which turned to yellow towards the higher pH values, upto pH 12.0. Similar reports have been published by other researchers that betalains are especially stable at pH 5.0, which could be stabilized against decolourizing and the action of antioxidants

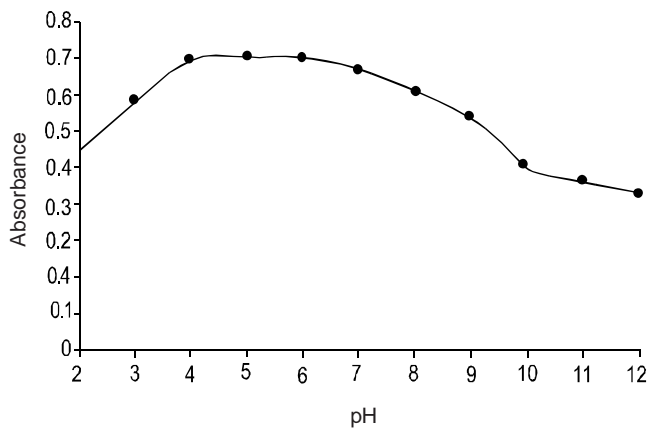


Fig. 1. Effect of pH on the stability of red colour extracted from beetroots.

by acidifying their solutions to pH 4.5 to 5.0 (Hamburg and Hamburg, 1991).

Effect of storage temperature. Colour was stored at different temperatures and best results were obtained at 15-35 °C (Table. 3). Above this temperature, the assayable contents reduced and the colour became unstable, which may be due to the degradation of the main colouring component (betanine) at the higher temperature. It was observed that at lower temperature, there was no remarkable change in the colour during storage period of one year. However, at higher temperature (60 °C), the storage period induced a drastic change in the assayable contents of the colour. There was no apparent trend of colour change at lower temperatures, suggesting that the colour remained stable at lower temperature during storage.

Table 2. Effect of different stabilizers on the stability of colour extracted from beetroots

Stabilizers (%)	Colour contents (%)										
	Sep 2002	Oct 2002	Nov 2002	Dec 2002	Jan 2003	Feb 2003	Mar 2003	Apr 2003	May 2003	June 2003	July 2003
Sodium benzoate (0.01)*	1.86	1.86	1.86	1.86	1.86	1.86	1.86	1.78	1.76	1.75	1.70
Sodium benzoate (0.01) + ascorbic acid (0.125)*	1.70	1.70	1.68	1.65	1.50	1.30	1.15	1.00	0.85	0.70	0.63
Sodium benzoate (0.01) + citric acid (0.125)*	1.60	1.60	1.50	1.35	1.32	1.25	1.22	1.00	0.80	0.68	0.50
Sodium chloride (0.5)*	0.9	0.63	0.50	0.28	0.15	0.10	0.05	-	-	-	-
EDTA (0.1)*	1.25	1.25	1.23	1.23	1.20	1.18	1.15	1.12	1.10	1.10	1.09
Sodium benzoate (0.01) + silicon dioxide (2.0)**	4.50	4.50	4.50	4.45	4.50	4.50	4.50	4.48	4.45	4.43	4.40

* = paste form; ** = powder form

Table 3. Effect of storage temperature on the stability of colour extracted from beetroots

Storage temperature (°C)		Colour contents (%)										
		Sep 2002	Oct 2002	Nov 2002	Dec 2002	Jan 2003	Feb 2003	Mar 2003	Apr 2003	May 2003	June 2003	July 2003
15	paste	1.86	1.86	1.86	1.86	1.86	1.86	1.86	1.86	1.86	1.85	1.83
	powder	4.50	4.50	4.50	4.50	4.50	4.50	4.50	4.43	4.40	4.38	4.35
25	paste	1.86	1.86	1.86	1.86	1.86	1.86	1.84	1.82	1.80	1.80	1.79
	powder	4.50	4.50	4.50	4.50	4.45	4.42	4.42	4.40	4.35	4.35	4.30
35	paste	1.86	1.86	1.86	1.85	1.85	1.85	1.80	1.78	1.75	1.71	1.69
	powder	4.50	4.45	4.43	4.40	4.40	4.38	4.35	4.32	4.30	4.25	4.00
60	paste	1.86	0.75	0.50	0.18	0.05	-	-	-	-	-	-
	powder	4.45	3.20	2.58	2.02	1.16	1.02	0.95	0.81	0.55	0.35	0.30

Toxicity and heavy metals. Toxicity test was performed on mice and it was observed that the extracted colour was non-toxic. Lead and arsenic were not detected in the extracted colour, while other heavy metals were found within the limits specified by FAO (1984).

Stability of colour during cooking. The effect of cooking time and temperature is shown in Fig. 2. It is evident that the colour remained stable upto 80 °C for 15 min. Above this time and temperature, colour intensity decreased and colour became unstable.

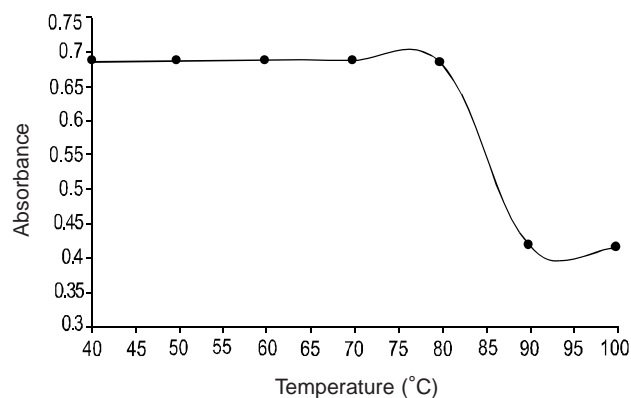


Fig. 2. Effect of temperature on the stability of colour extracted from beetroots during 15 min cooking; conditions: pH(4.0), stabilizer(sodium benzoate, 0.01%).

References

- Chorbanov, B., Ushanova, G., Lichev, V., Stamenov, S. 1988. Stabilized food coloring agent from red beets. *Khranit. Prom-st.* **37**: 38-40.
- Coulson, J. 1980. Naturally occurring colouring materials for food. In: *Developments in Food Colors*, J. Walford (ed.), pp. 208-210, Applied Science Publishers Ltd., London, UK.
- FAO. 1984. *Specifications for Identity and Purity of Colours*, **31/1**, pp. 23-26 (as prepared by the 28th Session of the Joint FAO/WHO Expert Committee on Food Additives), Food and Agriculture Organization, Rome, Italy.
- Feingold, B.F. 1975. Hyperkinesis and learning disabilities linked to artificial food flavours and colours. *American J. Nursing* **75**: 797-803.
- Hamburg, A., Hamburg, A. 1991. The stability properties of red beet pigments: influence of pH, temperature and some stabilizers. *Meded. Fac. Landbouwwet. Rijksuniv. Gent.* **56**: 1693-1695.
- Krasnikova, L.V., Filippov, V.I., Frolov, V.L., Tikhonov, L.A. 1996. Production of food dye concentrate from beets by using lactobacilli, ascorbic acid, and tannins. *Russ. Ru2,061,044 (cl. C09B61/00)*, May 1996 (from *Izobreteniya* **1996**: 221).
- Kutsakova, V.E., Frolov, S.V., Yakovleva, M.I. 1997. Mass transfer during freezing. *Zh. Prikl. Khim. (S-Petersburg)* **70**: 2061-2063.
- Liu, Z. 1981. Isolation and application of red pigment from beet. *Shipin. Kexue.* **20**: 3-6.
- Lozano, J., Rosales, J., Marcelo, A. 1993. Production of red coloring agent in powdered form from automation, from beet (*Beta vulgaris*). *Bol. Soc. Quim. Peru* **59**: 175-183.
- Zerebin, Yu.L., Kapustina, V.V., Veselova, L.V. 1991. Effect of ascorbic acid on betalain pigments of beet juice before and after fermentation. *Izv. Vassh. Uchebn. Zaved. Pishch. Tekhnol.* **1991**: 37-39.

The Effect of Substitution on the Dyeing and Spectroscopic Properties of Some Monoazo Disperse Dyes

Ausaf Aleem*, Mohammad Naeem, M. Aleem Ahmed, Kamran Ahmed and Mansoor Iqbal

Applied Chemistry Research Centre (Textile Section), PCSIR Laboratories Complex Karachi,
Shahrah-e-Dr. Salimuzzaman Siddiqui, Karachi-75280, Pakistan

(received December 17, 2005; revised August 6, 2006; accepted August 9, 2006)

Abstract. A range of monoazo disperse dyes has been synthesized. The colour, dyeing and fastness properties of the dyes on polyester, nylon and secondary acetate fibre at 1/1 standard depth have been examined and rationalized in terms of dye structure. The visible absorption behaviour of the dyes was also investigated. In general, substitutions on the diazo component have a significant effect on the visible absorption maxima of the dyes. Increasing the solvent polarity also had a pronounced effect on the absorption maxima.

Keywords: monoazo dyes, diazotization, dyeing, dye migration

Introduction

The disperse dyes arose out of the endeavour of many workers to find an easy and commercially satisfactory way to dye cellulose acetate. The importance of water insoluble disperse dyes has increased to a very great extent with the appearance of synthetic fibres, some of which, such as polyester and triacetate, are much more hydrophobic than cellulose acetate, and therefore very resistant to the conventional water soluble dyes (Trotman, 1984).

As with other classes, diverse properties are expected of disperse dyes according to the dyeing conditions that will be encountered during use. Disperse dyes for acetate are required to have brightness and fastness of shades, good build-up, and levelling properties. Some dyes, otherwise satisfactory, show a tendency to sublime under domestic ironing conditions. Others are sensitive leading to marked deterioration in their shades (Muller, 1970). Research efforts have been accordingly made to overcome these shortcomings and to determine such structural features that would confer improvements in these properties (Clark and Hildreth, 1973). These have been adapted to meet the requirements of polyester fibres and of different dyeing processes, mainly by varying the substituent types of the dye, which have quickly become important for dyeing acetate fibres (Stead, 1970).

Synthesis of some disperse dyes and their dyeing properties have been reported and discussed in the present paper. The findings of this study have been discussed in term of the structural features of the dye molecules. The focus has remained on dyes derived from conventional diazo component and aniline-based coupler.

*Author for correspondence

Materials and Methods

Synthesis of dyes. The dyes were synthesized by coupling the appropriate diazonium ions with N,N-diethylaniline. The amines used in the synthesis were 4-nitroaniline, 2-chloro-4-nitroaniline, 2,4-dinitroaniline, 4-nitroanisole, 2-cyano-4-nitroaniline, 2,6-dichloro-4-nitroaniline. All the amines were diazotized in aqueous hydrochloric acid and then gradually added to a well stirred dispersion of N,N-diethylaniline in a weakly basic system. These have been listed as **Ia-Ij**. The parent dye had the general structural formula as given in Fig. 1.

All the dyes were separated from the reaction mixture by filtration and then purified by dimethyl formamide (DMF) and their ϵ_{\max} in the visible region were measured on Nicolet evaluation spectrophotometer (Thermo Electron Corporation, Madison, Wisconsin, USA).

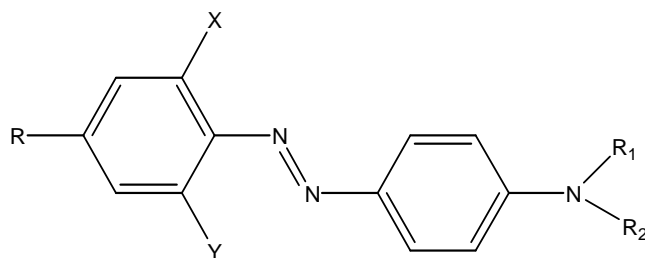
Dyeing of fabric at different concentrations. Dyeing of 0.5 %, 1% and 2% was carried on 5 g fabric at 130 °C for 75 min, using high temperature dyeing machine (Ahiba IR Laboratory Dyeing System, model D400ir/I, SDL Atlas Ltd., London, UK) containing 2 g/l dispersing agent, 3 ml/l acetic acid to maintain pH at 4.5-5.5, and the liquid to goods ratio of 1 : 20. After this period (75 min), the study specimens were removed from the dyeing bath and rinsed with cold water and dried. The dyeings were reduction cleared in an aqueous solution of sodium hydro-sulfite (2-3 g/l) and sodium hydroxide (2 g/l), using the liquid to goods ratio of 1 : 20 at 60 °C for 10 min. The samples were then rinsed with water and dried. The prepared dyes exhibited best dyeing properties on polyester and secondary acetate, dyeing on nylon being inferior to those on polyester and secondary acetate.

Assessment of dyeing properties. Build-up test. The concept of build-up can be related to the adsorption isotherm under high temperature conditions, since many dyes approach fairly close to the equilibrium adsorption within a practical dyeing time. The dyeing solution of different concentrations, 0.5 %, 1 % and 2 %, were prepared by the amount of dyes required to produce 1 : 1 standard depth at 80 °C (Derbyshire and Lemon, 1964). Dyeing was produced in the normal dyeing times at 100–130 °C. The dyed sample was assessed visually with the standard grey scale. The results are presented in Table 1.

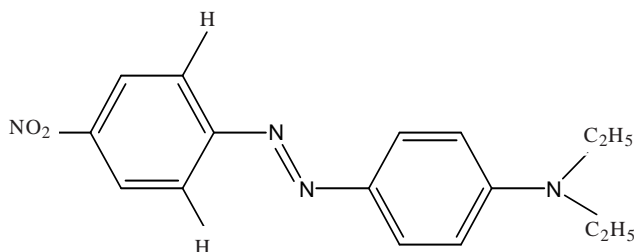
Migration test. The 1 : 1 ISO standard depth dyeing was prepared at 80 °C (Derbyshire and Lemon, 1964). Equal weights of this dyeing and similar undyed material were placed in a bath at 80 °C liquid to goods ratio of 50 : 1 and left immersed with agitation for one h. The difference between the two pieces was then assessed with the SDC Grey scale (Grey scale for assessment of the change in colour and staining; BS-1006, ISO-105, G-246-A; Atlas Material Testing Technology, Chicago, Illinois, USA). The results of migration test have been tabulated in Table 2.

Assessment of fastness properties. Colour fastness to light. The colour fastness to artificial light of the dyed samples was carried out by ISO-BO2 standard test procedure (SDC, 1999). The test specimen of the dyed fabric was exposed to artificial light (Xenon Arc Fading Lamp, model ci 3000+, Atlas Material Testing Technology, Chicago, Illinois, USA) under standard conditions, using sample of blue wool as the reference. The colour fastness was then assessed by comparing the change in colour with that of the reference blue wool sample. In all such cases, the light fastness exhibited on polyester was high, whereas on nylon it was poor. Light fastness assessment of dyes is given in Table 3.

Fastness to sublimation. This method of assessing sublimation fastness of the dye was carried out by ISO PO1 standard test procedure (SDC, 1999). The test sample was sandwiched



General structural formula of the parent dye



Structure of the parent dye (1a)

dye (1b) X = H, Y = Cl

dye (1c) X = H, Y = NO₂

dye (1d) X = H, Y = OCH₃

dye (1e) X = H, Y = CN

dye (1f) X = Cl, Y = Cl

Dyes synthesized from the parent dye (1a)

Fig. 1. The conventional structure of dyes and the general structural formulae of the dyes synthesized from the parent dye.

between two pieces of undyed material. The composite specimen was heated in an oven for 30 sec at 210 °C. The composite specimen was removed and left for 4 h in air, at room temperature and relative humidity of 65 %. The change in colour of the specimen and the staining of the adjacent fabric was assessed with the SDC Grey scale. The results of the study on fastness to sublimation are presented in Table 4.

Table 1. Dyeing properties of monoazo disperse dyes for 2% dyeing

Dye*	Polyester		Secondary acetate		Nylon	
	substantivity	build-up	substantivity	build-up	substantivity	build-up
1a	good	3-4	moderate	3	moderate	2
1b	moderate	3	moderate	2-3	poor	1
1c	good	3-4	good	3	moderate	2
1d	very good	3	good	3-4	moderate	1
1e	good	2-3	good	2	poor	1
1f	very good	3-4	good	3	poor	1

* = see Fig. 1 for the structure of parent dye and the derivative dyes; build-up has been reported in accordance with the standard Grey scale

Results and Discussion

Disperse dyes (**1a-1f**) were prepared by the conventional method of diazotization and coupling (Straley, 1970). The dyes were purified and their ϵ_{max} in the visible region were determined. The data presented in Table 5 show ϵ_{max} values of the parent and other dyes. The visible absorption band showed a bathochromic shift with increase in the solvent polarity (hexane to ethanol), confirming a $\delta - \delta^*$ transition involving the whole conjugated system. Substitution of a chlorine atom in the diazo component produced a bathochromic shift of approximately 5 nm in accordance with the electron donor properties of this substituent. With dyes (**Ic**) and (**Id**) the substituent caused a bathochromic shift in ϵ_{max} with respect to the unsubstituted dye (**Ia**). Variation in Y resulted in a bathochromic shift which increased in the order of H, Cl, NO₂, OCH₃, CN. Comparison of the dye (**Ib**) with (**Ic**) showed that the presence of NO₂ group ortho to the azo group in (**Ic**) gave a bathochromic shift of 7 nm in ethanol compared to the dye (**Ib**) containing the chlorine atom reflecting the greater electron withdrawing nature of NO₂ group. The presence of chlorine at 2,6 position

ortho to the azo group resulted in the possible steric effect on the azo benzene system. Steric hindrance prevents a planar alignment of the azobenzene molecule, which leads to a hypsochromic shift with simultaneous loss of clarity. These results are in agreement with similar observations reported in the literature (Peters, 1985; Marion, 1960). These results can be explained in terms of solvent solute interaction. With hexane, this interaction was minimal, since the solvent was non-polar and any stabilizing effect affected the ground and excited states equally. This resulted in a shift towards shorter wavelength. In ethanol, the interaction was much stronger, even to the possibility of formation of H-bonding between the solvent and the solute (Patrik and Svehle, 1977). All dyes exhibited good level of dyeing on polyester and secondary acetate fibre with a good build-up (Table 1), but had poor substantivity for nylon.

Migration test also showed a similar behaviour (Table 2), while the light-fastness test by Xenon Arc Lamp showed a very good stability for polyester and secondary acetate fibre (Table 3). The sublimation fastness (Table 4) clearly indicated that

Table 2. Migration test rating of disperse dyes on different fibres for 2 % dyeing (reported in standard Grey scale)

Dye*	Polyester	Secondary acetate	Nylon
Ia	4-5	4-5	3-4
Ib	3-4	4	2
Ic	4	4-5	3
Id	4-5	4	2-3
Ie	4-5	4	2-3
If	4-5	4	3

* = see Fig. 1 for the structure of parent dye and the derivative dyes

Table 3. Light fastness rating for 2% dyeing on different fibres (reported in standard Grey scale)

Dye*	Polyester	Secondary acetate	Nylon
Ia	4-5	4	2
Ib	4	4	2
Ic	5	5-6	3
Id	6	5-6	2-3
Ie	6	5	2-3
If	6-7	6	3

* = see Fig. 1 for the structure of parent dye and the derivative dyes

Table 4. Fastness to dry heat of disperse dyes for 2% dyeing (reported in standard Grey scale)

Dye*	For polyester			For secondary acetate			For nylon		
	change in shade	staining cotton	staining polyester	change in shade	staining cotton	staining polyester	change in shade	staining cotton	staining polyester
Ia	4-5	4	4-5	5	4-5	4-5	2-3	2-3	2-3
Ib	4	4	4	4-5	4	3-4	2-3	2-3	2
Ic	4-5	4	4	4	4	3-4	3	2-3	3
Id	5	4-5	4	4-5	4	4	2-3	2-3	2-3
Ie	4-5	4	4	4	4	3-4	3	3	3
If	3-4	4	4	4-5	4	4	2	3	2-3

* = see Fig. 1 for the structure of parent dye and the derivative dyes

Table 5. Effect of substitution on visible absorption values of disperse dyes ($R_1 = R_2 = C_2H_5$)

Dye*	R	X	Y	ϵ_{\max} (in ethanol)	Log ξ	ϵ_{\max} (in hexane)	Log ξ
Ia	NO ₂	H	H	514	4.410	482	4.381
Ib	NO ₂	H	Cl	519	4.410	490	4.380
Ic	NO ₂	H	NO ₂	526	4.416	495	4.389
Id	NO ₂	H	OCH ₃	534	4.417	495	4.388
Ie	NO ₂	H	CN	539	4.417	497	4.388
If	NO ₂	Cl	Cl	480	4.380	462	4.380

* = see Fig. 1 for the structure of parent dye and the derivative dyes

the dyes were quite stable at high temperature. The shades were generally reddish-violet to dull reddish-brown, depending on the nature of the substituent groups present in the diazo components as shown in Table 5.

Conclusion

The important conclusion that may be drawn from this work is that the synthesized disperse dyes showed good dyeing and fastness properties of an acceptable range. The strong electron donating influence of the substituted groups tended to stabilize monoazo disperse dyes. By increasing the solvent polarity there was a remarkable effect on the absorption maxima. The dyes are especially useful on polyester and secondary acetate, but more selective structural modifications are required for the colouration of nylons. A fair to good light fastness rating may be attributed in part to the non-polar nature of the dye molecule, which does not readily attract water molecules and other polar agents that may have a degrading effect. Further, the aromatic or benzene structure of the dyes gave them a relatively stable structure. The substitution variations in the diazo component demonstrated the facility with which different colours may be developed. Thus, the present data not only provide a base for assessing various disperse dyes but could also be extended to develop new disperse dyes with better exhaustion, built-up, colour, and fastness properties.

References

- Clark, M.C., Hildreth, J.D. 1973. Review articles on disperse dyes in annual reports on the progress of applied chemistry. *Society of Chemical Industry* **58**: 321-324.
- Derbyshire, Lemon, 1964. Development in disperse dyes. *J. Soc. Dyers Colourists* **80**: 243.
- Marion, D. 1960. The theory of colouration of textile. *American Dye Staff Report* **49**: 36-38.
- Muller, C. 1970. Recent developments in the chemistry of disperse dyes and their intermediates. *American Dye Staff Report* **61**: 37-44.
- Patrick, R.A., Svehle, G. 1977. The dyeing of cellulose acetate rayon with disperse dyes. *Anal. Chim. Acta* **88**: 363-364.
- Peters, A.T. 1985. Recent trends in the search for new azo dyes. Dyes for acetate rayon. *J. Soc. Dyers Colourists* **101**: 361-363.
- SDC. 1999. *Standard Methods for the Determination of Colour Fastness to Textile and Leather*, pp. BO2 (1-3), PO1 (1-2), 5th edition, The Society of Dyers and Colourists, SDC Publishers, Bradford, England.
- Stead, C.V. 1970. Chemical basis of technology of disperse dyes. *Review Progress Colouration and Related Topics* **1**: 26-31.
- Straley, J.M. 1970. *The Chemistry of Synthetic Dyes*, K. Venkatraman (ed.), vol. **III**, pp. 385-387, Academic Press, New York, USA.
- Trotman, E.R. 1984. *Dyeing and Chemical Technology of Textile Fibre*, pp. 435-437, 6th edition, Charles Griffin and Company Limited, Edward Arnold, London, UK.

Physicochemical Characteristics of Rayon Grade Dissolving Pulp and the Effects of Metallic-Ions on the Viscose Rayon Process

Atif Latif*, Asad Ullah Jan, Farid Ullah Khan and Amin Ur Rahman

PCSIR Laboratories Complex, Jamrud Road, Peshawar-25120, Pakistan

(received May 5, 2005; revised July 31, 2006; accepted August 2, 2006)

Abstract. Pakistan imports rayon grade pulp from different countries for viscose rayon fibre manufacturing. Samples of imported pulp were collected and analyzed for alpha-cellulose, hemicellulose, calcium, magnesium, silica, copper, manganese, and iron. Moisture, ash content, cuprammonium viscosity, degree of polymerization, alkali absorption, and colour brightness were also determined. The results showed that all these parameters varied from sample to sample. The cotton linter pulp contained high alpha-cellulose content (94-98%) as compared to the softwood pulp (89.7-95%). Degree of polymerization of all samples was above 500 and varied from 500-750 ml/g. The study showed that higher manganese and copper content in cotton decreased the degree of polymerization. Iron above the standard value (7-10 ppm) affected the brightness of fibre, as observed in the case of cotton linter pulp (imported from China). The percentage of ash was less than 0.25% in all the samples studied.

Keywords: rayon pulp, pulp characteristics, metallic ion effects, viscose, rayon fibre, viscose process, dissolving pulp

Introduction

The development and use of a great variety of man-made fibres have created a revolution in textile industry in the recent decades. Rayon is the commercial man-made fibre composed of regenerated cellulose. Pulp is chiefly prepared from wood and cotton linter and is used for the manufacturing of viscose rayon fibre (Shareve, 1977). The term 'dissolving pulp' is used for pulp dissolved in the form of alkali soluble cellulose xanthate in the viscose process. Bamboo is being used at present for the manufacture of dissolving pulp. The alpha-cellulose content of the dissolving pulp is important because the rayon yield depends upon it. If it is low, there will be difficulties in processing. The required alpha-cellulose content of dissolving pulp for viscose staple fibre is 89 to 93 %. Higher content of hemicellulose in the pulp spoils the caustic soda lye used for steeping in the viscose manufacture. The hemicelluloses are mostly lower polymers of pentoses and should be less than 4% for the rayon grade dissolving pulp (Mandelia, 1970). Degree of polymerization and cuprammonium viscosity of the pulp is very important for the reduction of molecular weight of the cellulose to get a viscose of right viscosity (Edwin, 1948). The polymerization degree (DP) of the hardwood dissolving pulp for the viscose rayon continuous filaments is generally 550 to 600.

An important quality index for the dissolving pulp is the filterability of viscose made from it. Before spinning, the viscose has to be filtered to avoid the plugging of the spinnerets. Although slow viscose filtration may be due to many causes,

*Author for correspondence

the pulp properties influence the viscose filterability to a large extent. Chlorine dioxide helps in increasing the pulp brightness and minimizing the colour reversion. Sulphur dioxide helps in reducing the ash content (Mandelia, 1970). Alkalis are able to swell cellulose at low concentrations and produce dispersion at high concentrations. Certainly, the alkali opens up the fibre structure and leads to enhanced reactivity of the pulp during the xanthation process.

The dissolving pulp, especially for viscose, must be highly purified and uniform in quality (Edwin, 1948). The ash and its constituents are very important in deciding the suitability of the pulp for rayon. Calcium and magnesium are usually found in pulps prepared by the sulphite process. Metallic ions give trouble in the manufacture of viscose and in its filtration (Mandelia, 1970).

The viscose industries convert the dissolving cellulose pulp into products such as staple fibre, cards, films, packing materials, and non-edible sausage casings. The materials are used in the clothing, drapery, hygiene, automobile, food, and packaging industries (Ewing and Stepanik, 2000).

Materials and Methods

Nine rayon grade pulp samples of cotton linter and wood pulp were collected from Chemi Viscose Fiber Pvt., Nawabshah, Sindh, Pakistan. The ash content was determined by igniting the sample of pulp at 580-600 °C in a muffle furnace (ASTM D-586-97, 2002), while silica was determined by heating the sample at 900 °C. The moisture content was analyzed at 105 °C in a drying oven for two h (ASTM D-644-99, 2002). Calcium and

magnesium were determined volumetrically (Furman, 1963). Atomic absorption spectrophotometer (Hitachi, model Z-8000) was used for the determination of iron, copper and manganese (ASTM D-4085-93, 2002).

For the determination of alpha-cellulose and the hemicellulose contents, standard testing method of TAPPI was used (TAPPI-T203-cm-99, 2000). Cuprammonium disperse viscosity of 1% solution of pulps was determined by using the capillary viscometer, in cuprammonium solution, having the copper concentration of 14.8-15.2 g/l and the ammonium concentration of 190-210 g/l (Scott, 1956). The brightness of pulp samples was determined by a photovolt model-577 brightness meter (ASTM D-985-97, 2002). The small round slices of pulp samples were immersed into 60 ml 17.50% NaOH solution for the determination of alkali absorption capacity (Charles, 1950).

Results and Discussion

Table 1 shows that alpha-cellulose ranged from 89.83 to 98.12%. Sulphide dissolving hardwood pulp (e) had the lowest alpha-cellulose content, while cotton linter pulp (i) had the highest alpha-cellulose. The alpha-cellulose is that fraction which is resistant to 17.5% sodium hydroxide at 20 °C. The amount of alpha-cellulose in the pulp should be more than 89%.

Hemicellulose is the principal non-cellulosic polysaccharide present in the pulp. The presence of hemicellulose in viscose pulp is not desirable because it causes deterioration of mechanical properties, such as the wet strength of the finished fibre (Mandelia, 1970). Hardwood contains more hemicellulose as compared to softwood (Table 1).

Moisture content showed little variation, as compared to other parameters. Moisture is also very important in the pulp as the

sorption of water affects the degree of swelling of the pulp. Therefore, the moisture content in the rayon grade pulp should not exceed more than 5%.

The percentage of ash was less than 0.25% in all the samples. Cotton linter pulp (g) had the highest ash content, which was 0.24%. The ash and its constituents are very important in deciding the suitability of the pulp for rayon. It should be under 0.1% of the weight of the pulp. The pulp ash contents mostly consist of salts and hydroxides of the multivalent elements, such as silica, calcium, magnesium and iron, which are not desirable in the pulp because they create troubles in the filtration of the viscose.

The degree of polymerization of all samples was above 500 and varied from 500-750. The cuprammonium viscosity of the pulp was directly proportional to the degree of polymerization. The degree of polymerization is necessary for regulating the viscosity of the viscose for spinning. The degree of polymerization of cellulose must be between 450-500, otherwise the strength, elongation, the spinning state, and dye affinity of the yarn is affected.

The brightness of most of the samples was below the standard values. The required brightness of the rayon grade pulp should be above 91% because it affects the brightness of the final product.

Many pulp properties have a significant effect on the viscose properties and subsequently the fibre properties. These include the degree of polymerization, the oxidation state of cellulose, the soda solubility, and the residual level of pulp impurities like iron and silica (Calvin, 2001). The pulp samples that contain high calcium, magnesium and silica contents in ash, may cause poor filterability after the ripening process.

Table 1. Physicochemical characteristics of the rayon grade wood pulps and cotton linter pulps

Test	Visconier-F-MP softwood (USA)	Fibernier-F softwood (USA)	Tembec softwood (Canada)	Domjoe softwood (China)	Sulphite dissolving hardwood (Canada)	Hardwood (Canada)	Goami cotton linter (China)	Nanjiang cotton linter (China)	Pulp-651 cotton linter (USA)
	a	b	c	d	e	f	g	h	i
α-Cellulose (%)	94.02	94.47	93.64	94.78	89.83	94.52	94.63	94.37	98.12
Hemicellulose (%)	3.78	4.59	7.80	5.23	4.44	3.91	5.57	5.18	1.9
Moisture (%)	5.27	6.95	6.40	5.57	5.84	6.04	5.54	5.96	4.83
Ash (%)	0.10	0.14	0.03	0.05	0.12	0.10	0.24	0.19	0.08
Depolymerization	710	727	692	510	590	518	506	715	745
Cuprammonium									
viscosity (centipoise)	12.80	13.0	11.40	7.50	10.41	8.70	7.70	11.80	16.30
Brightness (%)	90.5	87.3	92.7	88.6	91.0	91.10	77.40	89.10	87.40
Alkali absorption (%)	480	443	493	450	472	438	639	394	469

Table 2. Metallic ions (ppm) present in the rayon grade pulps

Test	Visconier F-MP softwood (USA)	Fibernier-F softwood (USA)	Tembec softwood (Canada)	Domjoe softwood (China)	Sulphite dissolving hardwood (Canada)	Hardwood (Canada)	Goami cotton linter (China)	Nanjiang cotton linter (China)	Pulp-651 cotton linter (USA)
	a	b	c	d	e	f	g	h	i
Calcium	31.50	17.60	23.17	68.61	75.02	82.1	128.04	105.3	13.60
Magnesium	16.09	8.99	11.49	29.84	32.57	39.50	61.50	47.0	7.88
Silica (ppm)	15.93	5.41	12.16	33.25	28.0	37.08	52.90	62.35	4.07
Copper	1.39	0.96	1.16	0.89	3.42	3.46	3.85	2.18	0.41
Iron	3.89	1.82	4.33	6.11	12.66	15.3	18.73	16.64	2.80
Manganese	0.07	0.12	0.17	0.92	1.29	1.77	1.21	1.58	0.18

The subsequent viscose ripening was combined with filtration through a metal sieve fabric to eliminate persistent fibre fragments and to reduce the gel particles content of a sufficiently low level. Good filtration of viscose was required before spinning for the production of a regular viscose rayon staple fibre. The viscose filterability characterizes the quality of a viscose solution (Sixta *et al.*, 2004).

Cotton linter (**g, h**) and hardwood pulp samples (**e, f**) contained high calcium and magnesium as given in Table 2. The metallic ions cause trouble in the manufacture of viscose, which in turn is responsible for poor filterability and choking of spinnerets during the spinning process. Manganese, copper, and iron are very harmful if present in the ash in more than the permissible minimum. Manganese and copper accelerate the degradation of cellulose rapidly during the ageing process of alkali cellulose. In the case of cotton linter and hardwood pulp samples, both manganese and copper contents were above the permissible limit (Table 2).

The maximum permissible content of manganese in the dissolving pulp for viscose is 0.2 ppm and that of copper is 3 ppm. Iron above the standard value (7-10 ppm) affects the quality of the viscose and lowering the brightness of fibre, as was observed in the case of cotton linter pulp.

References

- ASTM D-586-97. 2002. Test for ash in pulp, paper and paper products. In: *Annual Book of American Society for Testing and Material Standards*, vol. **15.09**: 11-13, Philadelphia, PA, USA.
- ASTM D-644-99. 2002. Test for moisture contents in paper and paperboard by oven drying. In: *Annual Book of American Society for Testing and Material Standards*, vol. **15.09**: 33-34, Philadelphia, PA, USA.
- ASTM D-985-97. 2002. Test for brightness of pulp, paper and paperboard. In: *Annual Book of American Society for Testing and Material Standards*, vol. **15.09**: 130-133, Philadelphia, PA, USA.
- ASTM D-4085-93. 2002. Test for metals in cellulose by atomic absorption spectrophotometry. In: *Annual Book of American Society for Testing and Material Standards*, vol. **6.03**: 596-598, Philadelphia, PA, USA.
- Calvin, W. 2001. *Regenerated Cellulose Fibre*, pp. 41-45, 1st edition, Woodhead Publishing Ltd., Cambridge, England.
- Charles, D. 1950. Disperse cellulose-mercerised cotton and rayons. In: *The Methods of Cellulose Chemistry*, pp. 84-95, 2nd edition, Chapman and Hall, London, UK.
- Edwin, S.B. 1948. Cellulose. In: *Chemistry of Pulp and Paper Making*, pp. 25-460, 3rd edition, Chapman and Hall, London, UK.
- Ewing, D.E., Stepanik, T.M. 2000. *Electron Treatment of Wood Pulp for the Viscose Process*, pp. 377-379, 1st edition, Elsevier Science Ltd., London, England.
- Furman, N.H. 1963. *Standard Methods of Chemical Analysis*, pp. 256, 6th edition, D. Van Nostrand Company, New York, USA.
- Mandelia, S.P. 1970. *Handbook of Rayon*, pp.71-96, 2nd edition, The Century Rayon Company, Bombay-20, India.
- Scott, W.W.D. 1956. Paper and paper making-materials. In: *Standard Methods of Chemical Analysis*, vol. **2**, pp.1884-1888, 5th edition, D. Van Nostrand Company, New Jersey, USA.
- Shareve, R.N. 1977. Pulp and paper-making materials. In: *Chemical Process Industries*, pp. 555-560, 2nd edition, McGraw-Hill Book Company, London, UK.
- Sixta, H., Harms, H., Dopia, J.C., Parajo, J., Puls, J., Roder, T. 2004. Evaluation of new organosolv dissolving pulps. Part I: preparation, analytical characterization and viscose processability. *Cellulose* **11**: 73-83.
- TAPPI-T203-cm-99. 2000. Test for determination of alpha, beta and gamma cellulose in pulp. In: *Test Methods of Technical Association of Pulp and Paper Industry*, vol. **1**, pp. 1-5, Technology Park, Atlanta, USA.

The Study of Electrolytes on the Dye Uptake of Bifunctional Reactive Red Dyes on a Cellulosic Substrate (Cotton K-68)

Javaid Mughal, Ausaf Aleem*, Qasim Siddiqui and Mansoor Iqbal

Applied Chemistry Research Centre (Textile Section), PCSIR Laboratories Complex Karachi, Shahrah-e-Dr. Salimuzzaman Siddiqui, Karachi-75280, Pakistan

(received December 19, 2005; revised September 12, 2006; accepted September 14, 2006)

Abstract. For obtaining optimum conditions for dyeing a cellulosic substrate (cotton K-68) with bifunctional reactive dyes, it was investigated as to how the dyeing results depended upon the properties of the dyes and the substrate. A cellulosic substrate (cotton K-68) was dyed by varying the nature and quantity of electrolytes. Experimental findings indicated that sodium chloride and sodium sulphate produced good dye exhaustion. An increase in the concentration of electrolytes (sodium chloride, sodium sulphate and potassium chloride) also improved the fastness properties of the dyed substrate.

Keywords: cellulose dyeing, dye exhaustion, dye uptake

During the recent years, demand of reactive dyes is increasing for the dyeing of cellulosic fibres because of their bright shades and excellent fastness properties. For the dyeing of cellulosic fibres with bifunctional reactive dyes, salts as well as alkalis are added at different stages. During the primary exhaustion stage, the dye is taken-up into the fabric in the presence of added inorganic salts. During the secondary exhaustion stage, alkali is added to the dyebath and the dye-fibre reaction takes place (Imada and Harada, 1992). When the dyeing is performed in an alkaline medium, the electrolytes tend to reduce the charge on the fibre, thus the transfer of dye from solution into the fibre is facilitated (Vickerstaff, 1954). UV-visible spectroscopy is a versatile technique of quantitative analysis for dye concentration, either in the dyebath or on the fabric. Measurements can be performed by absorbance spectrophotometry of the dye solution. The quantity of dye, which disappears from the bath during the dyeing process, may be determined by taking the absorbance of the solution (Venkataraman, 1995). An earlier work (Croft *et al.*, 1992) for the determination of dye uptake was based on taking the absorbance spectrum of the dye solution. The dye uptake was then defined in terms of the quotient of the dye covalently bounded to the fibre and the total amount of dye initially present in the bath:

$$T = (1 - A_s / A_b) \times 100 \quad (1)$$

where:

T = dye uptake

A_b = the maximum absorbance of the bath solution at dyeing

A_s = the absorbance of bath after stripping with 25% aqueous pyridine

In this connection it is further significant to refer to the studies of alkali metal electrolytes on the dye uptake of cellulosic fabrics. The results obtained by taking absorbance, at different electrolyte concentrations (Guo *et al.*, 1993), leads to the conclusion that sodium chloride was the most efficient salt for a short dyeing time. At an electrolyte concentration of 100 g/l, the dye uptake decreased in the order NaCl > KCl > CsCl > LiCl. It is well known that cellulosic fibres, when immersed in aqueous alkaline media, acquire a negative charge because their dielectric constant is lower than that of water. Due to a decrease in the negative surface potential of the fibre, the relative fibre-dye potential remains negative and involves a repulsive effect. By the addition of electrolytes, the adsorption of dyes on cellulosic fibre is influenced by the cations present in the dyebath (Peters, 1975). These cations influence the dye adsorption by disrupting the structure of hydrated water around the hydrophobic parts of the dye molecules and the structure of water bound to the surface of the fibre. This enables the dye anions to come closer to the surface of the cellulosic fibre thus making adsorption easier by virtue of their strong affinity for cellulose (Noah and Braimah, 1986).

The present study was conducted to assess the influence of electrolytes on the dye uptake of a bifunctional reactive dye on the cellulosic substrate (cotton K-68), which is a very low-grade cotton of Pakistan. Five electrolytes were used in order to assess their effectiveness in the dye uptake. Sodium chloride, lithium chloride, potassium chloride, caesium chloride

*Author for correspondence

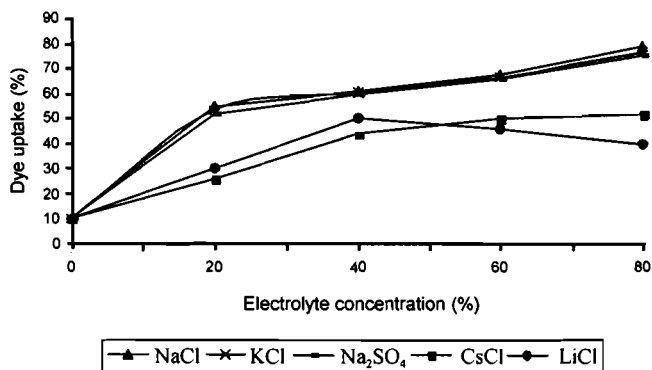


Fig. 1. Dye uptake of bifunctional reactive dye CI Red 194.

and sodium sulphate were used for this purpose. A series of measurements were carried out, at set intervals, until equilibrium was attained so that the optimum dyeing could be identified by the influence of the electrolyte addition. Dyeing was performed at 60 °C for 60 min. The values of the dye uptake, after 30 min, were determined and were calculated from UV-visible spectrophotometric measurements. It was observed that by using univalent electrolytes, the dye uptake increased with increasing electrolyte concentration, but with lithium chloride the dye uptake reached the maximum value at about 40 g/l, beyond this concentration the dye uptake of lithium chloride decreased (Fig. 1).

At an electrolyte concentration of 80 g/l, the value of (T) decreased in the order NaCl > KCl > Na₂SO₄ > CsCl > LiCl. Hence, increase in the electrolyte concentration always enhanced substantivity without impairing reactivity, provided the dye remained completely dissolved. It was also observed that an increase in the concentration of electrolytes

improved the fastness properties (wash fastness and light fastness) of the reactive red dye on cotton K-68.

The present studies have shown that sodium chloride and sodium sulphate produced good dyebath exhaustion during the complete dyeing process. It is also evident that increased electrolyte concentration improved the fastness properties of the dye on the cellulose substrate (cotton K-68). These results may give useful information for better use of electrolytes.

References

- Croft, S.N., Lewis, D.M., Orita, R., Sugimoto, T. 1992. Neutral-fixing reactive dyes for cotton. Part-I. Synthesis and application of quaternised S-triazinyl reactive dyes. *J. Soc. Dyers and Colourists* **108**: 195-197.
- Guo, Ln., Petit-Ramel, M., Gauthier, R., Jacquet, A. 1993. Interaction of vinylsulphone reactive dyes with cellulosic fabrics. Part-1. Dyeing mechanism, fibre characterization and effects of alkaline electrolytes. *J. Soc. Dyers and Colourists* **109**: 213-219.
- Imada, K., Harada, N. 1992. Recent developments in the optimized dyeing of cellulose using reactive dyes. *J. Soc. Dyers and Colourists* **108**: 210-214.
- Noah, A.O., Braimah, J.A. 1986. An investigation into the reaction of a bifunctional reactive dye at various pH levels. *J. Appl. Polymer* **32**: 5840-5842.
- Peters, R.H. 1975. *Textile Chemistry: The Dyeing of Cellulosic Fibres and Related Process*, pp. 580-582, Elsevier, Amsterdam, The Netherlands.
- Venkataraman, K. 1995. *The Analytical Chemistry of Synthetic Dyes*, pp. 149-194, Academic Press, New York, USA.
- Vickerstaff, T. 1954. *The Physical Chemistry of Dyeing*, pp. 238-240, 2nd edition, Oliver and Boyd, London, UK.